“Electrochemical and spectrochemical investigations into the determination of Niobium and Zirconium complexes in seawater”

Diploma Thesis

Kathrin Wuttig

November 2008

IFM-GEOMAR, Leibniz-Institut für
Meereswissenschaften an der
Christian-Albrechts-Universität Kiel

Table of Contents

1 Abbreviations

A	Absorbance
AC	Alternating current
ACP	Alternating current polarography
AE	Auxiliary electrode
BPHA	*N*-benzoyl-*N*-phenylhydroxylamine
CAdSV	Catalytic adsorptive tripping voltammetry
cit	Citrate
cm	Centimetre
conc.	Concentrated
CSV	Cathodic stripping voltammetry
Cupf	Cupferron, the ammonium salt of *N*-nitroso-*N*-phenylhydroxylamine
CV	Cyclic voltammetry
d	Day
DC	Direct current
DCP	Direct current polarography
DIC	Dissolved inorganic carbon
DME	Dropping mercury electrode
D-Nb/Zr	Dissolved
DOC	Dissolved organic carbon
DPCSV	Differential pulse cathodic stripping voltammetry
DPP	Differential pulse polarography
E_0	Standard potential
$E_{1/2}$	Half-wave potential
EDTA	Ethylenediamine-tetra-acetic acid
E_p	Peak potential
EPPS	4-(2-Hydroxyethyl)-1-piperazinepropanesulfonic acid
Fe	Iron
g	Gram
h	Hour
Hf	Hafnium
HFSE	High field strength elements
HMDE	Hanging mercury drop electrode

I,i	Current
ID-ICP-MS	Isotope dilution inductively coupled plasma mass spectrometry
IDMS	Isotope dilution mass spectrometry
I_p, i_p	Peak current
km	Kilometre
L	Litre
L	Ligand
LP-Nb/Zr	Labile particulate
m	Metre
M	Molar, M = mol L^{-1}
MES	2-(N-Morpholino)ethanesulfonic acid hydrate
min	Minute
mm	Milimetre
MQ	Ultrapure Milli-Q water
nA	Nanoampère
Nb	Niobium
NCE	Normal calomel electrode (with 1 mol L^{-1} KCL as a reference electrolyte)
NH_2OH	Hydroxylamine
nm	Nanometre
OD	Optical density = absorbance per unit length
ox	Oxalate
pA	Picoampère
PAR	4-(2-pyridylazo)-resorcinol
PIPES	1,4-Piperazinediethanesulfonic acid disodium salt
PP	Pulse polarography
ppb	Parts per billion (µg/kg)
ppm	Parts per million (mg/kg)
PSE	Periodic system of the chemical elements
RDE	Rotating disc electrodes
RE	Reference electrode
rpm	Rotation per minute
R.T.	Room temperature

S	Sensitivity
SCE	Saturated calomel electrode
sec	Second
SV	Stripping voltammetry
SW	Seawater
t	Time
Ta	Tantalum
tart	Tartrate
U	Voltage
WE	Working electrode
yr	Year
Zr	Zirconium
δ	Density
ε	Molecular extinction coefficient
ε_{mol}	Molar absorptivity
λ_{max}	Maximum absorption wavelength
$\tau_{1/2}$	Half-life

2 Abstract

The focus of this diploma work is on an electrochemical and spectrochemical investigation of Niobium and Zirconium speciation in seawater. Previously all published investigations of Nb and Zr were done at significantly higher concentrations (µmol L^{-1}) were the *in situ* speciation may be considerably different than that found in ambient seawater (nmol L^{-1} or pmol L^{-1}). At concentrations in the µmol L^{-1} range solubility issues coupled with the formation of dimeric and higher order polymeric hydroxy species complicate studies in seawater and presently our knowledge of the actual speciation in seawater and the potential role of organic complexation is very limited. Furthermore Nb and Zr belong to the "high field strength elements" (HFSE) (Barth et al. 2001) and are being investigated as oceanographic watermass tracers (McKelvey and Orians 1998). Thus there is some urgency to develop new methods to determine Nb and Zr speciation at low concentrations in seawater to improve our understanding of the basic biogeochemistry of these metals.

Wang et al. (1992a) published a sensitive electrochemical method for the detection of Nb with 5 µmol L^{-1} cupferron in 0.1 mol L^{-1} acetate buffer at pH 4. Their method was based on differential pulse cathodic stripping voltammetry (DPCSV). In the present work this method was extended to the pH range of 4.4-6.6 though the use of increased cupferron concentration was necessary for the achievement of the same sensitivity. With an increasing pH in both water and seawater the peak position of Nb was shown to move to a more negative potential, as observed previously by Ferrett et al. (1955). In order to apply this method to the determination of Nb in seawater, the cupferron concentration had to be further increased. This was due to the fact that there is a competition with Mg and Ca in seawater which are also able to form complexes with cupferron.

In seawater it was found that Nb can be determined by DPCSV with cupferron in the pH range of 3.9-6.5. An increased sensitivity of S = 0.55 nA $nmol^{-1}$ L can be obtained by adding 1 mmol L^{-1} cupferron as a chelator and 5.4 mmol L^{-1} $KBrO_3$ as an oxidizing agent at pH 6.4. The overall reaction is enhanced catalytically by the presence of an oxidizing agent and while cupferron itself can act as both complexing agent and oxidizing agent, $KBrO_3$ is more effective as an oxidizing agent under these pH conditions. Generally the catalytic cycle is the reduction of the Nb(V)-cupferron

complex to Nb(IV) with reoxidation back to Nb(V) in the presence of an oxidizing agent. At pH 7 another peak interfered at the same peak position as the Nb peak.
The results of this work suggest that a 1:1 Nb:cupferron complex is formed at pH 6 whereas a 1:2 Nb:cupferron complex is formed at a higher pH (6.5-7.1) in MQ.
For the polarographic determination of Nb an analogue of cupferron was also evaluated, *N*-benzoyl-*N*-phenylhydroxylamine (BPHA), as a chelator. BPHA is a stronger chelator for Nb than cupferron, but the catalytic cycle as with cupferron cannot be formed, because of the easy reduction of the Nb-BPHA complex.

It was previously published that Nb forms ternary red-coloured complexes with PAR and either tartrate, oxalate or citrate at pH 5-6. These ternary complexes can be determined spectrochemically, because the light is absorbed at a wavelength of λ_{max} = 550 nm. The composition of the formed Nb:PAR complex is 1:1 (Belcher et al. 1962a; Yamada et al. 1988; Yamada et al. 1990). The results of this thesis suggest that a 1:1 Nb-PAR complex is still formed at pH 7, but the formation takes far longer than at pH 5-6. The formation of the Nb:PAR complex without added chelator was significantly quicker indicating the absence of any competing complexation reactions.

Zr and Nb are often being complexed by the same organic compounds. Thus the electrochemical determination of Zr with the related complexing agents cupferron and BPHA was also tested, but it was not possible to find the corresponding Zr peak. Zr obviously forms no catalytic cycle and has no redox chemistry [Zr(IV)/Zr(III)] under the conditions used here.
Little is known about the marine chemistry of Nb and Zr. The oxidation state of Nb which dominates in seawater is probably +5 and the predominating hydrolyzed species could be primarily $Nb(OH)_6^-$ and secondarily $Nb(OH)_5$ (Greenwood and Earnshaw 1990; Sohrin et al. 1998a; Byrne 2002). In acidic streams (pH = 4.5-6.2) Astrom et al. (2008) found that the dissolved Nb is present in an anionic form. The results of this thesis are consistent with an anionic Nb species in seawater for pH higher than 5.8.
The dominating oxidation state of Zr under seawater conditions is presumably +4 and the predominant species is $Zr(OH)_5^-$ with a small fraction of $Zr(OH)_4$ (Byrne 2002). In a plot that is based on the pK-values published by Turner et al. (1981) it was found that with increasing pH the hydrolysis of Zr is increased and the dominating Zr species under seawater conditions agree with those published by Byrne (2002).

3 Introduction

3.1 Scientific background

3.1.1 Niobium and Zirconium in the Periodic System of Elements and their properties

3.1.1.1 Niobium (Nb)

Niobium belongs to the vanadium group in the Periodic System of Elements. It is the 5^{th} subgroup and 5^{th} group in the Periodic System of Elements respectively to which elements vanadium (V), niobium (Nb), tantalum (Ta) and dubnium (Db) belong as well (Hollemann and Wiberg 1995).

Vanadium, niobium and tantalum were discovered almost at the same time more than 200 years ago (in 1801 and 1802). Their discovery and naming was quite chaotic. They were detected at different places all around the world and, because of the lack of verification that it concerned the same elements, were named differently each time.

In 1830, the Swedish chemist Gabriel Sefström named vanadium after Vanadis, the Scandinavian goddess of beauty, as the compounds of vanadium show such a richness and variety of colours. Niobium was called columbium by Charles Hatchett in 1801 in honour of the discovery of his home country. He had found the mineral columbite in Colombia and extracted niobium from it. Columbium is the name for niobium still used in Northern America today.

At the same time the Swedish scientist Anders Gustaf Ekeberg also discovered a new element which was difficult to be extracted from the minerals. The minerals containing the new element could not easily be dissolved in acids either and were difficult to work on. This fact made Ekeberg think of the Greek half-god Tantalus, one of Zeus' sons who is supposed to have misbehaved at his father's table in Olympus and therefore was sent back to the earth. So Ekeberg named the new element after him tantalum.

That's the reason why only in 1844 Heinrich Rose was able to show that a sample of columbite (Fe, Mn)(Nb, $Ta)_2O_6$ contained not only tantalum, but a second element of the same group with an almost akin behaviour like Ta. Rose thought he had discovered a new element not knowing that he had discovered again columbium. He

named this element niobium after Tantalus' daughter Niobe (Greenwood and Earnshaw 1990; Greenwood 2003).

The lanthanide-contraction is an aperiodic property. It can be explained by the fact that the pulling force of the nuclear charge on a lonely 4f-electron is only very slightly shielded by the rest of the atomic electrons and hence in the direction of lanthanide row (from La^{3+} to Lu^{3+}) the increasing nuclear charge is becoming tighter and bound nearer to the nucleus. Because of the lanthanide-contraction Nb and Ta have an alike atomic and ionic radius and very similar properties and behave similar. The compounds of Nb and Ta differ a lot in their structure and formula from the compounds of the lighter vanadium.

In nature niobium is mostly found as iron niobate $(Fe, Mn)(NbO_3)_2$ or iron tantalate $(Fe, Mn)(TaO_3)_2$ in the same mineral. Depending on the amounts it can be either called niobite (columbite, pyrochlor) or tantalite. The mixed mineral $(Fe, Mn)(Nb, Ta)_2O_6$ contains 47-78 % Nb and trace-34 % Ta depending on its source. Due to the lanthanide contraction and hence their similar properties niobium and tantalum replace each other isomorphically in minerals.

In the continental crust there are 0.0019 mass-% of niobium. Just one stable natural isotope exists which is $^{93}_{41}Nb$.

Metallic niobium is light grey, melting at 2,468°C and boiling at 4,758°C. Its structure is cubic body centered with a density of δ=8.581 g/cm^3. It is comparably hard like wrought iron, good to roll and weld and it is insoluble in acids even in Aqua Regia. When niobium is exposed to the oxygen in air at room temperature it forms thin, protecting surface films of oxide and due to that is its general resistance to corrosion. At 300°C Nb reacts with oxygen to its pentoxide Nb_2O_5. It is oxidized by most non-metal elements like halogens and at very high temperatures also by nitrogen and carbon. The emerging products are often interstitial and non-stochiometric. In industry Nb is mostly used as a component in temperature resisting alloys, in superconductors and nuclear fuel rod coatings. Niobium is a lithophile element.

Like vanadium and tantalum, niobium forms compounds with quite a variety of oxidation states from +5 to -3. But the stability of those oxidation states differ. The most stable oxidation state of Nb and Ta is +5 like in their pentoxides. In contrast V "prefers" under normal circumstances the middle oxidation states +4.The stability of those middle oxidation states decreases from V down to Ta. V exists in water also in the oxidation states +2 and +3. This aqueous type of chemistry with those oxidation

states is unknown for Nb and Ta, but some halides and metalloxides in the range of +2/+3 and +1/+2 are known for them.
Some of the compounds of Nb are presumed to be toxic. Niobium is not essential for human beings, but it may be for some marine organisms like ascidians. (Greenwood and Earnshaw 1990; Hollemann and Wiberg 1995).

3.1.1.2 Zirconium (Zr)

Zirconium (Zr) belongs in the titanium group (4th subgroup and 4th group in the Periodic System of Elements respectively) along with titanium (Ti), hafnium (Hf) and rutherfordium (Rf). Their elemental properties are quite similar to their direct neighbours in the 3rd subgroup though their valency is one unit higher. Thus they can appear in multiple oxidation states and show a higher complexation tendency. The elements of the titanium group also show some affinity to the 4th maingroup (14th group in the Periodic System of Elements), which consists of carbon (C), silicon (Si), germanium (Ge), tin (Sn), lead (Pb), and ununquadium (Uuq), but there is the difference that the metals which belong to the titanium group corrode and oxidize more easily than the elements of the 14th group. These elements of the 4th group are hard refractory and base metals.
Because of the lanthanide-contraction zirconium and hafnium have nearly the same ionic and metalloatomic radius, though the atomic mass and density of Hf is twice as high as the atomic mass and density of Zr. Also their properties are very similar to one another –even more akin than the ones of Nb and Ta. Zirconium had already been identified in 1789, but because of their similar properties and the difficulty to separate the two elements, hafnium could not be identified before 1923. Hafnium just exists as an alloy in zirconium consisting minerals. Zirconium exists in nature only bound and mostly as silicate $ZrSiO_4$ (zircon) and as dioxide ZrO_2. Important deposits are found mostly in Australia, Brasilia and the USA.
Natural zirconium is composed of 5 isotopes: $^{90}_{40}Zr$ (51.45 %), $^{91}_{40}Zr$ (11.32 %), $^{92}_{40}Zr$ (17.28%), $^{94}_{40}Zr$ (17.19 %) and $^{96}_{40}Zr$ (2.76 %). The last one is slightly radioactive (ß$^-$-emitter with $\tau_{1/2} > 3.6 \times 10^7$ a). The two artificial nuclides have a very short $\tau_{1/2}$ which is in the range of hours and days and are used for tracer experiments.
In the continental crust there are 0.016 mass-% of Zr and thus it is found in nature more often than e.g. mercury, cadmium, silver, gold or platinum.

Pure zirconium is quite a supple, easily processible, heat and electricity conductive silver-shining metal. Under normal conditions it exists as a hexagonal tightest packing. It melts at 1,857°C and boils at 4,200°C. The melting and boiling points of Hf are very similar to the ones of Zr as well as their ionic radius and their energy, but they differ a lot in their density and superconducting properties (Zr: 0.55 K).
Zr doesn't corrode easily, because it builds a thin, protecting oxide surface film. Under higher temperatures it reacts with quite a lot of non-metallic elements. It is used e.g. to coat nuclear fuel rods.
The preferred oxidation state of Zr as well as of Hf is +4 (e.g. ZrF_4, ZrO_2), but also the oxidation states +3, +2. +1, 0 and in organic compounds <0 exist.
Zr is not essential and might be carcinogenic (Greenwood and Earnshaw 1990; Hollemann and Wiberg 1995).

3.1.2 Vanadium and Niobium in Ascidians

By now it has been known for nearly a century that vanadium is contained organically bound in the blood of some species of sea squirts (ascidiacea, ascidians) (Henze 1911) of the order of Phlebrobranchia (Kokubu and Hidaka 1965). Ascidians are marine, microphage filter feeders. They belong together with salps (thaliacea) and appendicularia (larvacea) to the group of tunicates (urchordata) and are members of the phylum chordate. They are an evolutionary effective sessile group from the continental shelf down to the deep sea, because they are suspension feeders. Tunicates exist in a big variety and richness of colours and sizes (Bone 1998). Figure 1 and Figure 2 show some colourful examples.

Figure 1. Pictures of tunicates. From left to right: Banded Messmate pipefish on Sea Squirts (Corythoichthys sp. 10), Pseudodistoma megalarva, Stalked Ascidian (Clavelina robusta) (Zubi 2006)

Fifty years ago, Carlisle suspected and developed spectrophotographic and chromatographic methods to show that not only vanadium but also niobium can be found in the blood of tunicates. However the amount of Nb depends on the species of tunicates, because only some of them contain Nb instead of or in addition to V (Carlisle 1958).

In other marine animals the V content in the dry weight does not exceed 39 µmol kg^{-1} / dry weight, but in ascidians it can reach numbers as high as 128 mmol kg^{-1} / dry weight (Kokubu and Hidaka 1965). Tunicates can enrich vanadium a million times more than the concentration of V in seawater (Bielig and Bayer 1954; Macara 1980) in which V behaves conservatively with an average concentration of 35 nmol L^{-1} (Nechay 1984). In ambient oxic seawater (pH 8) (Libes 1992; Faure 1998) vanadium(V) exists in equimolor amounts in the monomeric HVO_4^{2-} and $H_2VO_4^-$ species.

Figure 2. Pictures of tunicates. From left to right: Blue Club Tunicate (Rhopalaea crassa), Golden Sea Squirt (Polycarpa aurata), Moluccan blue spot Ascidian (Clavelina moluccensis) (Zubi 2006)

Tunicates seem to be able to extract monomeric vanadate species from the surrounding seawater (McLeod et al. 1975). Vanadium is reduced and organically bound in the phagocytic blood cells which was shown by electron-microscopic studies (Kalk 1963). V and other metals are stored in two types of phagocytic blood cells (vanadocytes or morula cells), the granular and vacuolar hyaline amoebocytes (Carlisle 1958; Macara et al. 1979; Rowley 1982; Rowley 1983). These cells might have the function to defend the tunicate against infections (Macara 1980; Rowley 1982; Rowley 1983; Michibata et al. 2002). Though the main oxidation state of

vanadium in seawater is +5, it is reduced in the vanadocytes to +3 and stored with abundant sulfate (Michibata et al. 2002).

For sea squirts found with a very high V content, the Nb content was not significantly high and vice versa. Apparently only one of the two elements can be concentrated in the blood cells (Carlisle 1958). The ability of the accumulation of Nb from seawater depends on the genera. Apparently the genus *molgula manhattensis* has the ability to accumulate Nb from seawater (Carlisle 1958) which can be seen in the measured amount of this element in the dry weight (Table 1).

Table 1. Different ascidian species and their V and Nb content (Carlisle 1958).

Species	V (µmol kg^{-1} / dry weight)	Nb (µmol kg^{-1} / dry weight)
Mytilus edulis	4	0.01
Phallusia mammillata	24,735	<0.01
Molgula manhattensis	314 Flesh without the tunic: 1,983	20 Flesh without the tunic: 603

Concentrations of iron (Fe) and vanadium in ascidians showed that they vary in the different body parts (tunic, blood, outer fluid) of the animals. In the genus *molgula manhattensis*, a Stolidobranchia, there was nearly no vanadium found- less than 393 µmol kg^{-1} / dry weight (Swinehart et al. 1974). This is far less than 1,983 µmol kg^{-1} / dry weight (flesh without the tunic) (Carlisle 1958), which might result from a genera difference (Monniot 1969). However the iron content was quite high compared to other sea squirt species: 16-30 mmol kg^{-1} / dry weight without tunic (Swinehart et al. 1974). This species is apparently an iron and niobium instead of a vanadium accumulator (Macara et al. 1979; Michibata et al. 1986).

The main oxidation state of niobium in seawater is normally +5 and this element has a restricted chemistry in aqueous solutions. Due to its low concentration in seawater ascidians need a strong ligand to coordinate the niobium. It has been suggested that α-hydroxy carboxylic acids take part in the complexation (Rayner-Canham 1984). If that's the case other metals like zirconium (Carlisle 1958) might also be complexed in ascidians, but no further investigations have yet been undertaken.

3.1.3 Sources and sinks of niobium and zirconium in seawater and continental crust

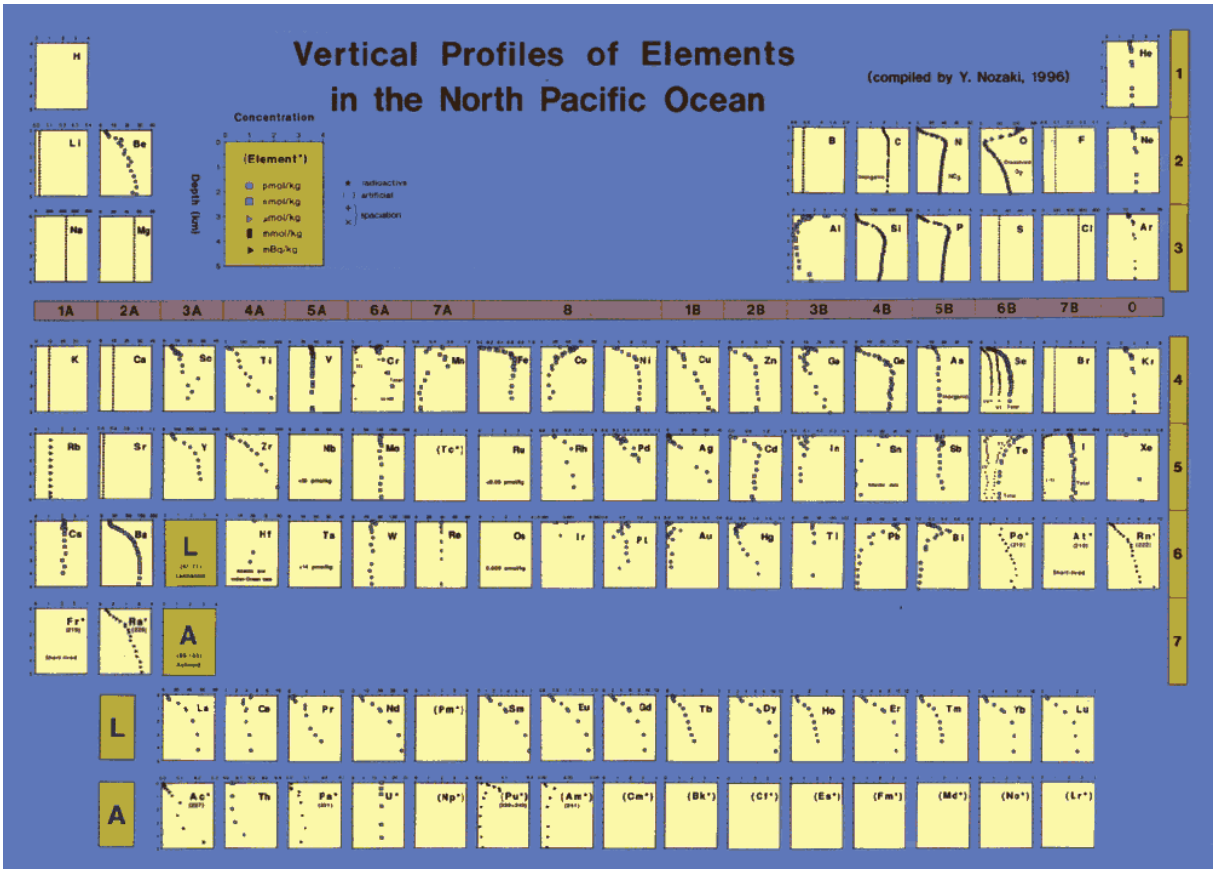

Figure 3. In this periodic table of elements the depth profiles of these Elements in the North Pacific are compiled by (Nozaki 1997), the source of the Nb data is (Carlisle and Hummerstone 1958) and the source of the used data set of Zr concentration is (McKelvey and Orians 1993).

In Figure 3 the periodic table of the chemical elements with their vertical profiles is shown as compiled by (Nozaki 1997). It can be seen that even in 1996 there was hardly any real data set for a vertical profile of dissolved niobium in the North Pacific and even the used data (Carlisle and Hummerstone 1958) was from before the development of contamination free sampling schemes.

The first depth profile of dissolved Zr in seawater Figure 3 and in more detail in Figure 6 was obtained in 1993 using isotope dilution inductively coupled plasma mass spectrometry (ID-ICP-MS) (McKelvey and Orians 1998; Firdaus et al. 2007). In this profile the Zr concentration monotonically increases with depth (McKelvey and Orians 1993).

3.1.3.1 Niobium

Ascidians take up Nb and V by filtering seawater and accumulating these elements in their blood (Carlisle 1958). With this discovery the interest on niobium chemistry in seawater was born. Nb was believed to be present in seawater in concentration as high as at least 538 pmol L^{-1} (Carlisle and Hummerstone 1958). In 1957 the first method to estimate the amount of Nb in seawater was paper-chromatography (Hunt et al. 1955). The reported concentration in unfiltered surface seawater was 108-1,078 pmol L^{-1} and in filtered seawater 54 pmol L^{-1} (Carlisle and Hummerstone 1958).

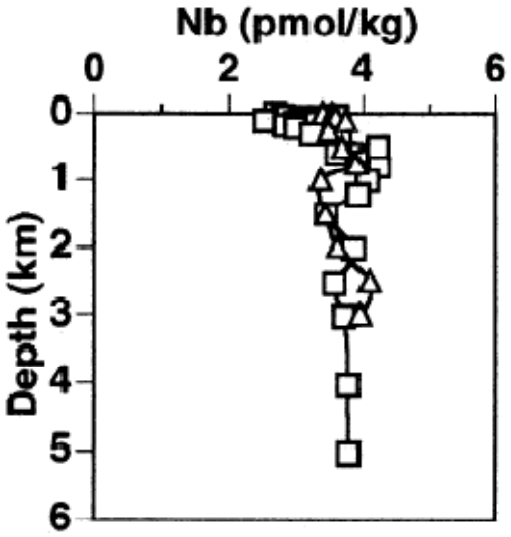

Figure 4. Distribution of dissolved Nb as a function of water column depth in the Northwest Pacific at different stations (Sohrin et al. 1998a).

Recent studies show that dissolved niobium in seawater is present at very low levels (Libes 1992; Faure 1998; Sohrin et al. 1998a) and that the concentration of dissolved niobium in water in European streams depends on the region, but is far higher than in seawater (Astrom et al. 2008).

The mean concentration of dissolved Nb in the oceans is <54 pmol L^{-1} (Libes 1992; Faure 1998). The average concentration of dissolved Nb in the surface seawater of the North Pacific is 3.0 pmol L^{-1} and in the deep North Pacific water it is 3.8 pmol/kg (Sohrin et al. 1998a) Figure 4 shows the distribution of the dissolved Nb through the water column at different stations.

According to Firdaus et al. the concentration of dissolved Nb in the western North Pacific Ocean (at 44°N, 155°E) ranges between 4.1 pmol L^{-1} and 6.7 pmol L^{-1} (Firdaus et al. 2006) and in a larger area of the North Pacific (35°-51° N, 155°-165° E) the Nb concentration reaches from 1.4 pmol L^{-1} to 9.5 pmol L^{-1} from the surface to the bottom waters (Firdaus et al. 2008) .

The range of the Nb to Ta ratio is 32-61. The ratio in the continental crust is lower and less fluctuating (Firdaus et al. 2006).

In the Atlantic coastal waters the niobium concentration is nearly twice as high as in the open Pacific Ocean where it varies between 6.7 pmol L^{-1} (Firdaus et al. 2008) and 7.8 pmol L^{-1} (Firdaus et al. 2007).

Variation of the distribution of Nb in the ocean is quite low and no specific relationship between the Nb-concentration and salinity, temperature or nutrient concentration has been observed up to now (Sohrin et al. 1998a).

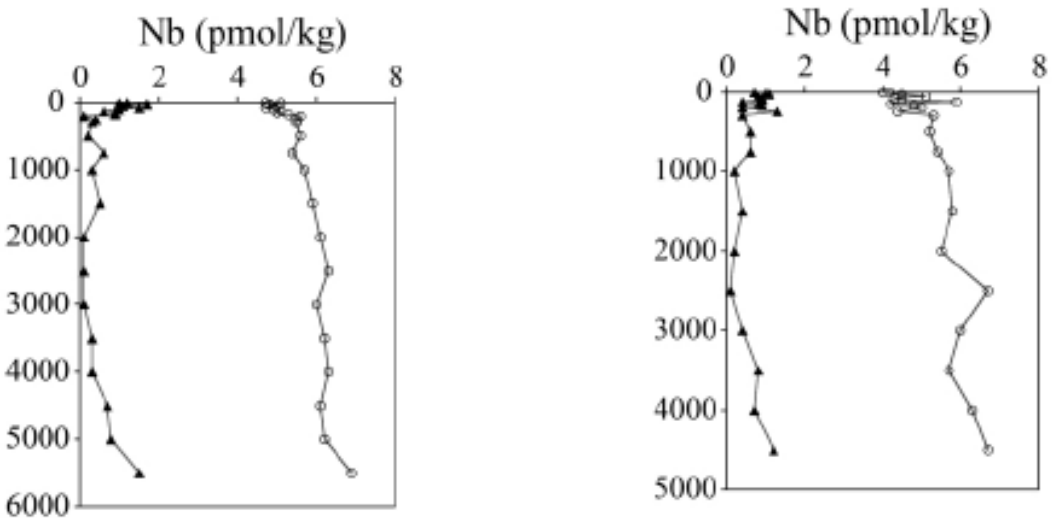

Figure 5. Distribution of labile particulate (dark triangles) and dissolved Nb (black surrounded circles) as a function of water column depth in the Northwest Pacific at two different stations at 51° N, 165° E and 35° N, 160° E (Firdaus et al. 2008).

The concentration of dissolved Nb is also quite uniform with the water column depth, though it shows a slight depletion in the surface water as can be seen in Figure 4 (Sohrin et al. 1998a) and Figure 5 shows the dissolved Nb (0.45 µm) and labile particulate Nb concentration. Labile particulate (LP) Nb is defined as its acid-dissolved species, which is a portion of seawater acidified without filtration, minus dissolved (D) Nb. It represents a chemically labile fraction of particulate species (Firdaus et al. 2008). In the bottom water (3.5-5.5 km) of the vertical profile in Figure 4 there is no indication for a change in the Nb concentration. In contrast to Figure 4 the dissolved Nb in Figure 5 shows a slight enrichment with depth in the water column, especially in depth greater than 5 km (Firdaus et al. 2008).

The data for niobum concentrations in Figure 4 and in Figure 5 were all measured by ICP-MS (Sohrin et al. 1998b; Firdaus et al. 2007).

The oxidation state of niobium which dominates in seawater is presumably +5 and the species may be $Nb(OH)_6^-$ and $Nb(OH)_5$ (Greenwood and Earnshaw 1990; Sohrin

et al. 1998a). According to Byrne, using the minimal speciation data available for Nb, the strongly hydrolyzed species dominate as principally $Nb(OH)_6^-$. A significant minor species is the uncharged species $Nb(OH)_5$ (Byrne 2002).

The calculated residence time for Nb in seawater is 4,600 years (Firdaus et al. 2008).

The concentration of niobium has scarcely been measured in freshwaters so far. In river water the Nb concentration seems to be strikingly higher than in the sea, but the level of Nb depends very much on the region. In European rivers (43 pmol L^{-1}) the Nb concentration is lower than in the Barents region (161 pmol L^{-1}). Dissolved Nb exists in acidic streams (pH = 4.5-6.2) in an anionic form. Also in streams the Nb level is presumably controlled by dissolved humic substances and colloidal Fe. Anomalies are formed by (clay-silt) deposits (Astrom et al. 2008). The river Uji in Japan for example contains 75 pmol L^{-1} of dissolved niobium (Firdaus et al. 2008).

Niobium and zirconium both belong - together with hafnium, tantalum and their two direct neighbours from the 6th group in the Periodic System of Elements: molybdenum and tungsten (also called wolfram) - to the so called “high field strength elements” (HFSE) (Barth et al. 2001). This means that during the fractional cristallization in the magma the HFSE cannot simply be concentrated, because of their lack to enter the cationic sites of minerals (Plank and Langmuir 1992; Plank and Langmuir 1998; Firdaus et al. 2006).

As a result of the similar properties and behaviour of these elements belonging to the same group of the Periodic System of Elements Nb and Ta, but also Zr and Hf, their abundance in the continental crust varies only very little (Jochum et al. 1986). The niobium content in the upper continental crust is 129 µmol kg^{-1} (Taylor and McLennan 1995; Rudnick and Gao 2003) which is the same estimated amount of Nb as in soils all over the earth (Reimann and Caritat 1998).

3.1.3.2 Zirconium

In 1964 when the first seawater measurements of Zr concentration were made, the measurements showed far higher Zr levels than today. The first published Zr concentrations in seawater was 2,150 nmol L^{-1} determined using a colorimetric method (Mauchline and Templeton 1964) which was followed by zirconium values that were in the range of 4.6 nmol L^{-1} to 15.8 nmol L^{-1} using optical spectrophotometry with Alizarin Red-S (Sastry et al. 1969).

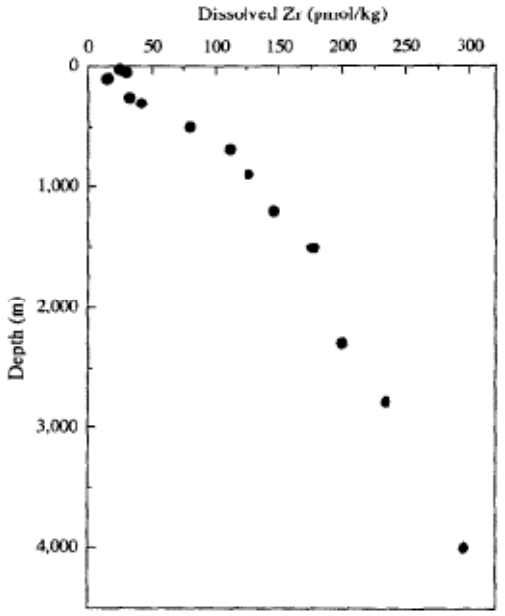

Figure 6. Vertical profiles of Zr in the central North Pacific (16°N, 168°W). The data points at 100m at 1500m were plotted (McKelvey and Orians 1993).

Due to more precise measurements the next reported dissolved zirconium values in seawater of the Indian and Atlantic Ocean were a hundred times lower than the ones reported before: 80-2400 pmol L^{-1}. This time they used isotope dilution mass spectrometry (IDMS) (Boswell and Elderfield 1988).

To measure the ultratrace Zr amount in seawater McKelvey, Firdaus and others used mostly isotope dilution coupled plasma mass spectrometry (ID-ICP-MS) in the last 15 years (McKelvey and Orians 1998; Firdaus et al. 2007). With this method the first depth profile of dissolved Zr in the North Pacific was gathered which is shown in Figure 6 (McKelvey and Orians 1993). This data was also used for the compiled periodic table of the chemical elements with their vertical profiles in Figure 3 (Nozaki 1997). In Figure 6 it can be seen that in the surface water there is quite a variability and a depletion of Zr in the first 100 m of the water column (12-95 pmol L^{-1}). With depth the Zr concentration increases nearly linearly until a maximum of 300 pmol L^{-1} which is reached in a depth of 4km.

The reported range of Zr values in the North Pacific has been confirmed by further measurements in Figure 7 (Firdaus et al. 2008).

Dissolved (D-) Zr concentration increases with depth and its concentration is in the range from 31-275 pmol L^{-1} (Firdaus et al. 2008) which is in a good agreement with the D-Zr concentration 12-300 pmol L^{-1} that can be seen in Figure 7 (McKelvey and Orians 1993). The same data field of the western North Pacific had also been published (30-250 pmol L^{-1}) by the same group (Sohrin et al. 1998a) that is shown in Figure 8 and will be explained further down.

Figure 7 shows that 10-14 % of Zr in seawater is labile particulate (LP-) Zr (dark triangles). This LP-Zr concentration is nearly constant from the surface to 3000 m and 1500 m respectively, then shows an increase with depth and also the percentage of LP-Zr rises with it. The particulate phase here is defined as those particles in a

seawater sample which do not pass through a 0.2 µm filter. An acidified seawater sample minus the D-portion represents the labile particulate part of the sample.
In Figure 7 the dissolved D-Zr (black surrounded circles) increases with depth (Firdaus et al. 2008).

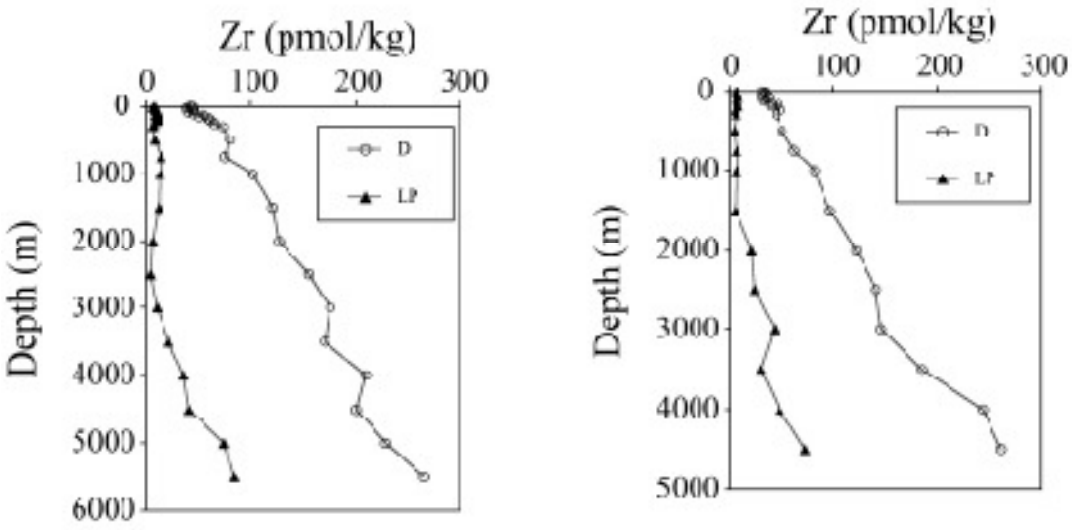

Figure 7. Labile particulate LP- (dark triangles) and dissolved D-Zr (black surrounded circles) distribution as a function of the water column depth in the Western North Pacific at two different stations at 51° N, 165° E and 35° N, 160° E (from left to right) (Firdaus et al. 2008).

Figure 8 shows the comparison of the measured depth profiles of Zr in the Northeast Atlantic (left) (Godfrey et al. 1996). In the right figure the dissolved niobium distribution versus depth in the Northwest Pacific can be seen (Sohrin et al. 1998a).
It shows that the Zr concentration ranges from 20 pmol L^{-1} at the surface to 240 pmol L^{-1} in deep water which is also in good agreement with the other data of the North Pacific published by (McKelvey and Orians 1993; Firdaus et al. 2006; Firdaus et al. 2008).
The left graph in Figure 8 represents a vertical depth profile of dissolved Zr in the northeastern Atlantic (47-50° N, 7-14° W, 50-4,500 m depth of water) and it shows that the Zr level increases from 81.1 pmol L^{-1} to 167 pmol L^{-1} (Godfrey et al. 1996). The Zr concentration is higher near the surface and lower in the bottom water than in the North Pacific. The total concentration range in the Northeastern Atlantic is smaller than in the data of the North Pacific. Godfrey et al. stated that this vertical profile of D-Zr indicates a nutrient-like scavenging behaviour, notwithstanding that below the nutricline there are big dissimilarities with silicate and nitrate.

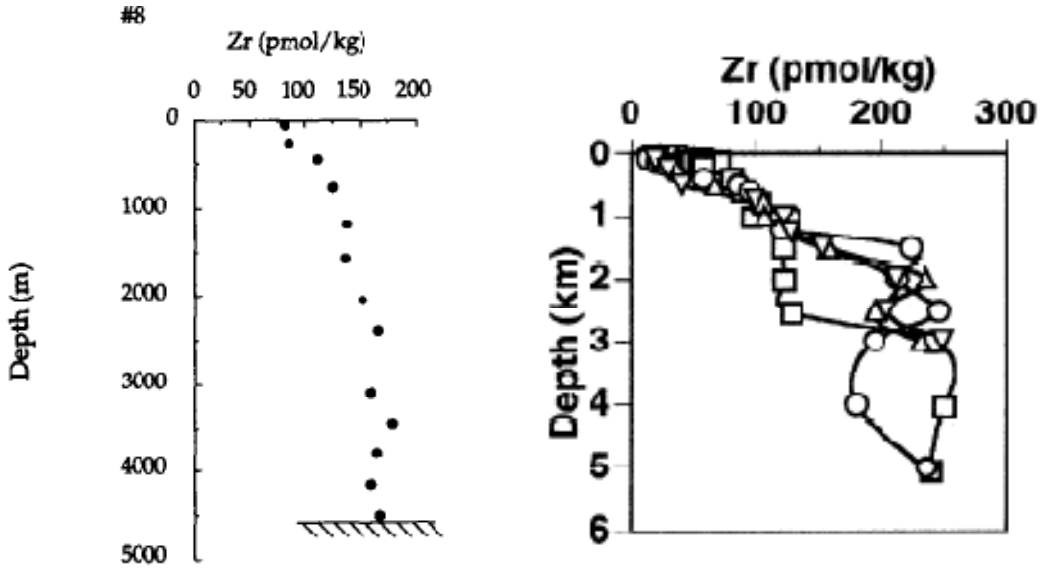

Figure 8. At the left hand side: Vertical depth profile of Zr in the Northeastern Atlantic (47°-50° N, 7°-14° W, 50-4,500m depth of water) (Godfrey et al. 1996).

At the right hand side: Dissolved Nb distribution versus depth in the Northwestern Pacific at different stations (25°-45° N and 139°-165° E) (Sohrin et al. 1998a).

The main oxidation state of dissolved Zr in seawater is +4 and the inorganic species are believed to be $Zr(OH)_4$ and $Zr(OH)_5^-$ (Turner et al. 1981). It has been calculated that over a wide pH-range the form $Zr(OH)_4$ is dominating, as long as there are no strong other ligands like F^-, SO_4^{2-} (Aja et al. 1995). On account of speciation calculations Byrne stated that Zr(IV) and Hf(IV) are strongly hydrolyzed in seawater and that the dominating form at this pH is $Zr(OH)_5^-$ (Byrne 2002).

The calculated residence time for Zr in seawater is 5,000 years (Broecker and Peng 1982). If you compare the behaviour of Ti, Zr and Be in seawater, Zr ranges in between Ti and Be. As a result McKelvey stated that the residence time of Zr also ranges in between the residence time of titanium and beryllium which means somewhere between a few hundred years (like Ti) and 3,000 years (like Be) (McKelvey and Orians 1993). Because of their results Godfrey et al. estimated a shorter residence time than Broecker and Peng (1982), but in agreement with McKelvey and Orians (1993) (in between 1,000 yr and 3,000 yr) (Godfrey et al. 1996).

The range of the Zr/Hf ratio is from 237 to 385, but in comparison to their ratio in continental crust, it is higher and more fluctuating (Firdaus et al. 2006). The dissolved Zr/Hf ratio, as well as the dissolved Nb/Ta ratio increase with the following order: continental crust, stream water, coastal seawater, seawater from the open North Pacific which was shown by Firdaus et al. The Zr/Hf ratio differs in abundance of the

origin of the water mass and therefore with the Zr/Hf ratio water masses can be traced throughout the Ocean (Firdaus et al. 2008).

In the upper continental crust the abundance of Zr is between 2,080 µmol kg^{-1} (0.019 %) (Taylor and McLennan 1995) and 1,120 µmol kg^{-1} (Rudnick and Gao 2003) and hence it is the twentieth most abundant element.

In rocks the Zr concentration depends highly on the type of rock. The Zr values can be lower than 220 µmol kg^{-1} in ultramafic rocks, can have intermediate values (1100-5500 µmol kg^{-1}) in andesites and trachytes or even be higher than 11,000 µmol kg^{-1} in granites (Aja et al. 1995). But the two most important Zr-bearing minerals are zircon ($ZrSiO_4$) and baddeleyite (ZrO_2) which are mostly accompanied by 1-2 % of Hf (Hall and Pelchat 1993). Zircon is very resistant to physical and chemical weathering (McKelvey and Orians 1993) and hence Zr is often used as a weathering index when studying other elements. Zirconium as the main compound of zircon was even found in samples of Western Saharan dust collected on Barbados (Gorbushina et al. 2007).

3.2 Hypothesis and objectives

The focus of this study is on electrochemical and spectrochemical investigations of both Niobium and Zirconium complexes in seawater. Currently all published works have treated the investigations of Nb and Zr at higher concentrations (µmol L^{-1}) than found in seawater where dimeric and higher order species may exist. Subsequently very little is known about the actual speciation in seawater and the potential for organic complexation. Thus the development of methods for determining Niobium and Zirconium speciation in seawater at nmol L^{-1} or pmol L^{-1} concentrations is urgently required. A further goal in this work was that the developed methods might also be easily practicable on a research vessel.

The marine chemistry of niobium and zirconium is not well known. As mentioned before niobium and zirconium belong to the “high field strength elements” (HFSE) (Barth et al. 2001) which might be, together with the alkali elements, linked to the detrital phase in the marine sediments (Plank and Langmuir 1998). The HFSE elements might also be good oceanographic tracers (McKelvey and Orians 1998). Especially the Zr/Hf ratio can be used as a tracer for the water’s age and as a tracer for the water masses (Godfrey et al. 1996).

Niobium and zirconium, together with their two adjacent elements tantalum and hafnium, are classified as “refractory metals” in seawater (McKelvey and Orians 1998). Probably in seawater they exist as hydroxides (Turner et al. 1981).
The main oxidation state of niobium in seawater is most likely +5. The dominating species might be $Nb(OH)_6^-$, $Nb(OH)_5$ and/or the corresponding oxyanion (Greenwood and Earnshaw 1990; Sohrin et al. 1998a). Notwithstanding little is known about the definite speciations.

1. Objective: An easy, quick and relatively cheap method for the detection of Nb(V) in seawater is necessary. ID-ICP-MS, AAS and AES are a lot more time consuming and expensive. Hence an existing voltammetric method to detect Nb(V) in aqueous solutions was modified for seawater measurements based on new findings related to Ti chemistry using the same ligand.

2. Objective: The development of a spectrophotochemical method to detect Nb(V) in seawater.

3. Objective: Nb(V) is present in seawater at ultratrace levels. Little is known about the speciation of Nb in seawater. Therefore it was a goal by using electrochemical and spectrochemical methods to determine which species are dominant under seawater conditions.

4. Objective: Our present knowledge of Zr(IV) speciation in seawater is also very limited. As many of the analytical reagents used for Nb also coordinate Zr it was thought prudent to also test the same analytical schemes as used for Nb for Zr.

4 Material and methods

4.1 Instrumental section

4.1.1 Polarography/Voltammetry

The artificial term voltammetry is created out of the words Volt- and Amperometry.
In polarography and voltammetry a continuously increasing voltage is applied to the used working and reference electrodes. The resulting current depends on the concentration of the analyte. It changes due to the reduction, oxidation or adsorption of the analyte on the surface of the electrode. This signal of the current (I) is plotted as a function of the voltage (U), the so called current-voltage curve. This permits sensitively quantitative and a qualitative determination of trace and ultratrace amounts of metals. This method is based on the different electrochemical potentials of the redox system. For the qualitative determination the peak position and for the quantitative determination the dependency of the peak current on the concentration of the electrolyte in the sample is used.

Figure 9. Voltammeter VA757 (Metrohm 2008)

Today common voltammeters - an example can be seen in Figure 9- consist of a three electrode system with a working electrode (WE), a reference electrode (RE) and, in addition, an auxiliary electrode (AE) also called the counter electrode. The setup is illustrated in Figure 10.
The analytically interesting redox process occurs at the WE in a polarographic or voltammetric cell. The most commonly used WE is a mercury electrode. A special kind of polarizable microelectrodes (WE) are rotating disc electrodes (RDE) for kinetic or mechanistic analysis.

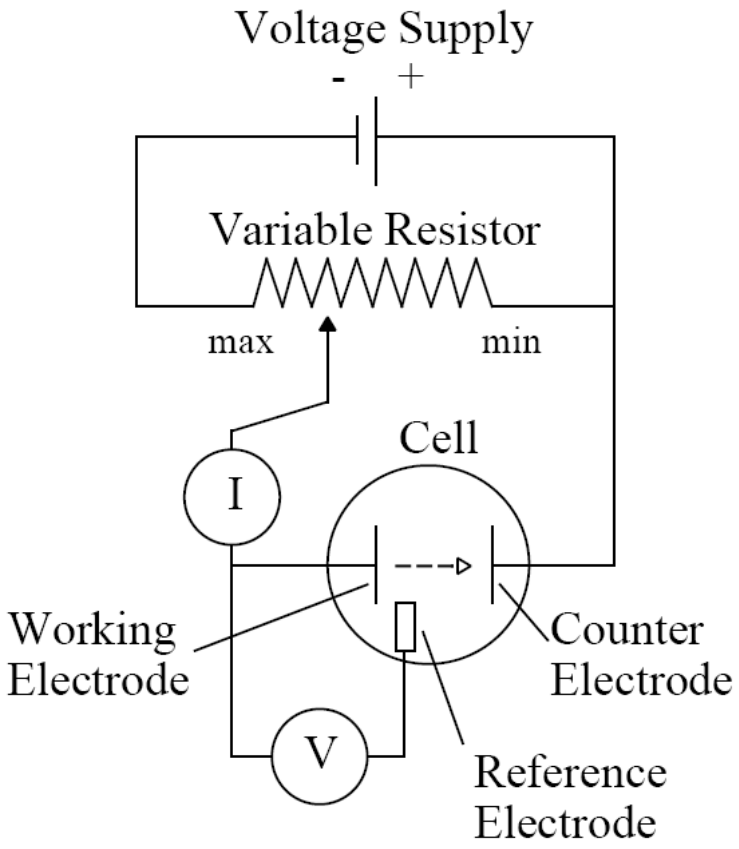

Figure 10. Schematic diagram of a voltammetric/polarographic setup with three electrodes (Bard and Faulkner 2001).

The RE has to be unpolarizable which means that the voltage must not change with the flowing electric current. RE are electrodes of the 2nd order which can be e.g. a calomel-KCl ($Hg/Hg_2Cl_2/KCl_{sat}$) or a silver/silverchloride ($Ag/AgCl/KCl_{3\ M}$) electrode.
The material of the AE should be conductive but chemically and electrochemically inert. Mostly platinum or glassy carbon electrodes are used.
In the cell should be a supporting electrolyte that is e.g. an alkali salt which does not react with the electrodes, but that has conductivity (seawater is a perfect electrolyte in this sense).
The difference between polarography and voltammetry is the type of working electrode which is used. According to the IUPAC ("International Union of Pure and Applied Chemistry") definition: voltammetry refers to work with a stationary or moveable hard electrode in contrast to polarography that implies the work with a solvent WE whose surface is continuously or periodically renewed (Irving et al. 1978; Rach et al. 1985). Dropping mercury electrodes (DME) and hanging mercury electrodes (HMDE) are widely used as WE. The advantages of the Hg-electrodes are that it is easy to generate a clean surface and due to the high Hg overvoltage it is

possible to measure even metals with high standard potentials without H_2 formation at the electrode. Disadvantages are that the Hg is easily oxidized and that Hg is toxic. In a stirred sample cell (hydrodynamic voltammetry) a diffusion layer, also called the Nernst diffusion layer, which has a thickness of 0.1-0.01 mm is formed near the electrode. In the simplest electrode reactions the mass-transfer-processes (migration, duffusion and convection) are far slower than the rates of the associated chemical reactions. In this case the homogeneous reactions can be regarded to be in equilibrium and the surface concentrations faradic species are connected to the electrode potential by the Nernst-equation.

The Nernst-equation demonstrates the connection between the potential E and the chemical activity a_i of the relevant species i.

$$E=E^0-\frac{R\cdot T}{n\cdot F}\cdot \ln(a_i) \tag{4.1}$$

$$E=E^0-\frac{R\cdot T}{n\cdot F}\cdot \ln\left(\frac{a_{ox}}{a_{red}}\right) \tag{4.2}$$

E^0 Standard potential of the electrode for $a_i = 1$

R 8.314472 J K^{-1} mol^{-1} is the universal gas constant

T Absolute temperature in Kelvin

n Number of electrons involved in the cell-reaction $O + n\ e^- \rightleftharpoons R$

F 9.64853 x 10^4 C mol^{-1} is the Faraday-constant

N Nernst-factor = 2.303 x (RT/F)

a Chemical activity

c Concentration

$$E = E^0-2.303\cdot\frac{R\cdot T}{n\cdot F}\cdot \log\left(\frac{a_{ox}}{a_{red}}\right) \tag{4.3}$$

$$E = E^0-\frac{N}{n}\cdot \log\left(\frac{a_{ox}}{a_{red}}\right) \tag{4.4}$$

Formulae 4.1-4.4 all refer to the standard potential and the chemical activity of the electroactive species.

The half wave potential ($E_{1/2}$) is the potential of the working electrode at which the polarographic step of the depolarizer is half-finished. Due to the half wave potential an electroactive species can be identified in a characteristic medium.

The concentration of the electroactive species can be determined due to the fact that the limiting current (I_c) is proportional to the concentration of the analyte (c_a):

$$I_c = k \cdot c_a \quad (4.5)$$

Polarography and voltammetry are split into direct current (DC) and alternating current (AC) methods, which can be combined with stripping voltammetry (SV). Important types are e.g. direct current polarography (DCP), differential pulse polarography (DPP), square-wave voltammetry and cyclic voltammetry (CV) (Eisenhardt 1991; Atkins 2001; Bard and Faulkner 2001; Wang 2006).

4.1.1.1 Differential pulse polarography (DPP)

In principal differential pulse polarography (DPP) is a combination of direct current polarography (DCP) and pulse polarography (PP) and is somewhat limited by nonfaradaic currents. The sensitivity of this method is increased by the electric current which is not measured throughout the whole lifetime, but shortly before the pulse increases and at the end of drop lifetime. This means that the current is measured twice in a single drop in a special time slice and that the differences of the measured currents are plotted as a function of the direct voltage. In the final spectra no steps are obtained but current peaks, and at the maxima is the half wave potential $E_{1/2}$. The peak current is direct proportional to the concentration (Rach et al. 1985; Bard and Faulkner 2001).

4.1.1.2 Cathodic Stripping Voltammetry (CSV)

Cathodic stripping voltammetry (CSV) is a special case of stripping voltammetry (SV). SV are the most sensitive voltammetric analytical procedures. CSV is used to determine a great variety of organic and inorganic species (mostly anions) that are able to form insoluble salts which can be enriched on the material of the working electrode. This requires usually that the WE is an Hg-electrode. The electrochemically enriched species builds a hardly soluble film on the surface of the WE. Because of the Nernst-equation the less soluble the film is, the more negative is the voltage at which the material of the electrode is oxidized. After this preconcentration step the deposit is stripped off and measured during a cathodic

potential scan. At higher concentrations of the enriched species, because of a surface saturation, sometimes a nonlinearity in the measurement is evolved (Rach et al. 1985; Wang 1985; Bobrowski and Zarebski 2000; Powell et al. 2000).

4.1.1.3 Apparatus

A Metrohm 757 VA Computrace which can be seen in Figure 11 is a three-electrode system typically used with a small-sized HMDE as a WE, a platinum wire auxiliary electrode and an Ag/AgCl (in 3 mol L^{-1} KCl) reference electrode to which the reported potentials were referred. The cell in which the sample is measured is a Teflon cup.

Figure 11. Metrohm 757 VA Computrace.

The used working parameters typically were:
Deposition time: 1 min
Deposition potential for Nb: from -0.2 V to -1.2 V
Deposition potential for Zr: from -0.2 V to -1.4 V
Preconcentration potential: -0.2 V
Pulse amplitude: 0.05 V
Pulse time: 0.01 sec
Voltage step: 0.002 V
Voltage step time: 0.1 sec
Sweep rate: 0.0200 V/sec
Stirring rate: 2,000 rpm

The determination method for Nb and Zr is based on differential pulse cathodic stripping voltammetry (DPCSV).
Deaeration was performed for 4min with nitrogen of high-purity grade, before each experiment that was performed under nitrogen atmosphere. All the experiments were obtained at R.T. (21 °C).

4.1.2 Spectrophotometry

Spectrophotometric methods, also called absorptiometry, are widely used in chemical analysis of metals. The determinable metals are complexed by chelates with which they form different coloured solutions and hence absorb light of different wavelengths. The absorbance is measured in both the UV- (1-380 nm) and visible part (380-750 nm) of the electromagnetic spectrum. A photoelectric cell measures the light which passes through the cell containing the solution. The absorbance is plotted as a function of the wavelength.

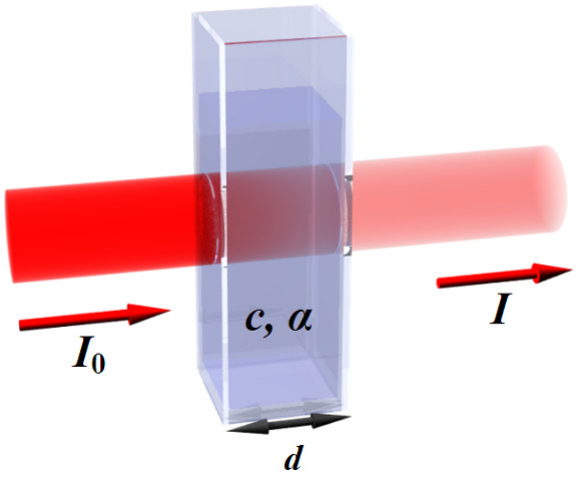

Figure 12. The law of Lambert-Beer says that the intensity of electromagnetic light of a special wavelength decreases exponentially with the concentration (c) of the absorbing species in the sample and the thickness of the sample (d).

According to the law of Lambert-Beer (formulae 4.5 and 4.6), which is the fundamental law of spectrophotometry, the intensity of a light beam decreases exponentially on its way through a sample.

$$I = I_0 \cdot e^{-\varepsilon \cdot c \cdot d} \tag{4.5}$$

$$A = \ln \frac{I}{I_0} = \varepsilon \cdot c \cdot d \tag{4.6}$$

I_0 Intensity of the incident light beam

I Intensity of the transmitted light beam

T Transmittance = I/I_0

ε A constant, the molar extinction coefficient which depends on the wavelength of the light, the temperature and upon the solvent

c concentration of the metal atoms in the sample that form a coloured complex

d Pathlength of the travelling light through the cuvette

A Absorbance of the sample, extinction

Transmittance (T) is the I_0 entering the cell divided by the intensity of the light beam leaving the cell (I) which is illustrated in Figure 12. The light which is transmitted by the cell which contains the coloured sample is in practice compared against the same cell containing just water or reagent as a blank. When multiplying c by d the mass of the light-absorbing substance in a column cross-sectional area can be calculated. The extinction of the light beam is proportional to the concentration of the metal atoms in the sample(Sandell 1959; Atkins 2001).

4.1.2.1 Apparatus

The spectrophotometer used here was an Ocean Optics USB4000 Miniature Fiber Optic Spectrometer for UV-VIS which can be seen in Figure 13.

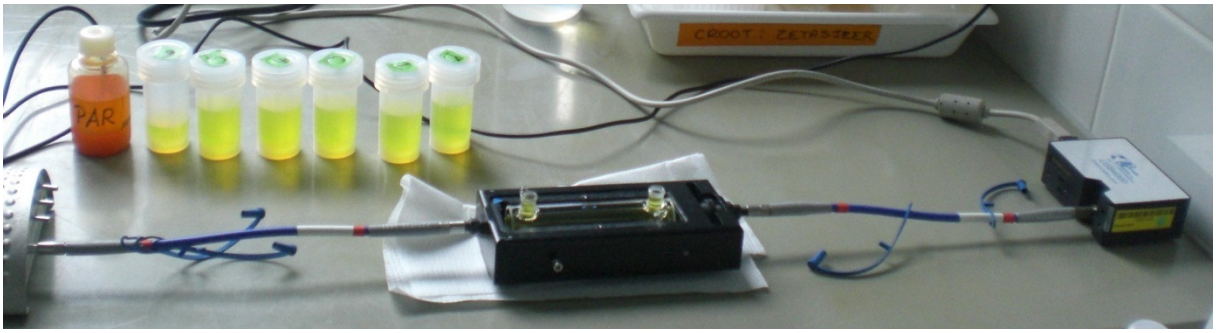

Figure 13. Ocean Optics USB4000 Miniature Fiber Optic Spectrometer for UV-VIS with a coloured sample set. From left to right: light source, optical fibre, cell holder with a 10.000 cm quartz cuvette, optical fibre and detector with a connection to the computer.

The apparatus is constructed out of: a light source, an optical fibre, a cell holder with a cuvette, a second optical fibre and a detector which relays the signal to a computer. The light source is a Micropack DT-Mini-2-GS which is applicable for measurements in the UV-VIS-NIR range as it contains both deuterium and halogen lamps. The electrical dark-level is corrected for and the wavelength range from 200 nm to 1,100 nm can be recorded using the USB4000 as the detector.

In the beginning a 1 cm quartz cuvette was used, then for the approach of measuring lower concentrations of Nb a 10 cm quartz cuvette (QS) was used which is shown in Figure 13 and Figure 14.
The blank which is compared to the samples was cleaned ultrapure Milli-Q (MQ) water.

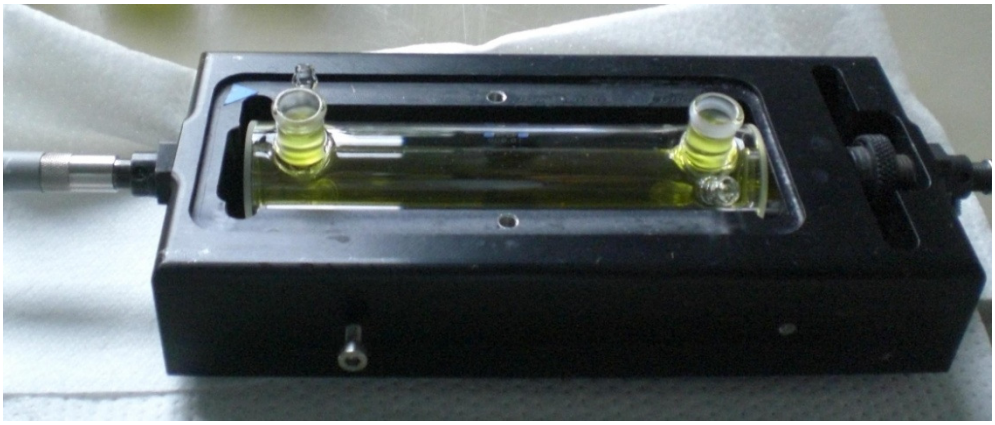

Figure 14. Cell holder and a 10 cm quartz cuvette with a coloured sample.

4.2 Reagents

All solutions were prepared with water that was cleaned in a Millipore Milli-Q water purification system.
Acids used for trace metal analysis were all quartz distilled.
All the chemicals were of analytical grade and were used without further purification.
The cupferron (benzenamine, *N*-hydroxy-*N*-nitroso-ammonium salt) was purchased from Sigma-Aldrich and stored at 4°C. At least every two weeks a fresh 0.1 mol L^{-1} solution was prepared by dissolving in 16.1 mL water.
53.8 mg 4-(2-pyridylazo) resorcinol (PAR) (Sigma-Aldrich) were dissolved in 50 mL water in a Teflon Bottle for a 5 mmol L^{-1} solution.
The BPHA (*N*-benzoyl-*N*-phenylhydroxylamin) was acquired from Sigma-Aldrich. A 0.1 mol L^{-1} solution was set up by solubilizing 0.25 g in 11.7 mL methanol.
1.5 mg potassium bromate ($KBrO_3$) (Sigma-Aldrich) was dissolved in 25 mL water for a 0.36 mmol L^{-1} solution.

The niobium atomic absorption standard solution (Aldrich) contains 11.09 mmol L^{-1} (1,030 ppm) of Nb in H_2O. The dilute 11.09 µmol L^{-1} Nb solutions were prepared for the spectrophotometry before every measurement containing 1 % distilled HCl (25 %).

The ammonium niobate(V) oxalate hydrate was on a 99.99 % metals basis. Stock solution (11.09 mmol L^{-1}) of Nb(V) was prepared by dissolving 67.2 mg $C_4H_4NNbO_9 \cdot xH_2O$ (Sigma-Aldrich) in water in a 100 mL volumetric flask.

The zirconium atomic spectroscopy standard solution Fluka (Aldrich) contains 10.96 mmol L^{-1} (1,000 ppm) Zr and was prepared with $ZrOCl_2$ and HCl (~2 mol L^{-1}).

The 0.1 mol L^{-1} and 1 mol L^{-1} acetate buffer solutions were prepared from sodium acetate (Merck) and acetic acid (J. T. Baker).

The biological "Good's" buffers MES (2-(N-Morpholino)ethanesulfonic acid hydrate), PIPES (1,4-Piperazinediethanesulfonic acid disodium salt) and EPPS (4-(2-Hydroxyethyl)-1-piperazinepropanesulfonic acid) were all purchased from Sigma-Aldrich. For the 1 mol L^{-1} MES and the 1 mol L^{-1} EPPS solutions the acids were dissolved in water and 1 mol L^{-1} NH_3 solution. For the 1 mol L^{-1} PIPES the disodium salt was dissolved in water and adjusted to the right pH with conc. HCl (Good et al. 1966; Zhao and Chasteen 2006)

4.2.1 Seawater

The used seawater (SW) was taken on the third leg of the 68th Meteor expedition in the tropical eastern north Atlantic in July 2007. Therefore it is called SW M68-3.

4.2.2 Carrier Gas

The compressed nitrogen was of high-purity grade (Air Liquide 5.0) and is used to purge dissolved oxygen from solutions.

4.3 pH meter

Electrochemical pH measurements are done with a pH meter "WTW Ino Lab Series pH 720" with a glass electrode and it is calibrated monthly with standard pH buffers (NBS).

4.4 Electrochemical and spectrochemical methods of Niobium determination

4.4.1 Voltammetric/Polarographic Nb determination

Most polarographic/voltammetric studies of Nb in the 1950's were done at low pH and sometimes even in very strong mineral acids like in 12 mol L^{-1} hydrochloric acid which is shown in Figure 15 (Cozzi and Vivarelli 1953; Elving and Olson 1956a) or in slightly acidic milieu in the presence of strong complexing agents like ethylenediamine-tetra-acetic acid (EDTA) which can be seen in Figure 16 (Ferrett and Milner 1955; Ferrett and Milner 1956; Kennedy 1961; Kirby and Freiser 1963).

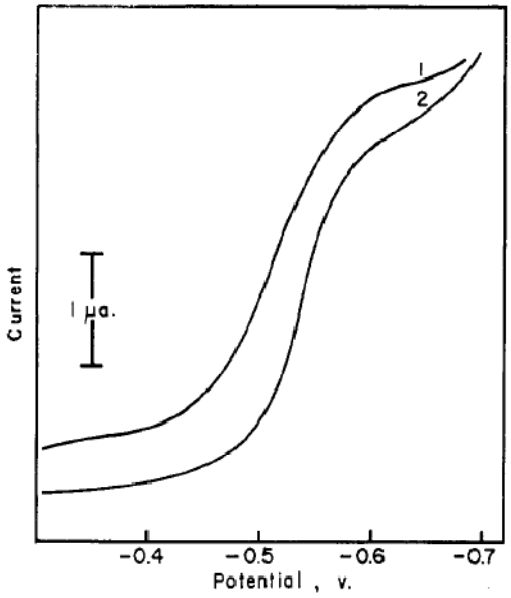

Figure 15. Polarogram (Elving and Olson 1956a) for 1.16 mmol L^{-1} in

1. 12 mol L^{-1} hydrochloric acid
2. 9 mol L^{-1} sulfuric acid

The irreversible reduction from Nb(V) to Nb(IV) was shown in nitric, sulphuric and hydrochloric acid, in tartrate and oxalate solutions (Cozzi and Vivarelli 1953; Elson 1953) and references included within these papers.

Due to the tendency of Nb to hydrolyse quickly in solutions, Nb was e.g. dissolved in concentrated hydrochloric acid to prepare a standard solution for the polarographic measurements. In a square-wave polarogram $E_{1/2}$ = -0.54 V is obtained against a mercury-pool anode (Ferrett and Milner 1956).

With direct current polarography (DCP) it is possible to detect 200 µmol L^{-1} Nb in 12.5 mol L^{-1} HCl in one step at $E_{1/2}$ = -0.46 V vs. SCE which is the reversible Nb(V) to Nb(IV) reduction. The sensitivity of the polarographic measurement is increased by adding hydroxylamine (NH_2OH) to the concentrated HCl solution or by adding a strong complexing agent like EDTA (Henrion and Adler 1975).

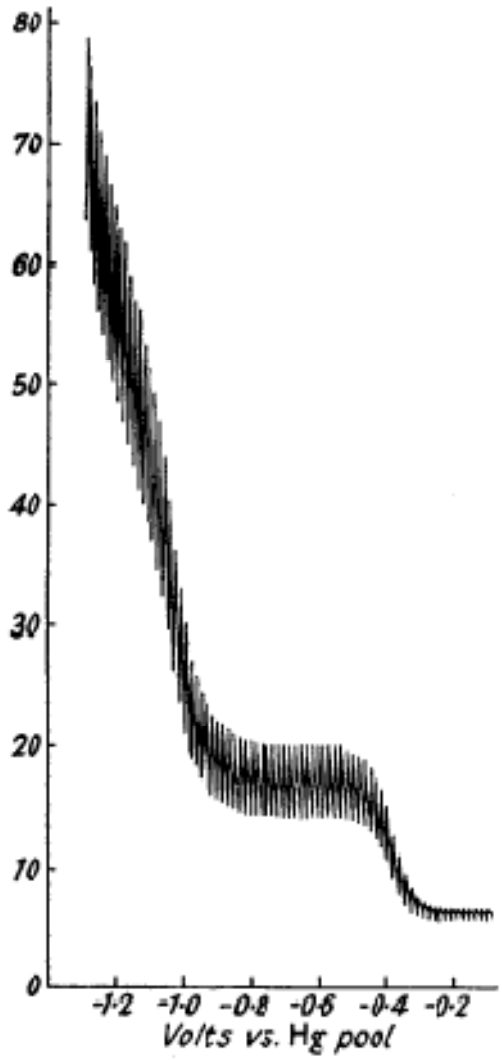

Figure 16. Nb-Polarogram in 0.1 mol L^{-1} EDTA, pH 3.1 with a Nb content of 1.62 mol L^{-1} (Ferrett and Milner 1956).

Figure 16 shows the reduction of Nb in EDTA at pH 3 produces two steps with $E_{1/2}$ = -0.61 V and -1.05 V versus a SCE (Ferrett and Milner 1955; Ferrett and Milner 1956). These half-wave potentials are very similar to the ones observed by Kennedy in EDTA: $E_{1/2}$ = -0.60 V and -0.95 V versus a SCE at pH 3 (1961). The first half-wave potential increases with the rising pH (from 2 to 4.8) and the second half-wave potential cannot really be observed because of the interaction with the hydrogen reduction wave. Below pH 3 the acid precipitates from solution and therefore the EDTA concentration is lower at pH 1-3 than at pH 3-5. Above pH 5 niobium precipitates out from EDTA-solution. If there is a reversible one-electron reduction the inverse slope should be 0.059 (Ferrett and Milner 1955; Ferrett and Milner 1956; Kirby and Freiser 1963). Table 2 shows that this seems to be the case below pH 3.2.

Table 2. pH-depending half-wave potentials for Nb in EDTA

pH	EDTA (in mmol L^{-1})	$E_{1/2}$	inverse slope*
1.1	1	-0.427	0.065
2.0	1	-0.419	0.060
3.0	1	-0.572	0.065
3.1	10	-0.609	0.059
3.2	10	-0.613	0.062
3.4	10	-0.615	0.069
3.6	10	-0.657	0.072
4.1	10	-0.767	0.100
4.8	10	-0.835	0.086

*inverse slope (=0.059/n) of U vs. $I/(I_d-I)$ with n=number of reversible electron exchange (Ferrett and Milner 1956)

At pH 4.5 in 0.01 mol L^{-1} EDTA two reduction waves were found and the first one was reversible: $E_{1/2}$ = -1.00 V and -1.40 V against Ag/AgCl (Gomes and Franco 1995). With DPP and against a DME using these amounts of analytes niobium can be quantified in pyrochlore ores $(Na,Ca)_2(Nb,Ti,Ta)_2O_6(OH,F,O)$ in a pH range between 2 and 5 in concentrations from 17-93 µmol L^{-1} (Lichtig and Andrade 2001).

The Nb-citrate complex is more stable than the Nb-EDTA complex. Ferrett and Milner observed at pH 4 in 2 mol L^{-1} citric acid $E_{1/2}$ = -1.13 V against a SCE. This one step wave was the reduction from Nb(V) to Nb(IV). In lower concentrations of citrate than 2 mol L^{-1} they could not observe any wave and advised pH 1 for further polarographic measurements of Nb (Ferrett and Milner 1956). Comparable results were found by Kennedy in 1 mol L^{-1} citric acid wherein the half-wave potential is $E_{1/2}$ = -0.95 ± 0.01 V versus a SCE (Kennedy 1961). The slightly more negative half-wave potential which was found by Ferrett could be due to the fluoride ions in the solution. Nb(V) and Nb(IV) are complexed with the same number of citrate ligands and the electroactive species takes a long time (2,000 min) to develop (Boodts et al. 1986).

Nb(V) is reduced in oxalate solutions to Nb(IV) which gives $E_{1/2}$ = -1.53 V and then to Nb(III) which gives a second step with $E_{1/2}$ = -2.18 V against a saturated calomel electrode (SCE) (Elson 1953). With a DME no signal could be observed for Nb in oxalate solutions (Ferrett and Milner 1956).

Nb peroxide complexes are stable in solution and the dominant complex varies with pH: in basic solutions the 4:1, in weak acids the 1:1 and in stronger acids the 2:1 complexes predominate (Adler and Hiskey 1957b; Adler and Hiskey 1957a). The optimum condition for the polarographic Nb-peroxide determination vs. SCE is with a fresh 0.01-1 mol L^{-1} peroxide solution at pH 5 and 400 µmol L^{-1} Nb can be detected. The measurements are possible in a pH range from 2 to 7 (Kennedy 1960).

4.4.1.1 Voltammetric/Polarographic Nb determination with cupferron, the ammonium salt of N-nitroso-N-phenylhydroxylamine

Cupferron has widely been used for the quantitative precipitation and separation of Nb from Ta and steel alloys (Majumdar and Ray Chowdhury 1958; Reed 1963).

Cupferron is also called benzenamine, *N*-hydroxy-*N*-nitroso-ammonium salt and ammonium *N*-nitrosophenyl-hydroxylamine. Structure 1 shows the structure of cupferron which is a strong chelating agent and can be used for the determination of

a number of trace metal ions amongst others for Cu, Fe, Ti, V and Nb by optical measurements and gravimetric methods (Kolthoff and Sandell 1952). Cupferron binds with two oxygen atoms to the metal cations and it forms preferably five-membered rings.

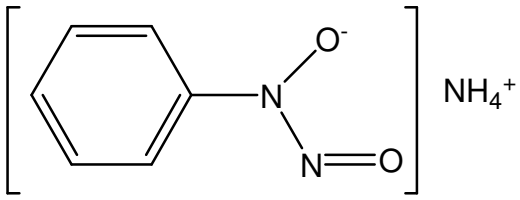

Structure 1. Ammonium *N*-nitrosophenylhydroxylamine whose trivial name is cupferron.

In cold water cupferron forms with hydrous niobium(V) oxide a white precipitate which was identified after recrystallization from ethanol as the neutral complex oxytris (N-phenyl-N-nitrosohydroxylamino) niobium(V) $[NbO(C_6H_5N_2O_2)_3]$ (Land and Sanchez-Caldas 1967).

Wang et al. (1992a) published a sensitive method to determine trace concentrations of Nb with cupferron. This method based on adsorptive stripping voltammetry was found to have a high sensitivity (Wang 1985; Wang 2006). Trace concentrations of Nb in water can be reduced and complexed by the ligand cupferron. The Nb-cupferron complex is enriched on the surface of a medium-sized HMDE at an accumulation potential of -0.2 V for 150 sec. As a supporting electrolyte and for the achievement of the right pH 4 the measurements are conducted in 0.1 mol L^{-1} acetate buffer at room temperature. The amount of the measured sample is 10 mL containing 5 µmol L^{-1} cupferron. The solution is purged with nitrogen for 8 min to deoxygenate the sample while stirring it. 15 sec after stopping the stirring they record the voltammogram by DPCSV. The applied scan rate is 10 mV/sec and recorded from -0.2 V to -1.2 V with a 25 mV amplitude. The well detectable amount of niobium in water with this method is 0.89 nmol L^{-1}. The well-defined Nb peak is observed at a peak position E_p = -0.97 V (Wang et al. 1992a).

4.4.1.2 Voltammetric/Polarographic Nb determination with cupferron and an oxidizing reagent

The combination of a catalytic reaction with an adsorptive accumulation on the electrode is called catalytic adsorptive stripping voltammetry (CAdSV). It is often used in combination with the sensitive DPP and this leads to a better selectivity and sensitivity of the determination of the electroactive species (Bobrowski and Zarebski 2000). Possible oxidizing reagents are NO_2^-, NO_3^-, H_2O_2, ClO_3^- and BrO_3^-. With cupferron (0.02 mmol L^{-1}) as a complexing and $NaBrO_3$ (6 mmol L^{-1}) as an oxidizing agent using DPP vs. HMDE the detection limit of vanadium is 4.9 pmol L^{-1} (Wang et al. 1992b).

In analogy to the vanadium-cupferron complex and its catalytic and adsorptive responses, the niobium-cupferron complex relies on:

$$Nb(V)Cupf_{solution} \xrightarrow{\text{accumulation}} Nb(V)Cupf_{surface} \quad (4.7)$$

$$Nb(V)Cupf_{surface} + e^- \rightarrow Nb(IV)Cupf_{surface} \quad (4.8)$$

$$6\ Nb(IV)Cupf_{surface} + BrO_3^- + 6\ H^+ \rightleftharpoons 6\ Nb(V)Cupf_{surface} + Br^- + 3\ H_2O \quad (4.9)$$

In the first reaction (4.7) the Nb-Cupf complex is accumulated from solution onto the surface of the HMDE. On the surface Nb is reduced from Nb(V) to Nb(IV) (4.8). In the third reaction (4.9) the Nb-Cupf complex is reoxidized by BrO_3^-. Due to this reaction Nb can be measured several times and the detection limit can be improved.

Using the same reagents but a mercury film coated glassy carbon electrode (MFGCE) V can be also detected in natural and seawaters (Greenway and Wolfbauer 1995).

4.4.1.3 Voltammetric/Polarographic Nb determination with N-benzoyl-N-phenylhydroxylamine (BPHA)

Structure 2 shows the structure of *N*-benzoyl-*N*-phenylhydroxylamine (BPHA) whose synonyms are *N*-Hydroxy-*N*-phenylbenzamide and *N*-Phenylbenzohydroxamic acid.

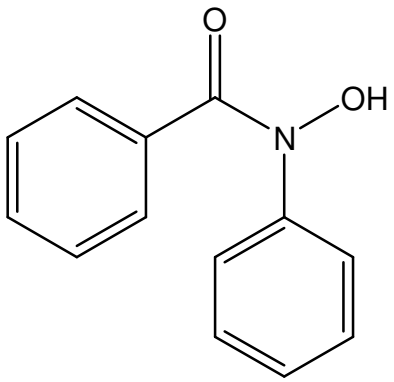

Structure 2. *N*-benzoyl-*N*-phenylhydroxylamine (BPHA)

Like cupferron BPHA has been used in the 1950's and 60's as a chelating resin for the separation of Nb and Ta in metals, alloys and rocks (Moshier and Schwarberg 1957; Majumdar and Mukherjee 1958; Majumdar and Pal 1961; Pobi and Das 1993). Nb forms a stable complex with BPHA of the composition $NbO(C_{13}H_{10}NO_2)_3$ and the Nb content can then be determined gravimetrically (Majumdar and Mukherjee 1959). Cupferron is unstable as a solid to UV-VIS light and in solution it is sensitive to heat. It decomposes to benzene and ammonia. Therefore other comparable hydroxylamines which are more stable and also strong chelators are interesting for the voltammetric/gravimetric determination of Nb in seawater. BPHA is more stable in air and heat than cupferron, but the disadvantage is that it is less soluble in water. The solubility of cupferron in water is 12 g/100 mL and the one of BPHA is only 0.04 g/100 mL, but it is easily soluble in organic solvents (Shendrikar 1969).

BPHA is a complexing agent for the polarographic determination of Ti(IV) and V(V). The half-wave potentials in 0.1-2 mol L^{-1} sulphuric solution were $E_{1/2}$(Ti) = -0.42 V and $E_{1/2}$(V) = -0.41 V to -0.50 V against a DME. In the range of +0.1 V to -1.0 V BPHA shows no polarographic activity (Donoson et al. 1975). Because of its stability and the possible determination of Ti(IV) and V(V), BPHA is a promising chelate for the voltammetric/polarographic determination of Nb.

4.4.2 Spectrophotometric Nb determination with 4-(2-pyridylazo)-resorcinol

Before the 1960's the knowledge of the spectrophotmetric determination of Nb was very limited. It was known that lots of elements of the 4th, 5th and 6th group of the PSE form coloured peroxy complexes in sulphuric acids (Palilla et al. 1953; Adler and Hiskey 1957b).

In the 1960's it was published that different reagents form coloured complexes with Nb and that they can be determined spectrophotometrically. One of these reagents was Xylenol Orange whose red coloured complex with Nb absorbes light at λ_{max} = 530 nm at pH 5.50 (Agarwala and Dey 1969). Other reagents were azo-dyestuffs which contain a *O*,*O*'-dioxyazo group. Reagents with such an analytical functional group are often used for spectrophotometric determinations and e.g. Lumogallion, Arsenazo and PAR belong to this group (Alimarin and Savvin 1966). PAR which is the abbreviation for 4-(2-pyridylazo)-resorcinol is shown in Structure 3.

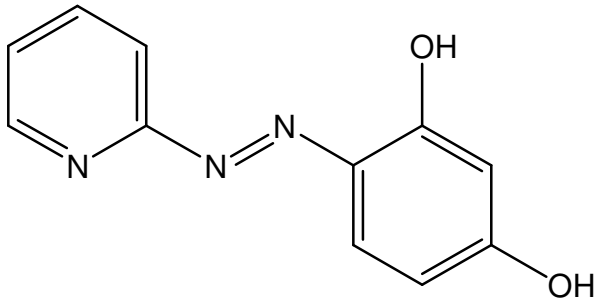

Structure 3. PAR which is the abbreviation for 4-(2-pyridylazo)-resorcinol

PAR is yellow in neutral and acid solutions which can be seen in the cell in Figure 14. It forms well detectable complexes with quite a lot of metal ions like Cd, Cu, Zr, Ti and Nb. The Nb-PAR complex exhibits in solution a red colour and according to Belcher et al. it is a 1:1 complex at pH 5.8 in a tartrate-buffered solution. The maxima of this complex occurs at λ_{max} = 550 nm with a molecular extinction coefficient ε(550 nm) = 38,700 and the detection limit is 1.08 µmol L^{-1} Nb. It takes 45 min for the colour of the Nb-PAR chelate to be generated. The measured absorption spectra can be seen in Figure 17 (Belcher et al. 1962b; Belcher et al. 1963).

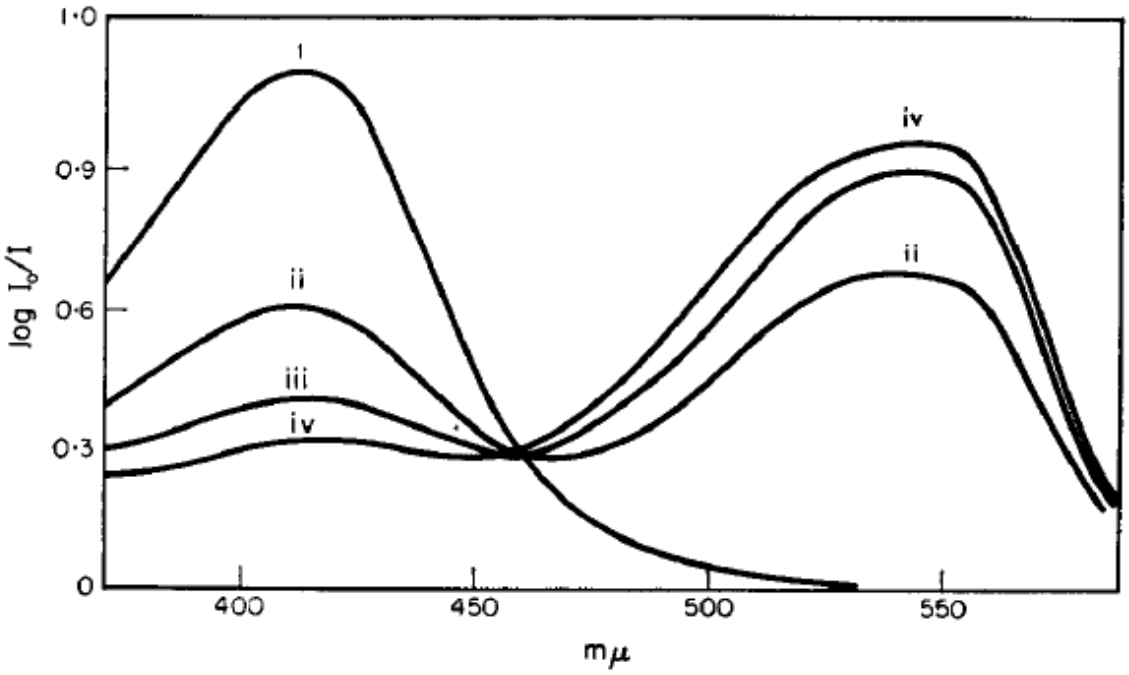

Figure 17. Absorption spectra of PAR and Nb-PAR at pH 5.8 with a 4 cm cell (Belcher et al. 1963).

(i) 10 mL 1 mmol PAR + 5 mL buffer

(ii) 10 mL 1 mmol PAR + 5 mL buffer + 5 mL 10^{-4} mol L^{-1} Nb-solution

(iii) 10 mL 1 mmol PAR + 5 mL buffer + 10 mL 10^{-4} mol L^{-1} Nb-solution

(iv) 10 mL 1 mmol PAR + 5 mL buffer + 15 mL 10^{-4} mol L^{-1} Nb-solution

The optimum pH is 6, but the spectrophotometric detection of the Nb-PAR in tartrate solution works in a broader range from 3 to 7 (Agarwala and Dey 1967).

Alimarin et al. stated that the colour is not only of the Nb-PAR complex, but of a ternary complex. This ternary complex can only evolve if a third compound like EDTA, tartaric, oxalic or citric acid is present in the solution (Alimarin and Savvin 1966).

In pH 5.5 oxalate-buffered solution the maximum absorption takes place at λ_{max} = 545 nm. The amount of PAR compared to the amount of Nb has an influence on the intensity of the coloured complex. The optimal ratio for Nb:PAR is 1:3 in oxalic solutions (Siroki and Djordjev 1971).

Yamada et al. (1988; 1990) used aqueous solutions buffered to pH 5.5-6.0 which contain 0.1 mmol L^{-1} PAR and either oxalate, citrate or tartrate. The equilibration time depends on the pH, but for Nb(V)-ox, Nb(V)-cit and Nb(V)-tart $\tau_{1/2} \leq 1$ min at pH 3-5. The spectra are recorded at λ_{max} = 550 nm.

$$\text{Nb(V)-L} + \text{PAR} \underset{k_2}{\overset{k_1}{\rightleftharpoons}} \text{Nb(V)-PAR} + \text{L} \qquad (4.10)$$

Equation 4.10 shows the substitution of the L(igand) which can be ox(alate), cit(rate) or tart(ate) for PAR. k_1 and k_2 are the conditional rate constants for the forward and the reverse reaction. The kinetics of this substitution is of first-order. In agreement with Belcher et al. (1962b) the formation of a 1:1 Nb:PAR complex at pH 5 in citrate was reported (Yamada et al. 1988; Yamada et al. 1990).

Yamada et al. (1988) stated that at pH lower than 4 a protonated 1:1 Nb:PAR complex is formed and that this complex has a smaller molar extinction coefficient than the complex which is not protonated at higher pH. At a higher pH the protonated complex releases a proton and the strongly coloured complex is formed. In reaction 4.11 the L(igand) can be citrate or tartrate. The colour reaction 4.12 shows the formation of the ternary complex with oxalate.

$$\text{NbO(L)(HPAR)} \rightleftharpoons \text{NbO(L)(PAR)}^- + \text{H}^+ \qquad (4.11)$$

$$\text{NbO(ox)}^{3-} + \text{H}_2\text{PAR} \rightleftharpoons \text{NbO(ox)(PAR)}^- + 2\text{H}^+ + 2\text{ox}^- \qquad (4.12)$$

Table 3 shows the determined data by Yamada et al. (1990). They used the following concentrations: c(PAR) = 0.1 mmol L^{-1}, c(Nb) = 10 µmol L^{-1}, c(ox) = 1-10 mmol L^{-1}, c(cit) = 15-20 mmol L^{-1}, c(tart) = 0.2-1 mmol L^{-1}. Changes in the ligand concentration did not influence the reaction. The determined molar absorptivity data were used in further calculations of the expected absorptions.

Table 3. Thermodynamic parameters for the colour reaction with PAR at 25°C, d = 0.1 cm and 550 nm (Yamada et al. 1990).

Nb(V)-L	log K	ε_{mol} (PAR) in mol^{-1} dm^3 cm^{-1}	ε_{mol} (HPAR) in mol^{-1} dm^3 cm^{-1}
Nb(V)-oxalate	-10.05	25,500	
Nb(V)-tartrate	-4.59	39,400	2,280
Nb(V)-citrate	-5.16	34,400	480

4.5 Electrochemical methods of Zirconium determination

Zirconium is difficult to detect by polarography, because the standard potential is very negative and the wave then coincides with the hydrogen wave (Zhang et al. 1995).
For the polarographic determination of Zr in 0.1 mol L^{-1} KCl the wave is at $E_{1/2}$ = -1.64 V (vs. calomel electrode) and it is not possible to use this quantitatively (Laubengayer and Eaton 1940). Figure 18 shows the current-voltage curve of this determination.

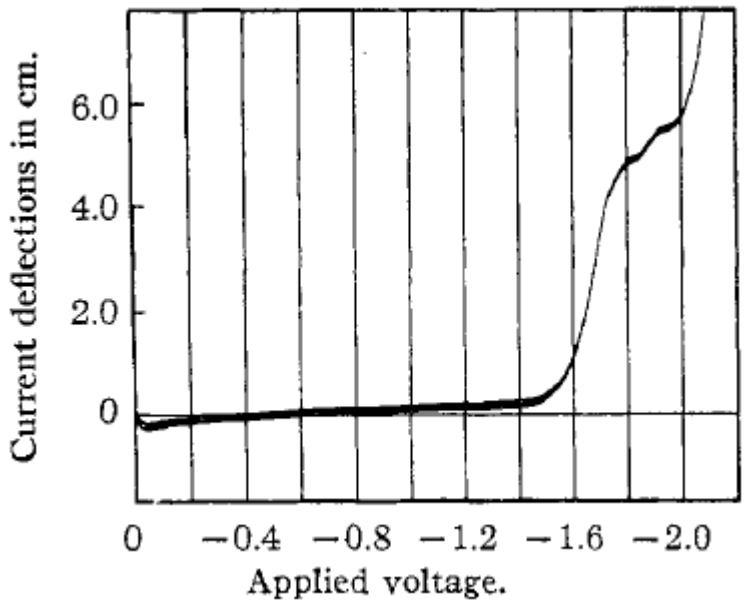

Figure 18. Polarogram of 1 mmol L^{-1} $ZrOCl_2$ in 0.1 mol L^{-1} KCl at pH 3 (Laubengayer and Eaton 1940)

Voltammetric and spectrophotometric determination of Zr with Alizarin Red S whose IUPAC name is 1,2-dihydroxy-9,10-anthracenedione was performed by Zittel et al. (1967) and they found that a 1:1 complex is formed within the determined pH range. In the voltammetric determination they discovered that with increasing Alizarin Red S concentration from 2.2 µmol L^{-1} to 194 µmol L^{-1} the half-wave potential increases but remains in the range of $E_{1/2}$ = +0.7 V vs. SCE. With increasing pH (0.1-9.4) the half-wave potential decreases ($E_{1/2}$ = +0.76-0.35 V). The detection limit with this method for Zr is 1.1 µmol L^{-1}.
A sensitive stripping voltammetric Zr determination method was reported by Wang et al. (1987) who used Solochrome Violet RS also called Acid Alizarin Violet in a

concentration of 1.5 µmol L^{-1}. The half-wave potential is $E_{1/2}$ = -0.446 V vs. HMDE with a detection limit of 2.3 µmol L^{-1}.

Zirconium forms with phenylfuorene and hexadecyl pyridinium chloride a ternary complex in 0.15 mol L^{-1} HCl. The complex can be measured by linear potential sweep voltammetry and has a determination limit of 5 nmol L^{-1} (Zhang et al. 1995).

The voltammetric determination of Zr with three different *O*,*O*'-dihydroyazo compounds was studied by Orshulyak et al. (2008). The azo compounds and their detection limits for Zr were 2.19 µmol L^{-1} (Erichrome Red B), 0.38 µmol L^{-1} (Calcon) and 0.17 µmol L^{-1} (Calcion).

4.5.1 Voltammetric/Polarographic Zr determination with cupferron

As for the separation of Nb and Ta, cupferron and BPHA can be used for the separation of Zr from other metal like Nb, Ta, Hf, Fe or Ti (Alimarin and Tse 1962; Hála 1967).

In the 1950's, cupferron was used as a standard solution for titrimetric determinations of Zr in magnesium alloys in strong sulphuric and hydrochloric acids. This determination is essential because Zr is added to alloys for high temperature applications (Olson and Elving 1954; Elving and Olson 1956b).

Elving and Olson also reported a method to determine Zr polarographically as a cupferrate in 0.1 mol L^{-1} and 2 mol L^{-1} sulphuric acid with $E_{1/2}$ = -1.06 V against a SCE (Elving and Olson 1955; Elving and Olson 1956a).

5 Results and discussion

5.1 Results of Niobium determination

5.1.1 Voltammetric/Polarographic determination with cupferron

The sensitive method DPCSV was used to determine the Nb-cupferron complex which was accumulated on the surface of a HMDE.

Various buffers were used to achieve different pH-values: acetate buffer for the pH-range from 3 to 6, MES for pH 5.5-6.7, PIPES for pH 6.1-7.8 and EPPS for pH 7.3-8.7.

The amount of the sample was 10 mL containing different amounts of cupferron from 4 µmol L^{-1} to 1 mmol L^{-1}. Wang et al. (1992a) used a cupferron concentration of 5 µmol L^{-1} to determine Nb in acetate buffer. To enable the utilization of this method not only for the determination of Nb in water but also in seawater it had to be modified to increase the sensitivity by using more cupferron and in addition an oxidizing reagent.

The sensitivity (*S*) of this method can be described as the relationship between the peak current and the Nb concentration. By plotting the peak current (I_p) against the added Nb concentration [Nb] in solution, the slope can be calculated which represents the sensitivity in the following equation 4.13:

$$S = \frac{I_p}{[Nb]} \qquad (4.13)$$

For a clearly visible peak the optimum amount of cupferron was 20 mmol L^{-1} especially for seawater samples. The oxidizing reagent was $KBrO_3$ which does not work well at pH 4, because the reduction wave for the $KBrO_3$ interferes with the Nb peak. $KBrO_3$ works rather at pH 6-8, but nearly all the previous studies which were described above were done at low pH (below 4).

The sample was purged for 240 sec before the first measurement and purged for 20 sec after each addition to keep the sample under a nitrogen atmosphere. Each addition was measured twice. The 0.1-0.01 mol L^{-1} buffered samples were measured at room temperature (21 °C). The accumulation on HMDE was carried out at a potential of -0.2 V for 60 sec. Then it was stripped off for 5 sec before the current was measured. The scan range was varied depending on the detected exact peak

position. In the beginning -0.2 V to -1.2V were used to find the peak position. After the localization of the peak the applied scan range for Nb-cupferron was from -0.5 V to -1.2 V in MQ around pH 4 or from -0.7 V to -1.1 V in seawater at pH 6 and more.

5.1.1.1 Reproduction of the Nb determination by DPCSV in acetate buffer solution at pH 4 with cupferron (Wang et al. 1992a)

Name	080507-Nb-Test1-5.dth
pH value	4.0
Peak position	-0.731 V
Reagents	10 mL 0.1 mol L^{-1} acetate buffer 200 µL 11.09 µmol L^{-1} Nb 20 µL 0.002 mol L^{-1} cupferron

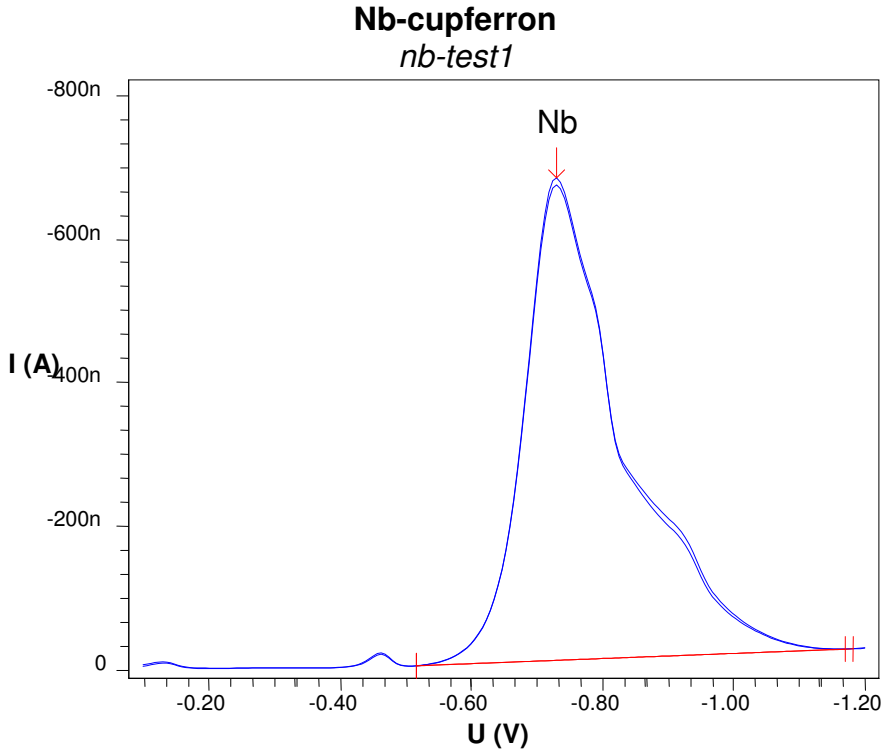

Figure 19. Total scan from 0.0 V to -1.2 V with the polarographic curve of Nb at -0.731 V.

In Figure 19 a total DPCSV scan with a high Nb concentration (215 nmol L^{-1}) in 0.1 mol L^{-1} acetetate buffer can be seen. This scan was recorded to try out and confirm the applicability of the published method by Wang et al. (1992a) and to localize the peak position of Nb-cupferron.

Name	080508-Nb-Test2-3b.dth
pH value	4.4
Peak position	-0.774 V
Reagents	10 mL 0.1 mol L^{-1} Nb acetate buffer 20 µL 11.09 µmol L^{-1} Nb 20 µL 0.002 mol L^{-1}Cupferron
Additions	4 times 20 µL 11.09 µmol L^{-1} Nb

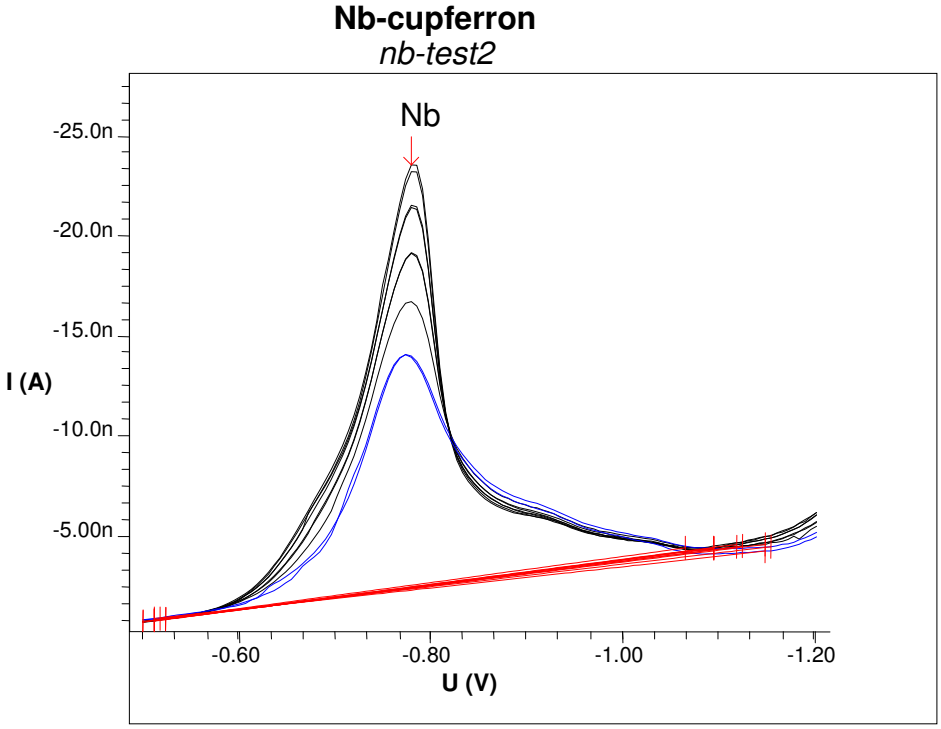

Figure 20. Current-voltage curves for 21.5, 42.9, 64.2, 85.4, 106.6 nmol L^{-1} Nb(V) in 0.1 mol L^{-1} acetate buffer (pH 4.4).

Figure 20 shows the rising polarographic curves for linearly increasing amounts of Nb (21.5, 42.9, 64.2, 85.4, 106.6 nmol L^{-1}) in 0.1 mol L^{-1} acetate buffer containing 4 µmol L^{-1} Cupferon at pH 4.4. The measured peak current is well reproducible for each amount of Nb and the peaks are well defined which can also be seen in Figure 21. In comparison to the values of -0.97 V published by Wang et al. (1992a) the peak position is shifted to a less negative potential of -0.77 V.

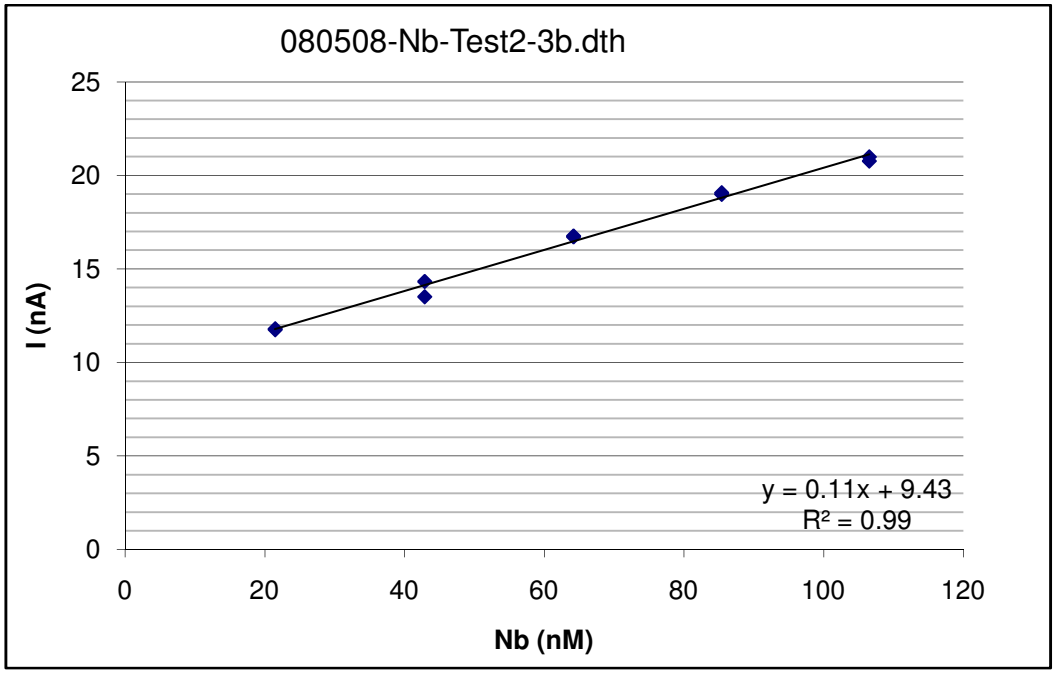

Figure 21. The measured currents are plotted as a function of the Nb concentrations.

In Figure 21 the measured peak currents are plotted as a function of the added Nb concentrations. The slope represents the sensitivity of the measurement which is S = 0.11 nA nmol^{-1} L.

5.1.1.2 Nb determination by DPCSV in acetate buffer solution at pH 5 with cupferron

Name	080514-Nb-acetate(pH5)-1b.dth
pH value	5.0
Peak position	-0.839 V
Reagents	10 mL 0.1 mol L^{-1} acetate buffer 20 µL 11.09 µmol L^{-1} Nb 20 µL 0.002 mol L^{-1} cupferron
Additions	4 times 20 µL 11.09 µmol L^{-1} Nb

It can easily be seen in Figure 22 that there is an apparent low signal to noise ratio and the curves seem to be scattered. The whole curves shift very much in their height. Not withstanding the measured peak current of the replicated curves of each addition of Nb were acceptable which is demonstrated in Figure 23. The correlation of the measured peak currents and the Nb concentration is linear with R^2 = 0.99.

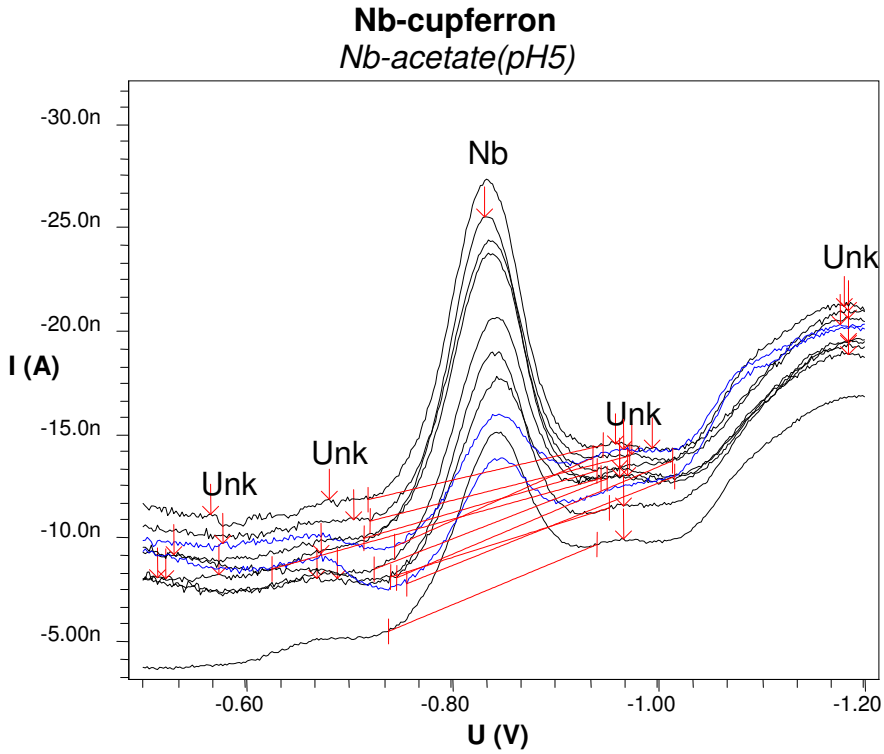

Figure 22. Current-voltage curves for 21.5, 42.9, 64.2, 85.4, 106.6 nmol L^{-1} Nb(V) in 0.1 mol L^{-1} acetate buffer (pH 5.0) containing 4 µmol L^{-1} cupferron.

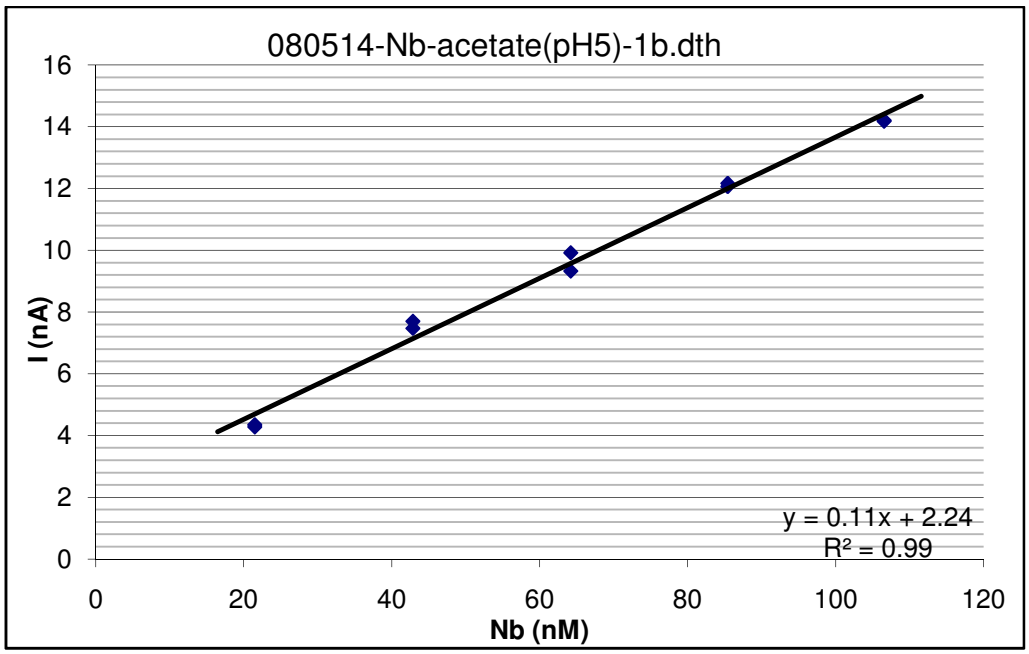

Figure 23. The measured peak currents are plotted as a function of the added Nb concentrations.

In Figure 23 the sensitivity with 4 µmol L^{-1} cupferron at pH 5 is exactly the same as for pH 4. Due to the low sensitivity and the close curves of the experiments with 4 µmol L^{-1} cupferron in the solution, the cupferron concentration was increased to

200 µmol L^{-1} for the next Nb determinations at the same pH. With this increase the peak current rose by the factor of 12 in Figure 24. The peak position shifted only a fraction. The replicates are a lot more defined and closer together than in Figure 23. Furthermore it was possible to increase the sensitivity nearly by a factor of 6 from S = 0.11 nA $nmol^{-1}$ L to S = 0.65 nA $nmol^{-1}$ L as shown in Figure 25. It can be clearly seen that with an increase of the cupferron concentration the sensitivity increases.

Name	080521-Nb-acetate(pH5)-3b.dth
pH value	4.9
Peak position	-0.823 V
Reagents	10 mL 0.1 mol L^{-1} acetate buffer 20 µL 11.09 µmol L^{-1} Nb 20 µL 0.1 mol L^{-1} cupferron
Additions	4 times 20 µL 11.09 µmol L^{-1} Nb

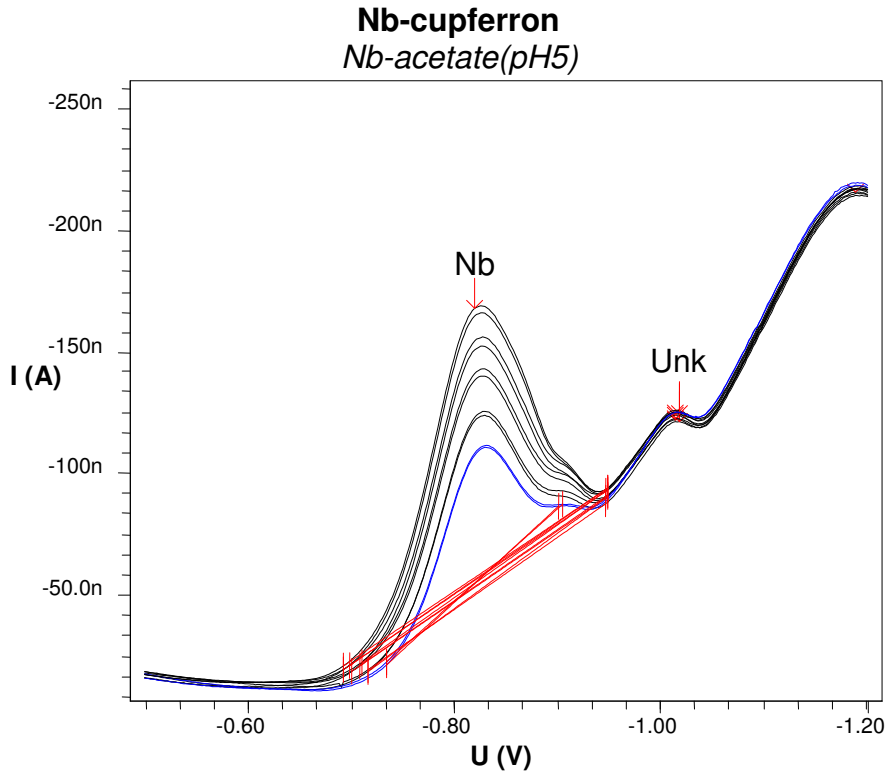

Figure 24. Current-voltage curves for 21.5, 42.9, 64.2, 85.4, 106.6 nmol L^{-1} Nb(V) in 0.1 mol L^{-1} acetate buffer (pH 5.0) containing 200 µmol L^{-1} cupferron.

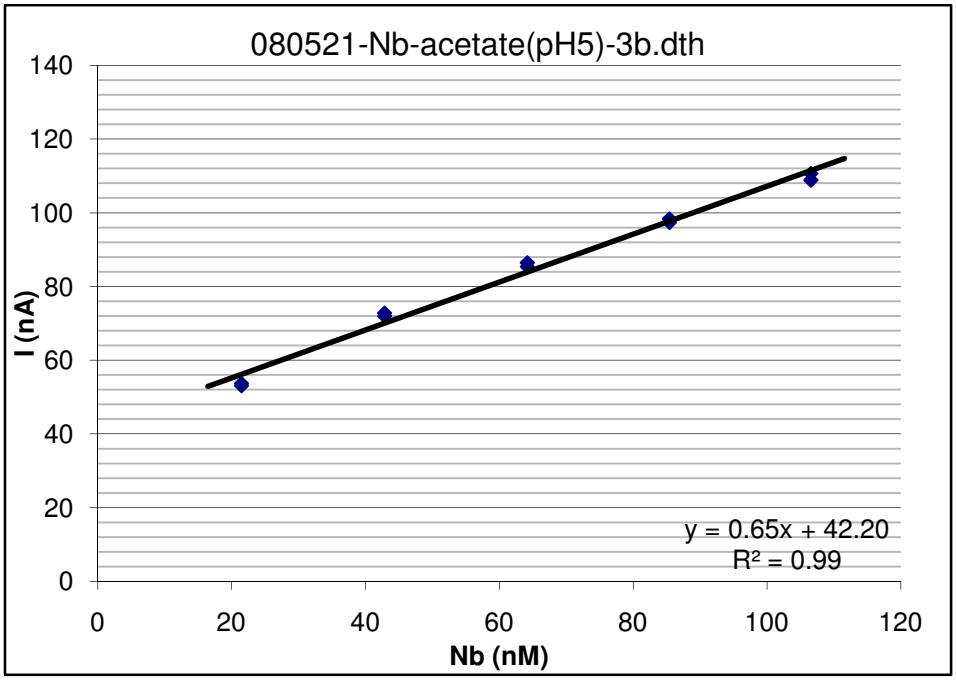

Figure 25. Plot of the peak current as a function of the added Nb concentration.

5.1.1.3 Nb determination by DPCSV in MES buffer solution at pH 6 with cupferron

Name	05271125_080527-Nb-MES-1b.dth
pH value	6.1
Peak position	-0.857 V
Reagents	10 mL 0.1 mol L^{-1} MES buffer 20 µL 11.09 µmol L^{-1} Nb 20 µL 0.005 mol L^{-1} cupferron
Additions	4 times 20 µL 11.09 µmol L^{-1} Nb

Figure 26 shows the current-voltage curves for nanomolar Nb concentrations in 0.1 mol L^{-1} MES buffer. The results demonstrate that polarographic Nb measurements are possible at pH 6.

The replicate measurements of the peak current of the Nb-cupferron complex were always lower than the first measurements. In Figure 27 the R^2 value of this determination is nonetheless 0.99.

The sensitivity of this Nb determination at pH 6.1 is S = 0.31 nA $nmol^{-1}$ L.

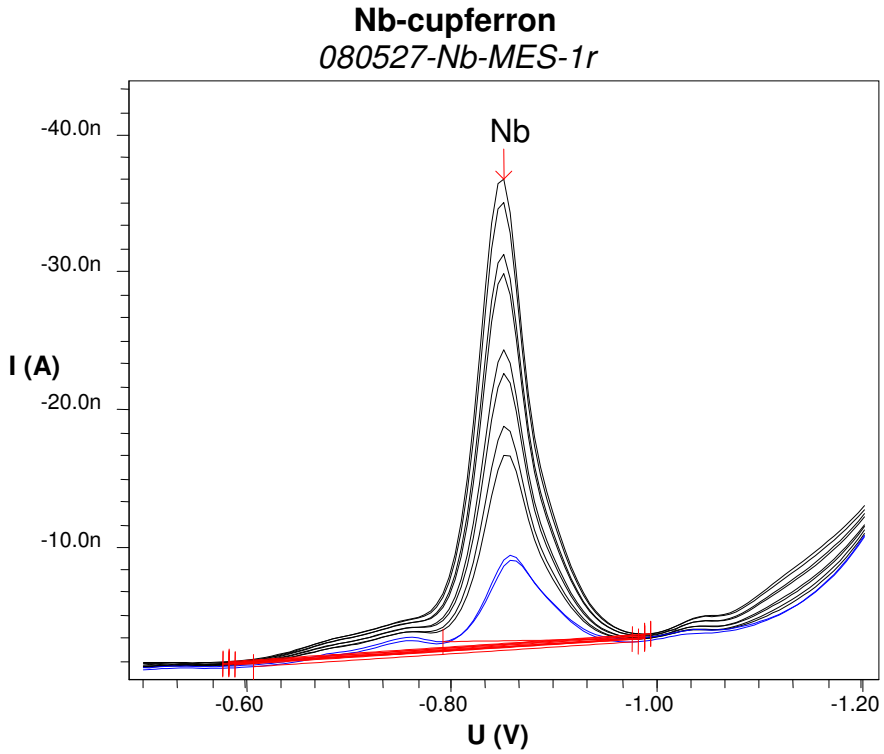

Figure 26. Current-voltage curves for 21.5, 42.9, 64.2, 85.4, 106.6 nmol L^{-1} Nb(V) in 0.1 mol L^{-1} MES buffer (pH 6.1) containing 10 µmol L^{-1} cupferron.

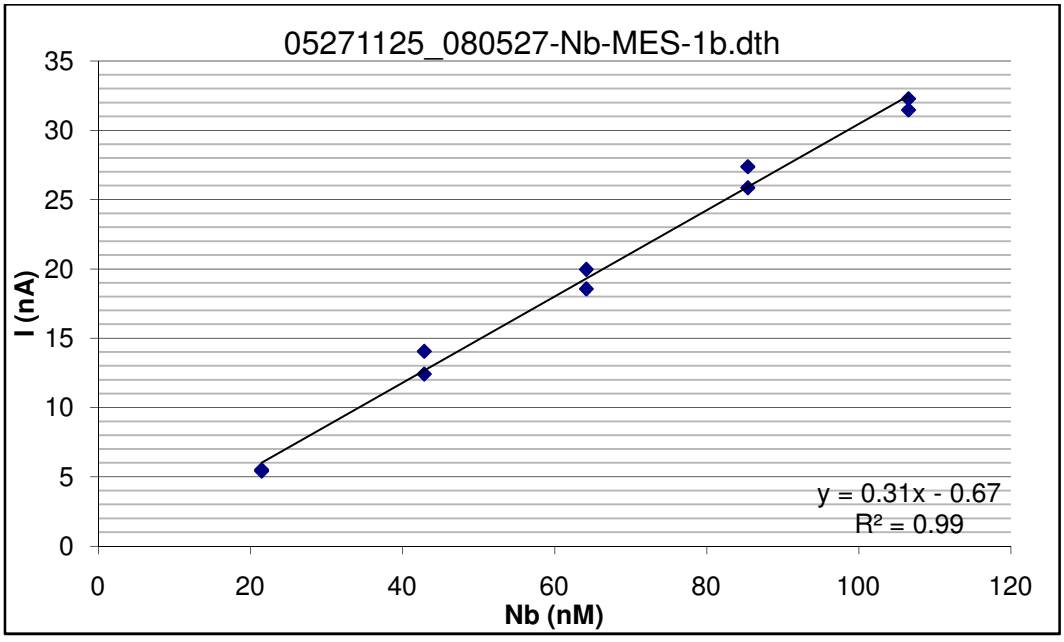

Figure 27. Plot of the the peak current as a function of the added Nb concentration (21.5, 42.9, 64.2, 85.4, 106.6 nmol L^{-1}).

5.1.1.4 Nb determination by DPCSV in MES buffer solution at pH 6 with cupferron and with the oxidizing agent $KBrO_3$

Name	11060746_081007-BrAdd01.dth
pH value	6.1
Peak position	-0.857 V
Reagents	10 mL 0.1 mol L^{-1} MES buffer 100 µL 11.09 µmol L^{-1} Nb oxalate 100 µL 0.1 mol L^{-1} cupferron
Additions	15 times 20 µL 0.36 µmol L^{-1} $KBrO_3$ solution

Figure 28 shows the current-voltage curves for the increasing concentration of $KBrO_3$ in 10 mL 0.1 mol L^{-1} MES buffer at pH 6.1 containing 10 mmol L^{-1} cupferron and 106.6 nmol L^{-1} Nb(V). The peaks increase slightly with the increasing $KBrO_3$ concentration and the peak forms change with it. They lose the shoulder at -0.89 V and get sharper. Figure 29 shows the linear correlation of the measured peaks and the $KBrO_3$ concentrations.

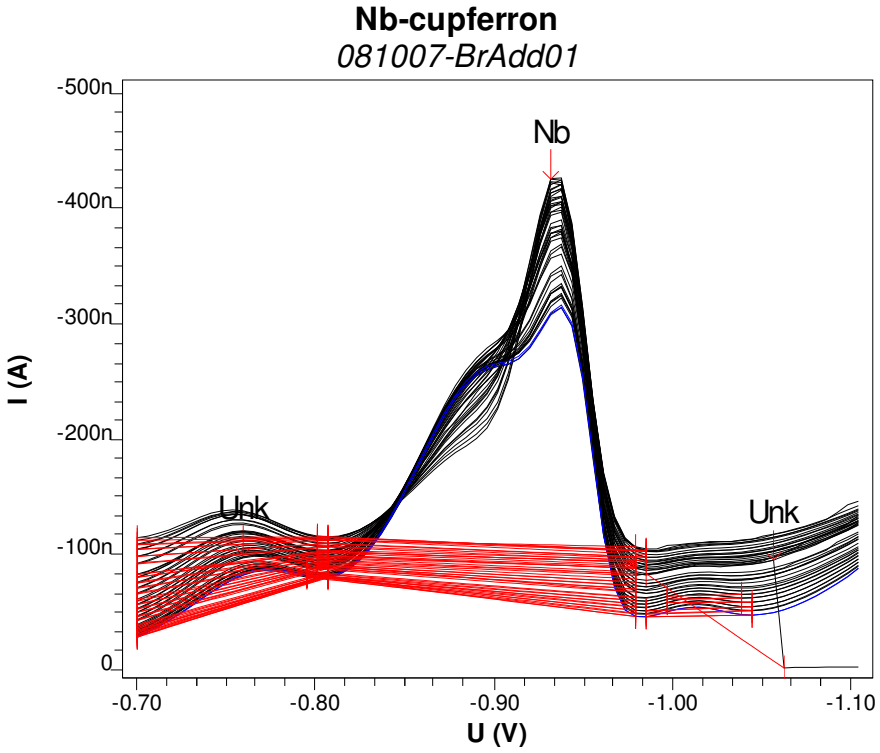

Figure 28. Current voltage curves for 0 to 2.8 µmol L^{-1} $KBrO_3$ in 10 mL 0.1 mol L^{-1} MES buffer (pH 6.1) containing 10 mmol L^{-1} cupferron and 106.6 nmol L^{-1} Nb(V).

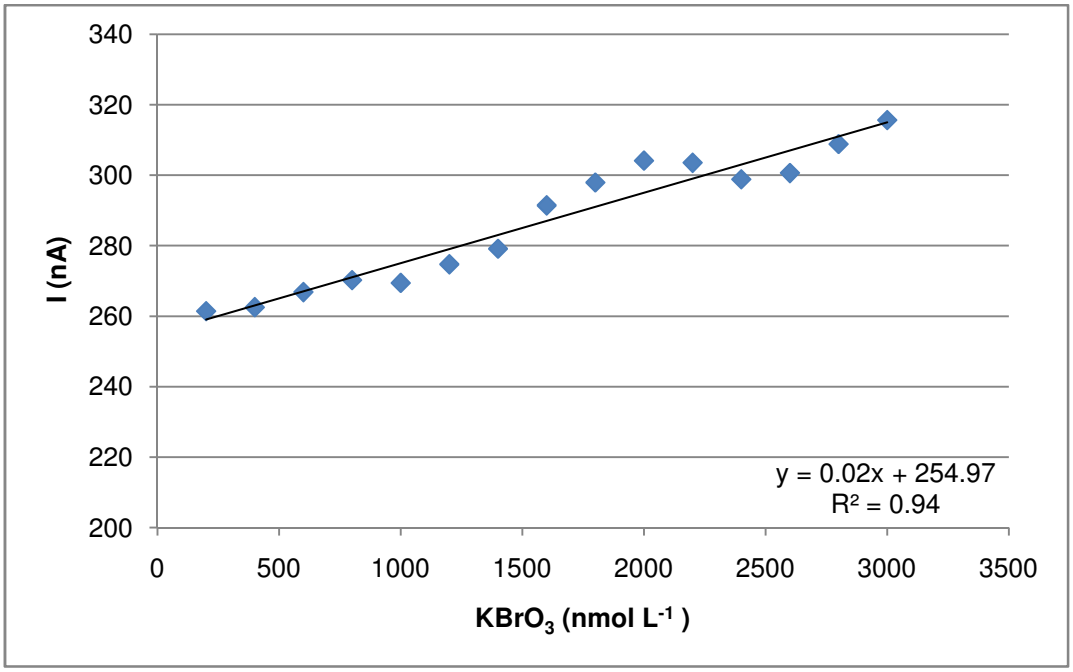

Figure 29. Plot of the measured peak current as a function of the $KBrO_3$ concentration in 10 mL 0.1 mol L^{-1} MES buffer (pH 6.1) containing 10 mmol L^{-1} cupferron and 106.6 nmol L^{-1} Nb(V).

5.1.1.5 Nb determination by DPCSV in PIPES buffer solution at pH 6.7 with cupferron

Name	06121336_080612-Nb-PIPES1.dth
pH value	6.7
Peak position	-0.889 V
Reagents	10 mL MQ 100 µL 1 mol L^{-1} PIPES buffer 20 µL 11.09 µmol L^{-1} Nb 20 µL 0.005 mol L^{-1} cupferron
Additions	4 times 20 µL 11.09 µmol L^{-1} Nb

Figure 30 shows the current-voltage curves for an increasing concentration of Nb (21.5, 42.9, 64.2, 85.4, 106.6 nmol L^{-1}) at pH 6.7 with 10 µmol L^{-1} cupferron in 10 mmol L^{-1} PIPES buffer .The high sensitivity of this Nb determination is S = 0.49 nA $nmol^{-1}$ L with a linear correlation of the peak current and the Nb content (see Figure 31).

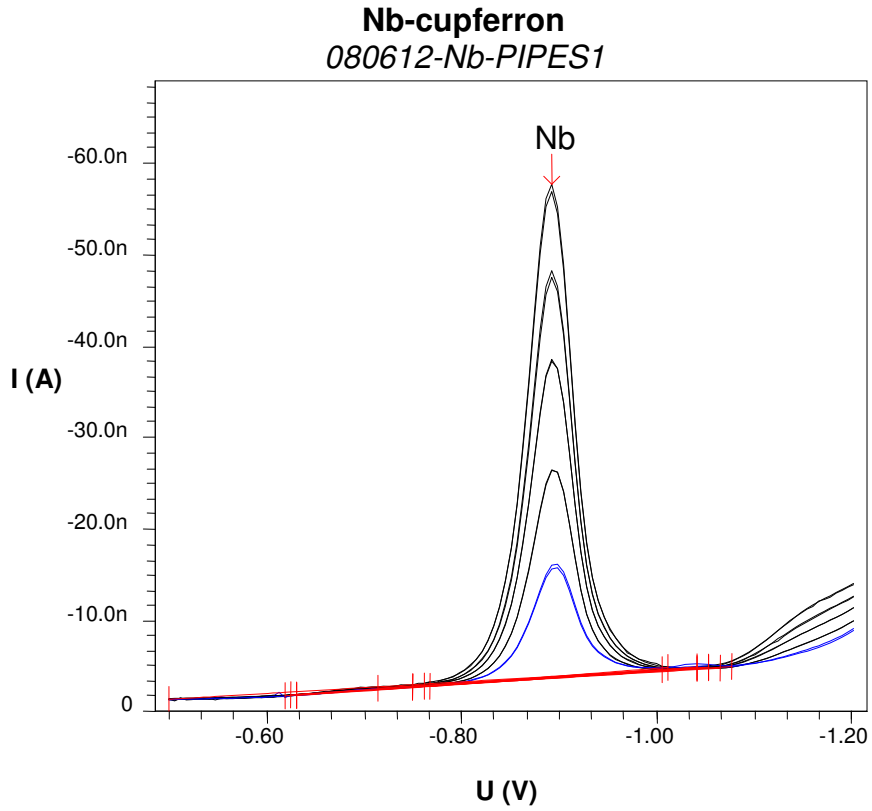

Figure 30. Current-voltage curves for 21.5, 42.9, 64.2, 85.4, 106.6 nmol L^{-1} Nb(V) in 10 mmol L^{-1} PIPES buffer (pH 6.7) containing 10 µmol L^{-1} cupferron.

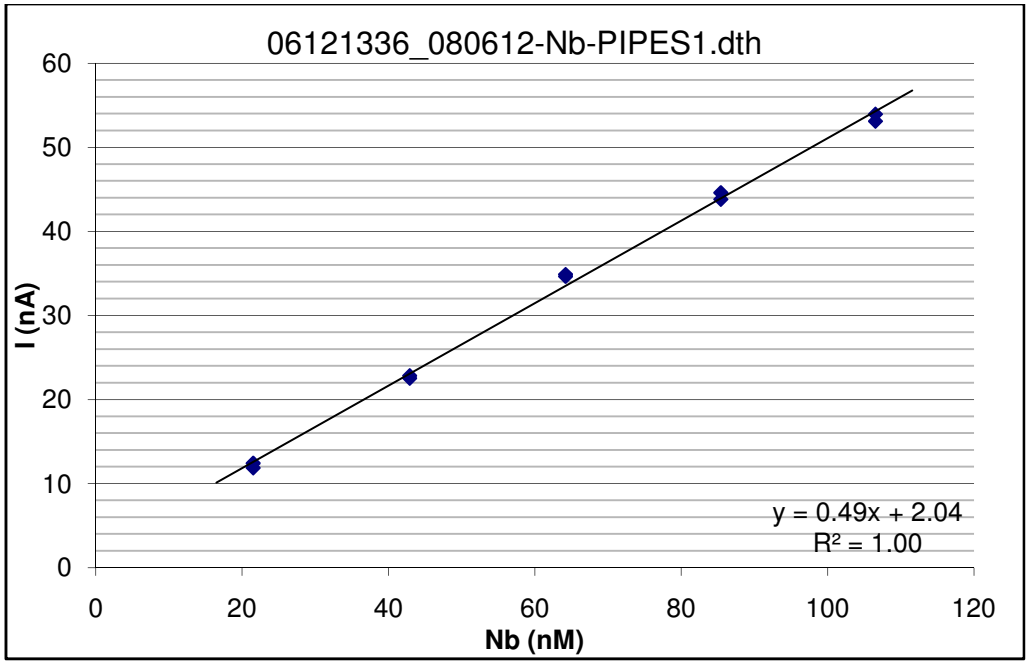

Figure 31. Plot of the the peak current as a function of the added Nb concentration (21.5, 42.9, 64.2, 85.4, 106.6 nmol L^{-1}).

5.1.1.6 Nb determination by DPCSV in PIPES buffer solution at pH 6.6 with cupferron and smaller Nb concentrations

Name	06121441_080612-Nb-PIPES3.dth
pH value	6.6
Peak position	-0.928 V
Reagents	10 mL MQ 100 µL 1 mol L^{-1} PIPES buffer 200 µL 110.9 nmol L^{-1} Nb 200 µL 0.005 mol L^{-1} cupferron
Additions	4 times 200 µL 110.9 nmol L^{-1} Nb

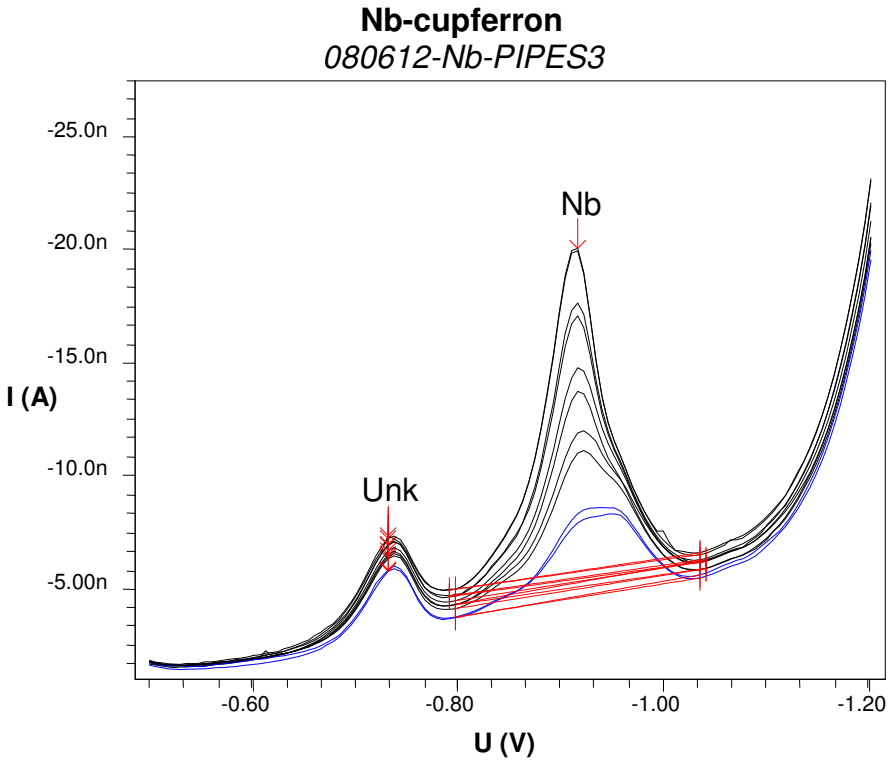

Figure 32. Current-voltage curves for 2.1, 4.1, 6.1, 8.0, 9.8 nmol L^{-1} Nb(V) in 10 mmol L^{-1} PIPES buffer (pH 6.6) containing 100 µmol L^{-1} cupferron.

Figure 32 shows the current-voltage curves for the determination of the increasing concentration of Nb (2.1, 4.1, 6.1, 8.0 and 9.8 nmol L^{-1}). The cupferron concentration was 100 µmol L^{-1} in a 10 mL 10 mmol L^{-1} PIPES buffer solution at pH 6.6.

The sensitivity is fantastic $S = 1.39$ nA $nmol^{-1}$ L for the low Nb concentrations (see Figure 33). The sensitivity could be increased to $S = 2.07$ nA $nmol^{-1}$ L with the increase of the cupferron concentration to 2 mmol L^{-1}. The replicates of the current-voltage curves looked good.

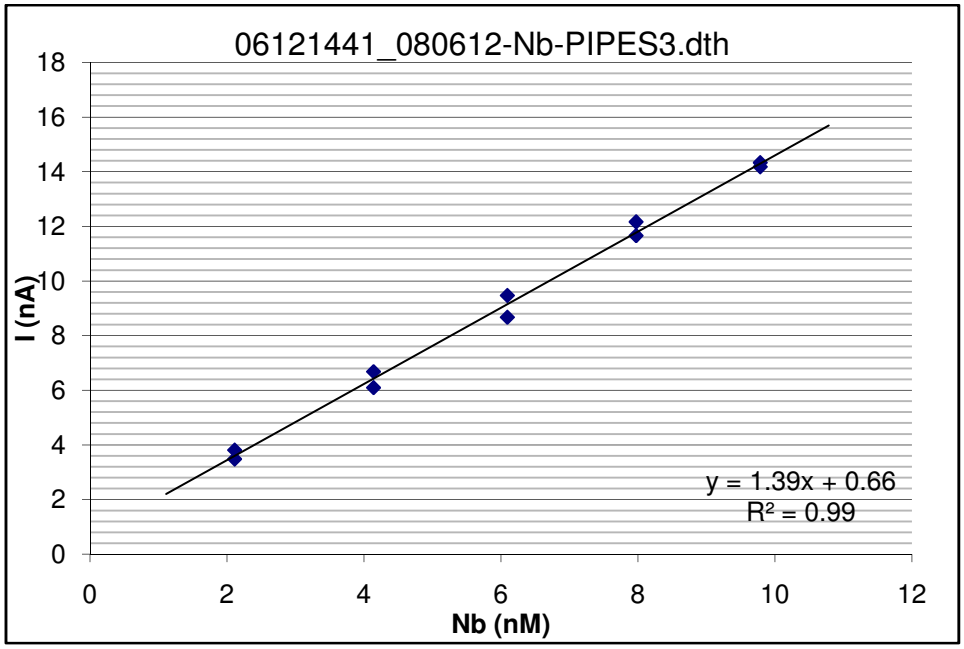

Figure 33. Plot of the the peak current as a function of the added Nb concentration (for 2.1, 4.1, 6.1, 8.0, 9.8 nmol L^{-1} Nb) in 10 mmol L^{-1} PIPES buffer (pH 6.6) containing 100 µmol L^{-1} cupferron.

5.1.1.7 Nb determination by DPCSV in PIPES buffer solution at pH 6.6 with cupferron and the oxidizing agent $KBrO_3$

Name	06130929_080613-Nb-PIPES1.dth
pH value	6.6
Peak position	-0.916 V
Reagents	10 mL MQ 100 µL 1 mol L^{-1} PIPES buffer 200 µL 110.9 nmol L^{-1} Nb 200 µL 0.005 mol L^{-1} cupferron 150 µL 0.36 µmol L^{-1} $KBrO_3$ solution
Additions	4 times 200 µL 110.9 nmol L^{-1} Nb

Figure 34 shows the polarogram for 2.1, 4.1, 6.1, 8.0 and 9.8 nmol L^{-1} Nb in 10 mL 10 mmol L^{-1} PIPES buffer solution at pH 6.6 containing 100 µmol L^{-1} cupferron and 5.4 µmol L^{-1} $KBrO_3$. It looks very similar to the one without $KBrO_3$ (see Figure 32). Also the sensitivity did not change S = 1.36 nA $nmol^{-1}$ L with the addition of the $KBrO_3$ which can be seen in Figure 35. With the increase of the cupferron concentration to 2 mmol L^{-1} and the sensitivity could be increased to S = 2.56 nA $nmol^{-1}$ L which was higher than the sensitivity in the Nb determination without $KBrO_3$.

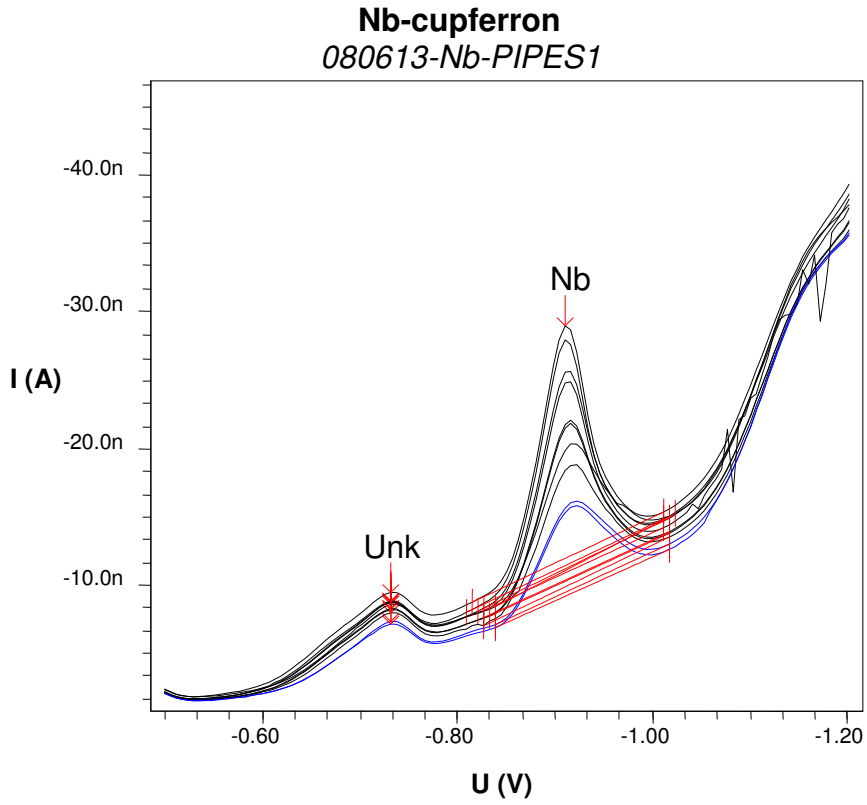

Figure 34. Current-voltage curves for 2.1, 4.1, 6.1, 8.0, 9.8 nmol L^{-1} Nb(V) in 10 mmol L^{-1} PIPES buffer (pH 6.6) containing 100 µmol L^{-1} cupferron and 5.4 µmol L^{-1} $KBrO_3$.

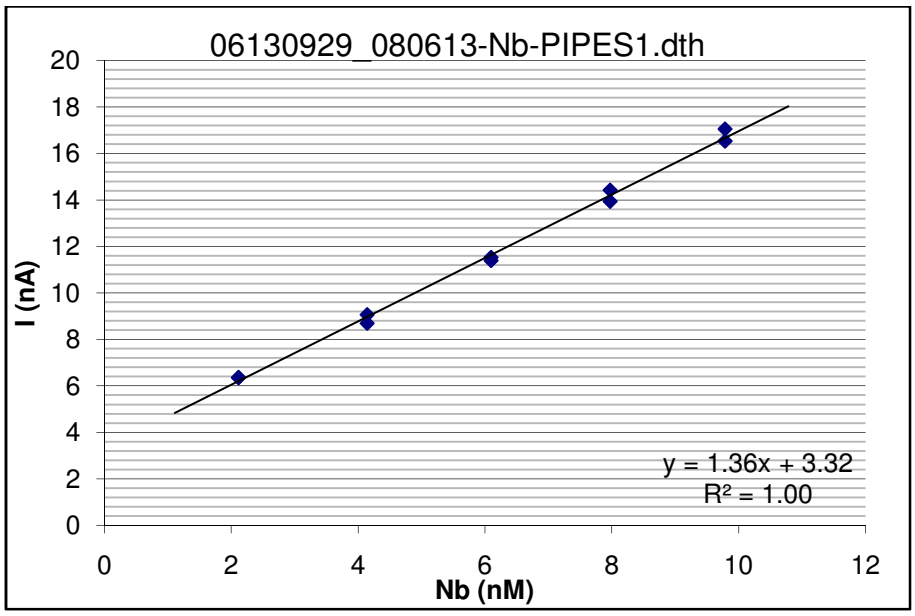

Figure 35. The peak current is plotted as a function of the Nb concentration (2.1, 4.1, 6.1, 8.0, 9.8 nmol L^{-1}) in 10 mmol L^{-1} PIPES buffer (pH 6.6) containing 100 µmol L^{-1} cupferron and 5.4 µmol L^{-1} $KBrO_3$.

5.1.2 Voltammetric/Polarographic determination of Nb with cupferron in seawater

5.1.2.1 Nb determination by DPCSV with cupferron in seawater with acetate buffer to pH 4

Name	080513-Nb-Test3-3b.dth
pH value	3.9
Peak position	-0.736 V
Reagents	5 mL 0.1 mol L^{-1} acetate buffer 5 mL SW M68-3 20 µL 0.002 mol L^{-1} cupferron
Additions	4 times 20 µL 11.09 µmol L^{-1} Nb

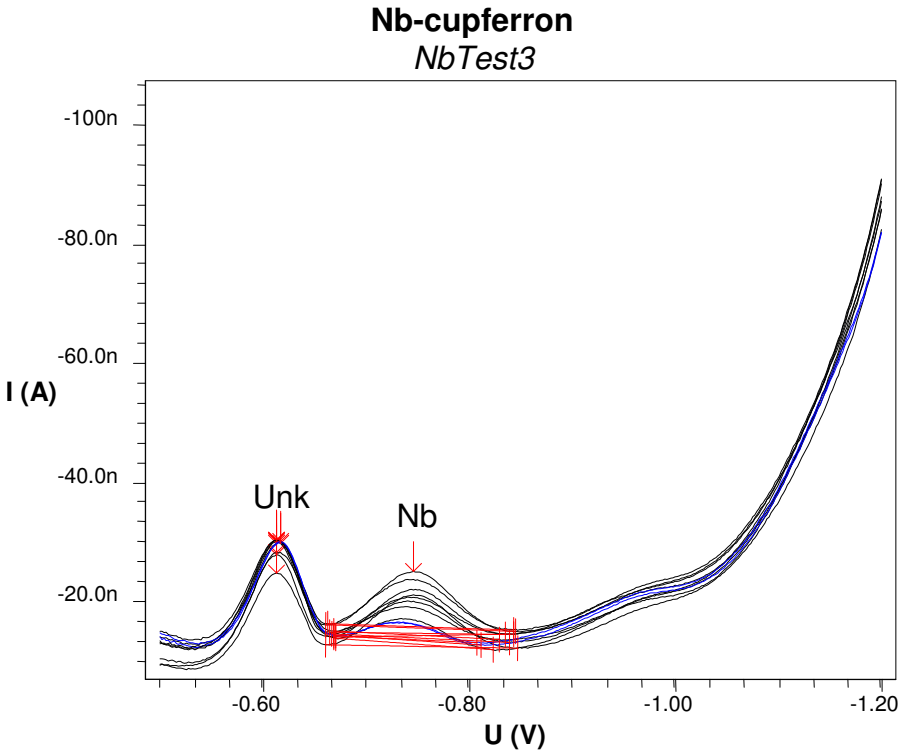

Figure 36. First polarogram of Nb additions (21.5, 42.9, 64.2, 85.4, 106.6 nmol L^{-1}) in seawater.

Figure 36 shows the first trial of a polarograhic determination of Nb seawater. It was carried out in 5 mL seawater and 5 mL 0.1 mol L^{-1} acetate buffer to continue the already done measurements in pure acetate buffer. The Nb-cupferron peak is located at -0.736 V. The increasing Nb amount cannot directly be seen in the curves, because the whole curves move upward and downward, though the correlation of the

peak current and the Nb concentration is linear with $R^2 = 0.99$. But Figure 37 shows that the sensitivity is very low with $S = 0.07$ nA nmol^{-1} L. The sensitivity in seawater with cupferron was expected to be lower than in MQ, because of the presence of Ca and Mg in seawater which can also bind the cupferron and makes it less available for the complexation with Nb.

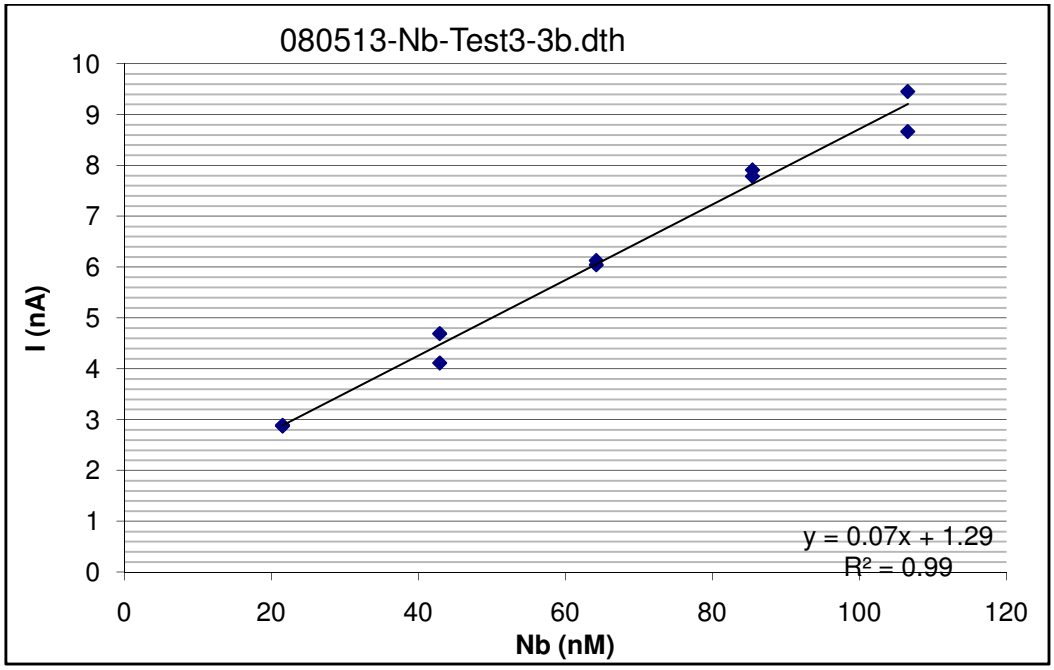

Figure 37. The measured peak current is plotted as a function of the added Nb concentration.

Name	05281606_080528-Nb-ac4-S1b.dth
pH value	4.3
Peak position	-0.756 V
Reagents	9 mL SW M68-3 1 mL 0.1 mol L^{-1} acetate buffer 20 µL 0.005 mol L^{-1} cupferron
Additions	4 times 20 µL 11.09 µmol L^{-1} Nb

To increase the sensitivity, in contrast to the measurement at pH 3.9, an increased cupferron concentration of 10 µmol L^{-1} in 9 mL seawater and 1 mL 0.1 mol L^{-1} acetate buffer was used at pH 4.3.

Figure 38 shows the current-voltage curves with a nicely increasing Nb-cupferron peak at -0.756 V. The other two visible peaks are decreasing with an increasing Nb concentration, because the cupferron is complexed by the Nb.

Figure 39 shows the measured peak currents plotted as a function of the added Nb concentrations. The sensitivity is S = 0.72 nA nmol^{-1} L.

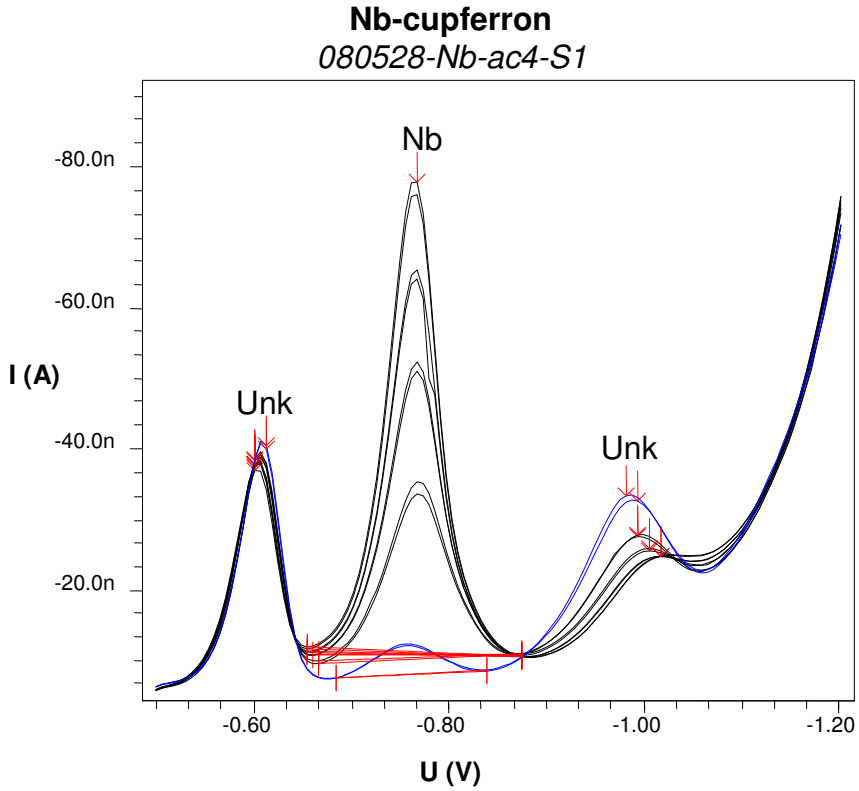

Figure 38. Current-voltage curves for Nb (0, 21.5, 42.9, 64.2, 85.4 nmol L^{-1}) 9 mL SW M68-3 and 1 mL 0.1 mol L^{-1} acetate buffer (pH 4.3) containing 10 µmol L^{-1} cupferron.

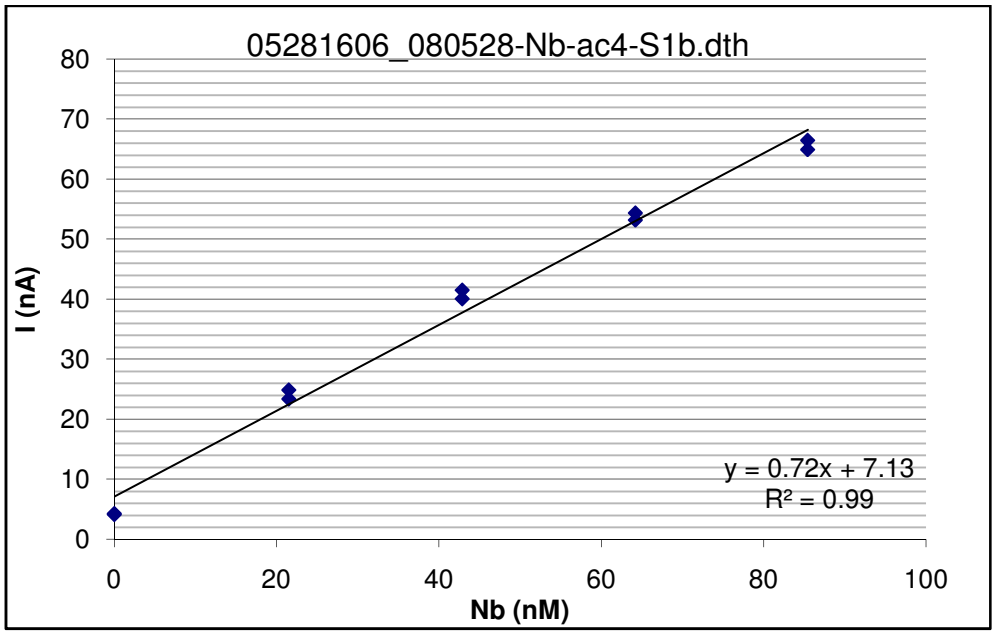

Figure 39. Plot of the measured peak current as a function of the added Nb concentration (0, 21.5, 42.9, 64.2, 85.4 nmol L^{-1}) for 9 mL SW M68-3 and 1 mL 0.1 mol L^{-1} acetate buffer (pH 4.3) altogether containing 10 µmol L^{-1} cupferron.

5.1.2.1 Nb determination by DPCSV with cupferron in seawater with acetate buffer to pH 5

Name	05281638_080528-Nb-ac5-S1b.dth
pH value	5.3
Peak position	-0.815 V
Reagents	9 mL SW M68-3 1 mL 0.1 mol L^{-1} acetate buffer 200 µL 0.005 mol L^{-1} cupferron
Additions	4 times 20 µL 11.09 µmol L^{-1} Nb

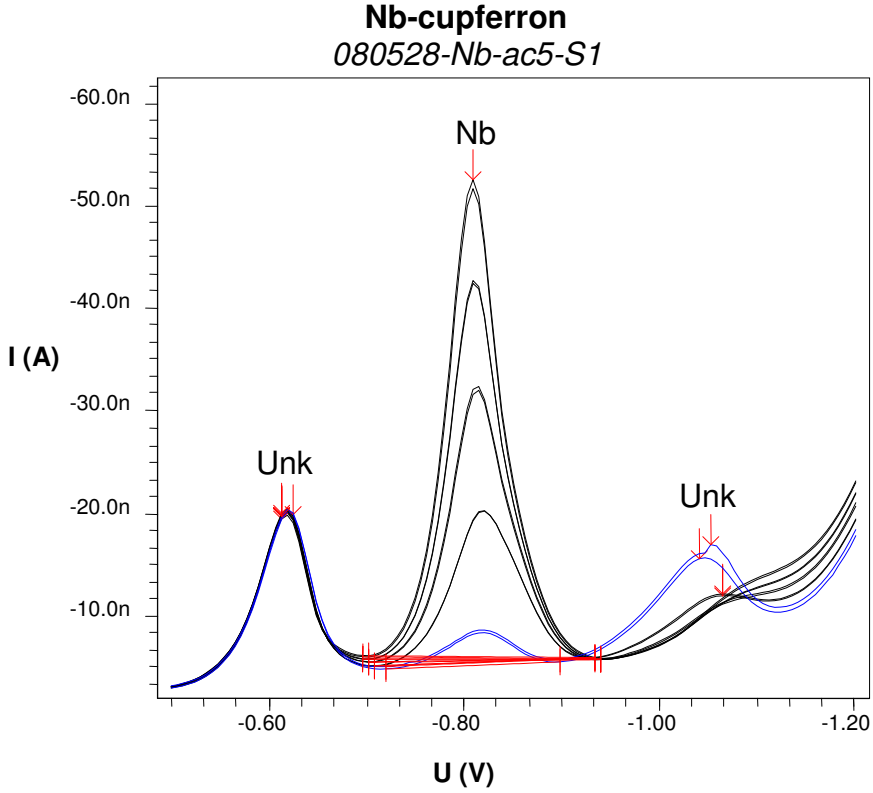

Figure 40. Current-voltage curves for 9 mL SW M68-3 and 1 mL 0.1 mol L^{-1} acetate buffer (pH 5.3) altogether containing 10 µmol L^{-1} cupferron. The added Nb concentration was 0, 21.5, 42.9, 64.2, 85.4 nmol L^{-1}.

Figure 40 shows the current-voltage curves for the mixture of 9 mL SW M68-3 and 1 mL 0.1 mol L^{-1} acetate buffer containing 100 µmol L^{-1} cupferron at pH 5.3. The peak at -0.815 V increased nicely with the added Nb concentration.

Figure 41 shows the plot of the added niobium concentration as a function of the measured peak current and that the determined sensitivity is $S = 0.51$ nA nmol^{-1} L. This is a decrease of 0.21 nA nM^{-1} compared to Figure 39 with a pH increase from 4.3 to 5.3.

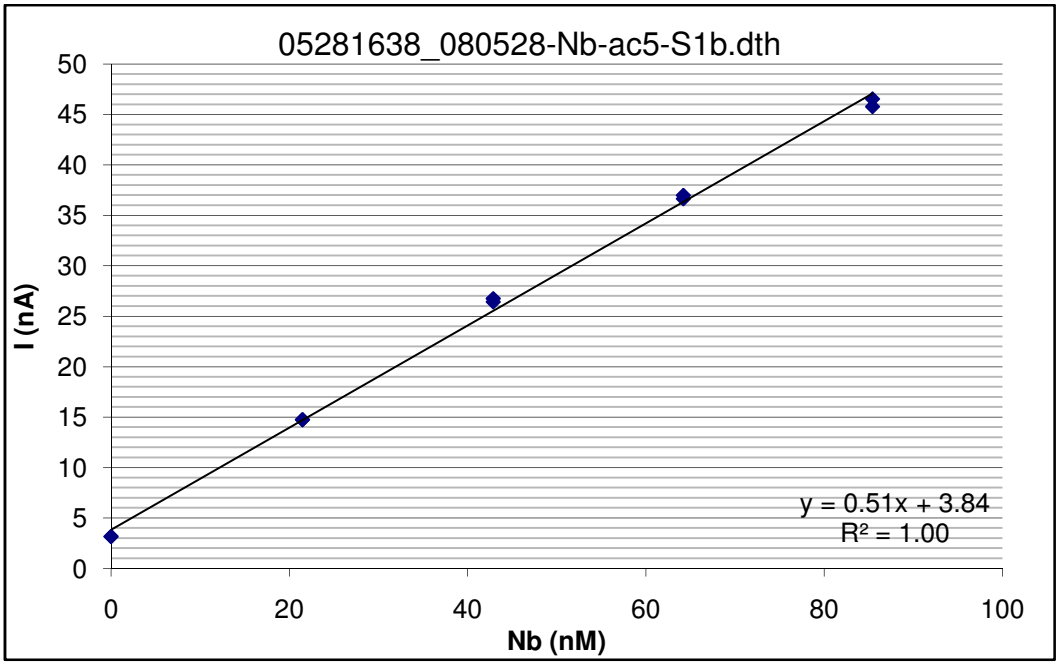

Figure 41. The measured peak currents are plotted as a function of the added Nb concentrations.

5.1.2.2 Nb determination by DPCSV with cupferron in seawater buffered by MES to pH 6

Name	05281502_080528Nb-MES-S1b.dth
pH value	6.1
Peak position	-0.869 V
Reagents	9 mL SW M68-3 1 mL 1 mol L^{-1} MES buffer 200 µL 0.005 mol L^{-1} cupferron
Additions	4 times 20 µL 11.09 µmol L^{-1} Nb

Figure 42 shows the current-voltage curves for 0, 21.5, 42.9, 64.2, 85.4 nmol L^{-1} Nb in 9 mL SW M68-3 and 1 mL 1 mol L^{-1} MES buffer (pH 6.1) containing 100 µmol L^{-1} cupferron.

The sensitivity is S = 0.05 nA $nmol^{-1}$ L (see Figure 43).

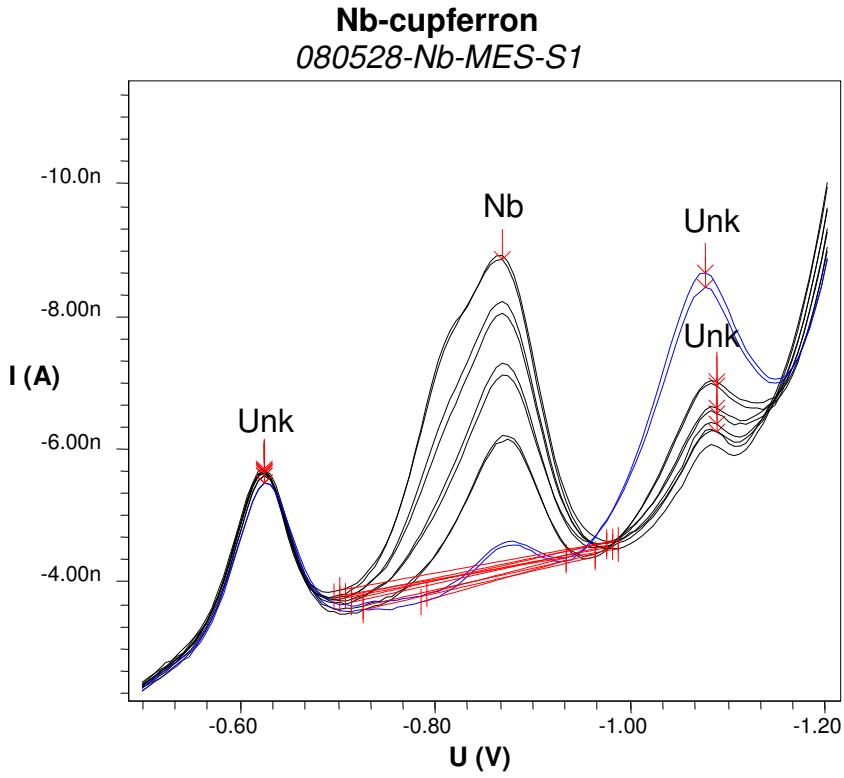

Figure 42. Current-voltage curves for 9 mL SW M68-3 and 1 mL 1 mol L^{-1} MES buffer (pH 5.6) altogether containing 200 µmol L^{-1} cupferron. The added Nb concentration was 0, 21.5, 42.9, 64.2, 85.4 nmol L^{-1}.

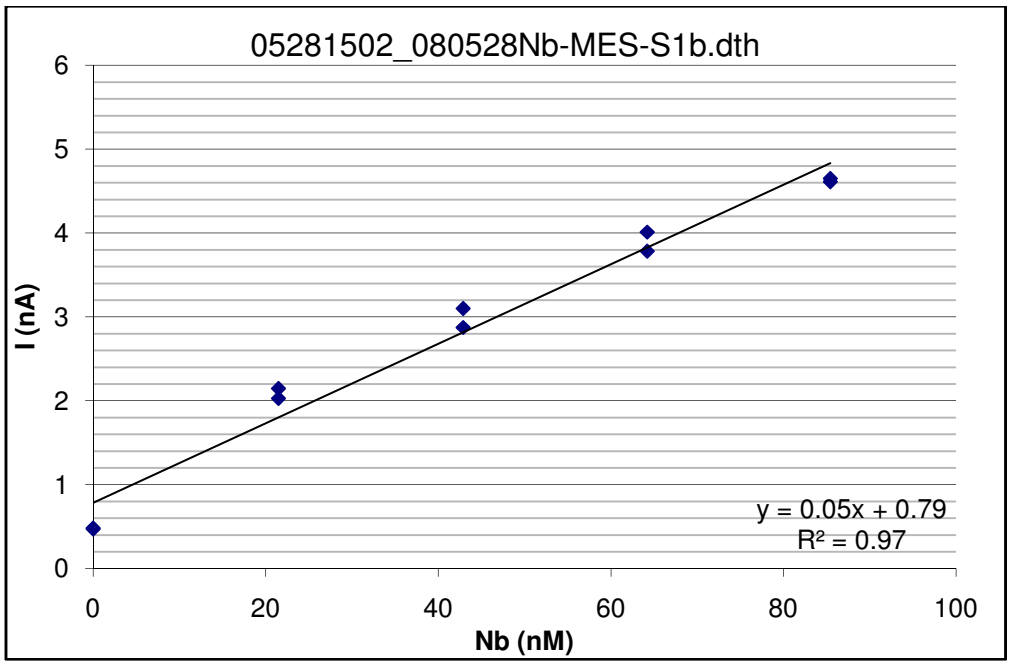

Figure 43. Plot of the peak currents as a function of the added Nb concentrations (0, 21.5, 42.9, 64.2, 85.4 nmol L^{-1}).

5.1.2.3 Nb determination by DPCSV with cupferron and the oxidizing agent $KBrO_3$ in seawater buffered by MES to pH 6.4

Name	08131058_080813-Nb-test03.dth
pH value	6.4
Peak position	-0.890 V
Reagents	10 mL SW M68-3 100 µL 1 mol L^{-1} MES buffer 100 µL 0.1 mol L^{-1} cupferron 150 µL 0.36 mmol L^{-1} $KBrO_3$ solution
Additions	4 times 20 µL 11.09 µmol L^{-1} Nb ox

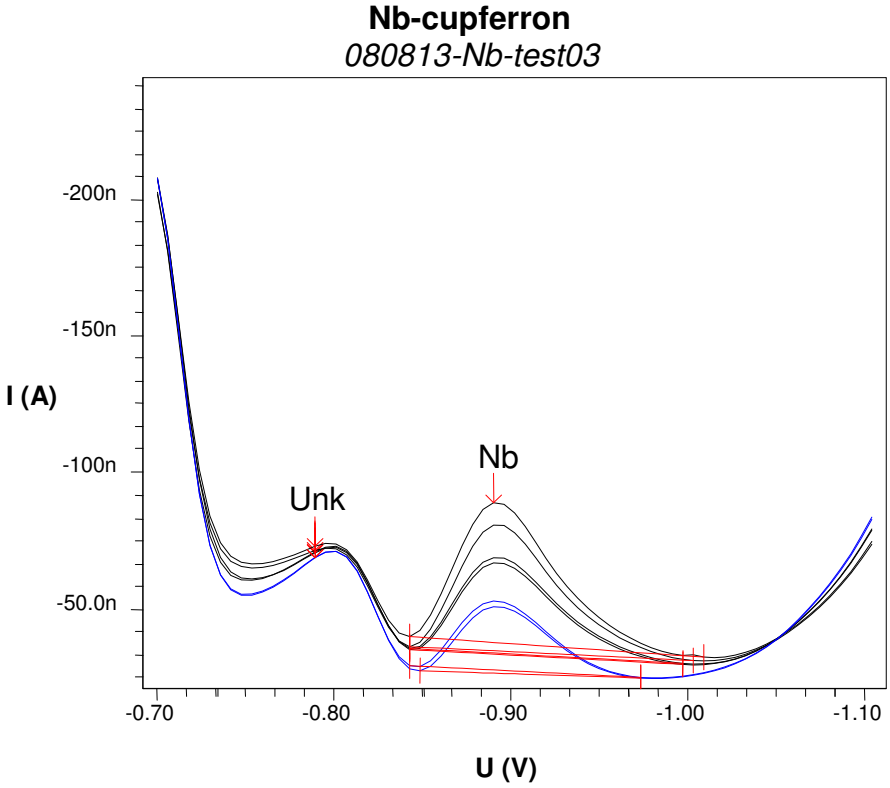

Figure 44. Current voltage curves for 0, 21.5 and 42.9 nmol L^{-1} Nb in 10 mL seawater containing 10 mmol L^{-1} cupferron, 5.4 µmol L^{-1} $KBrO_3$ and 10 mmol L^{-1} MES buffer (pH 6.4).

Figure 44 shows the current-voltage curves for two additions of Nb in 10 mL seawater containing 10 mmol L^{-1} cupferron, 5.4 µmol L^{-1} $KBrO_3$ and 10 mmol L^{-1} MES buffer at pH 6.4. The sensitivity was S = 0.56 nA $nmol^{-1}$ L. The correlation was linear with an R^2 value of 0.96.

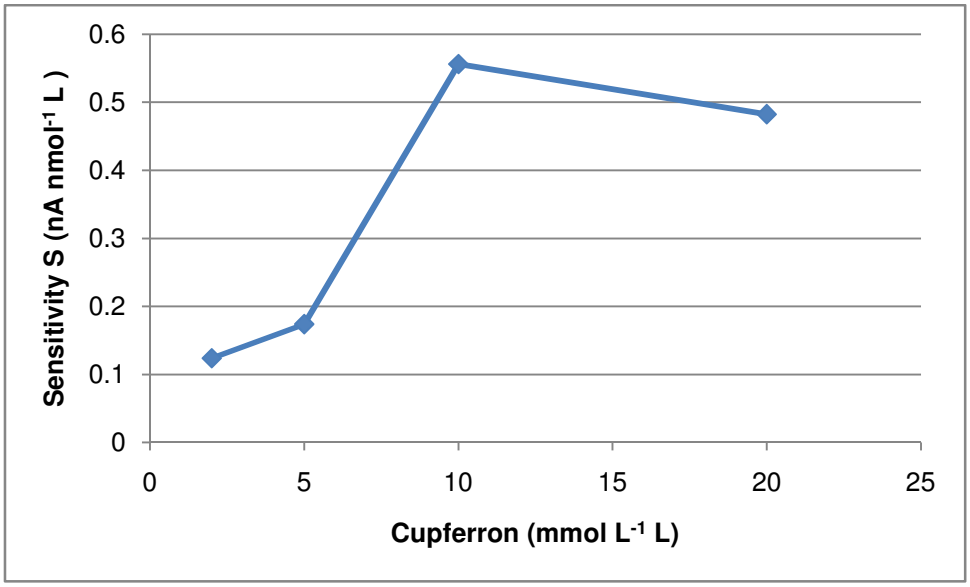

Figure 45. Plot of the calculated sensitivity as a function of the cupferron concentration in 10 mL seawater containing 5.4 µmol L^{-1} $KBrO_3$ and 10 mmol L^{-1} MES buffer (pH 6.4).

Figure 45 shows the plot of the sensitivity as a function of the cupferron concentration in the sample. Only the cupferron concentrations were varied. All of the samples contained 10 mL seawater with 5.4 µmol L^{-1} $KBrO_3$ and 10 mmol L^{-1} MES buffer (pH 6.4-6.5). The highest sensitivity was achieved with 10 mmol L^{-1} cupferron (see Figure 44).

5.1.2.4 Nb determination by DPCSV in seawater at pH 6.4 buffered by MES with cupferron and with addition of $KBrO_3$

Name	11060956_081007-BrAdd02.dth
pH value	6.4
Peak position	-0.890 V to -0.905 V
Reagents	10 mL SW M68-3 100 µL 1 mol L^{-1} MES buffer 100 µL 11.09 µmol L^{-1} Nb oxalate 100 µL 0.1 mol L^{-1} cupferron
Additions	21 times 20 µL 0.36 µmol L^{-1} $KBrO_3$ solution

Figure 46 shows the polarogram of 10 mL SW containing 10 mmol L^{-1} MES buffer (pH 6.4), 10 mmol L^{-1} cupferron and 106.6 nmol L^{-1} Nb(V). The $KBrO_3$ concentration was increased from 0 to 4 µmol L^{-1} in the solution. With the increase of the $KBrO_3$ concentration the peak position moved from -0.890 V to -0.905 V and the peak at -0.77 V rose, too. The correlation of the peak current and the $KBrO_3$ concentration

increased linear by 0.01. In water the peak current increased twice as much as in seawater with the increase of the $KBrO_3$ concentration (compare Figure 47 and Figure 29).

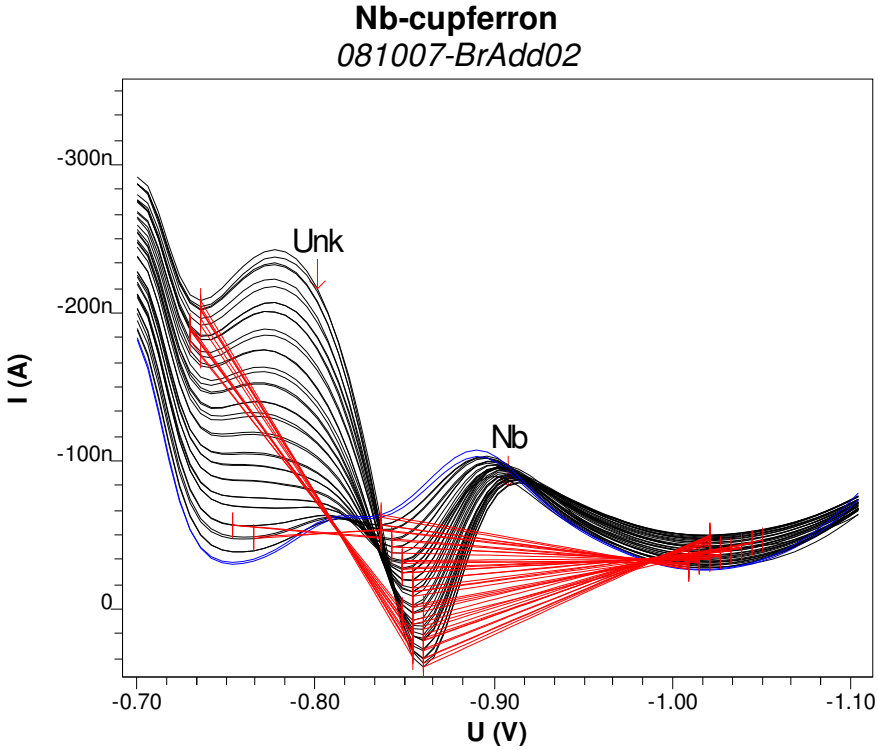

Figure 46. Current voltage curves for 0 to 4 µmol L^{-1} $KBrO_3$ in 10 mL SW containing 10 mmol L^{-1} MES buffer (pH 6.4), 10 mmol L^{-1} cupferron and 106.6 nmol L^{-1} Nb(V).

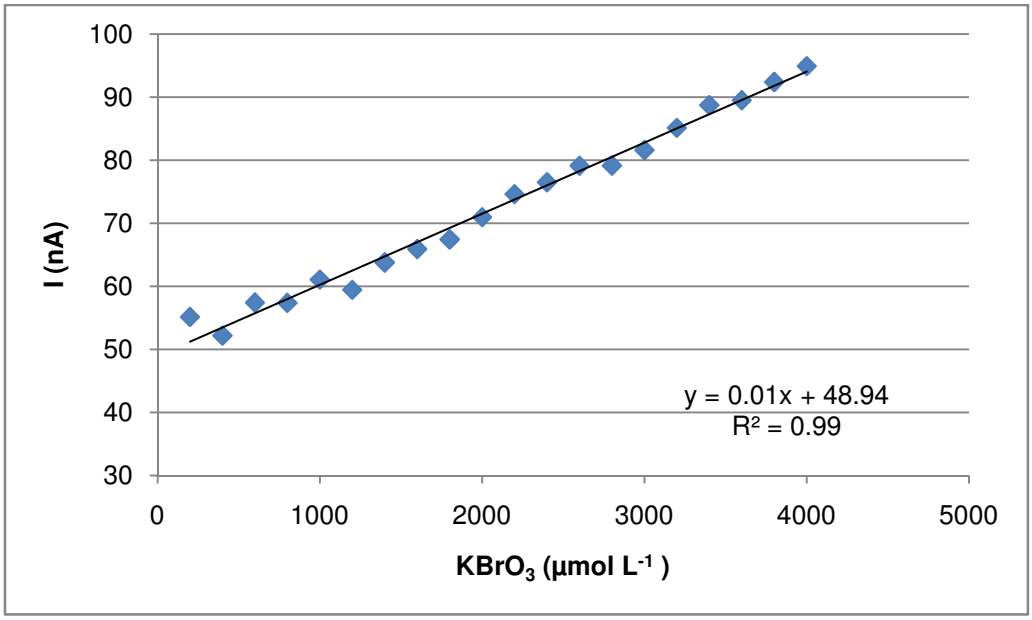

Figure 47. Plot of the measured peak currents as a function of 0 to 4 µmol L^{-1} $KBrO_3$ in 10 mL SW containing 10 mmol L^{-1} MES buffer (pH 6.4), 10 mmol L^{-1} cupferron and 106.6 nmol L^{-1} Nb.

5.1.2.5 Nb determination by DPCSV in PIPES buffer solution at pH 6.9 with cupferron in seawater

Name	06191130_080619-Nb-PIPES2.dth
pH value	6.9
Peak position	-0.845 V to -0.905 V
Reagents	10 mL SW M68-3 100 µL 1 mol L^{-1} PIPES buffer 200 µL 0.1 mol L^{-1} cupferron
Additions	4 times 20 µL 11.09 µmol L^{-1} Nb

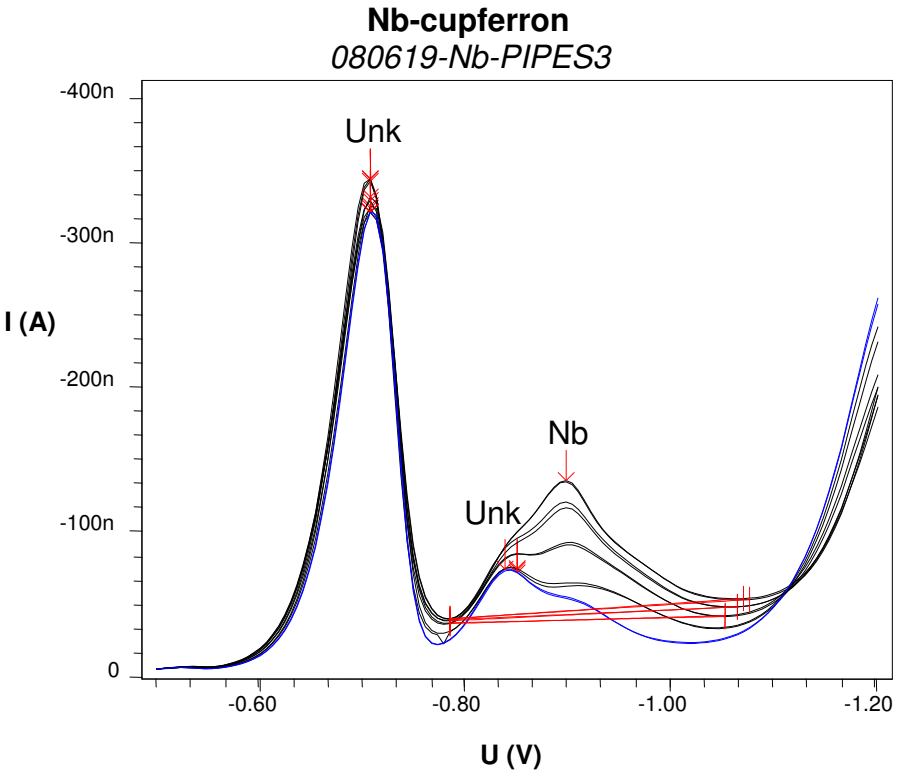

Figure 48. Current-voltage curves for 10 mL SW M68-3 containing 200 mmol L^{-1} cupferron and 10 mmol L^{-1} PIPES buffer (pH 6.9). The added Nb concentration was 0, 21.5, 42.9, 64.2, 85.4 nmol L^{-1}.

Figure 48 shows the polarogram for the Nb determination in seawater at pH 6.9. It can be clearly seen that the peak position moved strongly from -0.845 V to -0.905 V, because there seemed to be another peak at -0.845 V. Therefore the correlation of the added Nb concentration and the peak current was not linear. This happened in all of the Nb determinations at this pH which were buffered with PIPES. It made no difference what the cupferron concentration was and whether $KBrO_3$ was added or not.

5.1.3 Comparison of the Nb determinations by DPCSV with cupferron

Table 4. Compiled data of the polarographic Nb determinations with cupferron.

pH	peak position V	Sensitivity nA $nmol^{-1}$ L	reagents 10 mL	Buffer Conc. mmol L^{-1}	cupferron conc µmol L^{-1}	$KBrO_3$ conc. µmol l^{-1}	smallest added Nb conc. nmol L^{-1}
4.4	-0.774	0.11	MQ	0.1	4		21.5
5.0	-0.839	0.11	MQ	0.1	4		21.5
4.9	-0.823	0.65	MQ	0.1	200		21.5
6.1	-0.857	0.31	MQ	0.1	100		21.5
6.7	-0.889	0.49	MQ	0.01	100		21.5
6.6	-0.928	1.39	MQ	0.01	100		2.1
6.6	-0.916	1.36	MQ	0.01	100	5.4	2.1
3.9	-0.736	0.07	SW	0.05	4		21.5
4.3	-0.756	0.72	SW	0.01	100		21.5
5.3	-0.815	0.51	SW	0.01	100		21.5
6.1	-0.869	0.05	SW	0.1	100		21.5
6.4	-0.890	0.12	SW	0.01	200	5.4	21.5
6.5	-0.872	0.17	SW	0.01	500	5.4	21.5
6.4	-0.878	0.56	SW	0.01	1000	5.4	21.5
6.5	-0.890	0.48	SW	0.01	2000	5.4	21.5
6.9	-0.845 V to -0.905 V		SW	0.01	2000		21.5

Table 4 shows the compiled data for the polarographic Nb determination in MQ and in seawater.

In MQ the Nb determination works fine at the pH range from 4.4 to 6.6. With increasing pH a higher cupferron concentration is needed to achieve the same sensitivity.

In seawater Nb can be determined from pH 3.9 to 6.5, but above that pH it does not work, because of another interfering peak at the same peak position. A very good sensitivity can be achieved at pH 6.4 with 1 mmol L^{-1} cupferron and 5.4 mmol L^{-1} $KBrO_3$.

5.1.4 Nb-cupferron stoichiometry

Name	11051200_081006-CupfAdd01.dth
pH value	6.0
Peak position	-0.896 V
Reagents	10 mL MQ 100 µL 1 mol L^{-1} MES 150 µL 0.4 mmol L^{-1} $KBrO_3$ 100 µL 11.09 µmol L^{-1} Nb oxalate (fresh)
Additions	17 times 20µL 0.1 mol L^{-1} Cupf

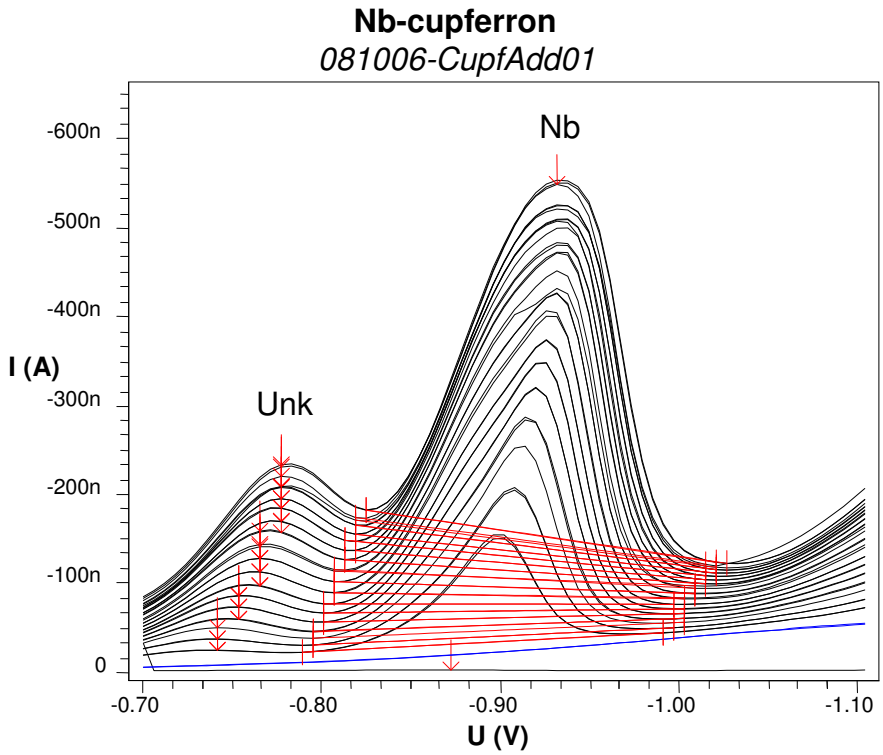

Figure 49. Current-voltage curves for 106.6 nmol L^{-1} Nb at pH 6 with 17 additions of 20 µL 0.1 mol L^{-1} cupferron.

Figure 49 shows the polarogram of seventeen cupferron additions (each 2 mmol L^{-1}) at pH 6 in 10 mmol L^{-1} MES buffer containing 106.6 nmol L^{-1} Nb and 5.4 µmol L^{-1} $KBrO_3$. With the increasing concentration of cupferron the peak current increased less. After the tenth addition (20 mmol L^{-1} cupferron in the solution) the peak increased far less than before (see blue squares in Figure 51). The same behaviour can be observed in Figure 50 in seawater (red squares).

Figure 50 shows the polarogram of seven cupferron additions (each 2 mmol L^{-1}) in seawater at pH 6.5 containing 10 mmol L^{-1} MES buffer containing 106.6 nmol L^{-1} Nb and 5.4 µmol L^{-1} $KBrO_3$.

Name	11051327_081006-CupfAdd02.dth
pH value	6.5
Peak position	-0.867 V
Reagents	10 mL SW M68.3 100 µL 1 mol L^{-1} MES 150 µL 0.4 m mol L^{-1} $KBrO_3$ solution 100 µL 11.09 µmol L^{-1} Nb oxalate (fresh)
Additions	7 times 20 µL 0.1 mol L^{-1} Cupf

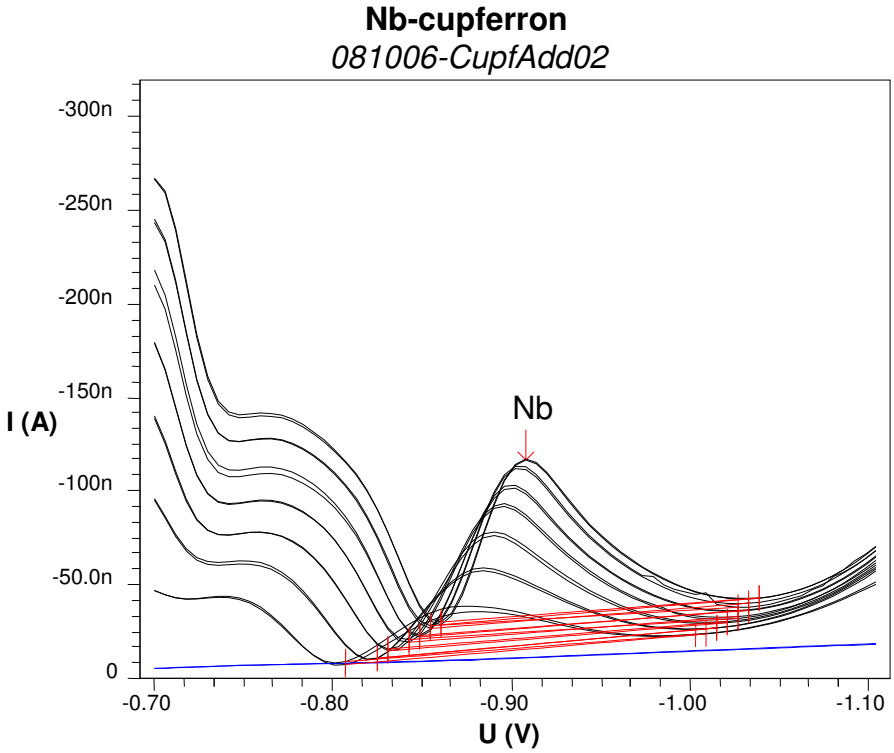

Figure 50. Current-voltage curves for 106.6 nmol L^{-1} Nb in SW at pH 6.5 with 7 additions of 20 µL 0.1 mol L^{-1} cupferron.

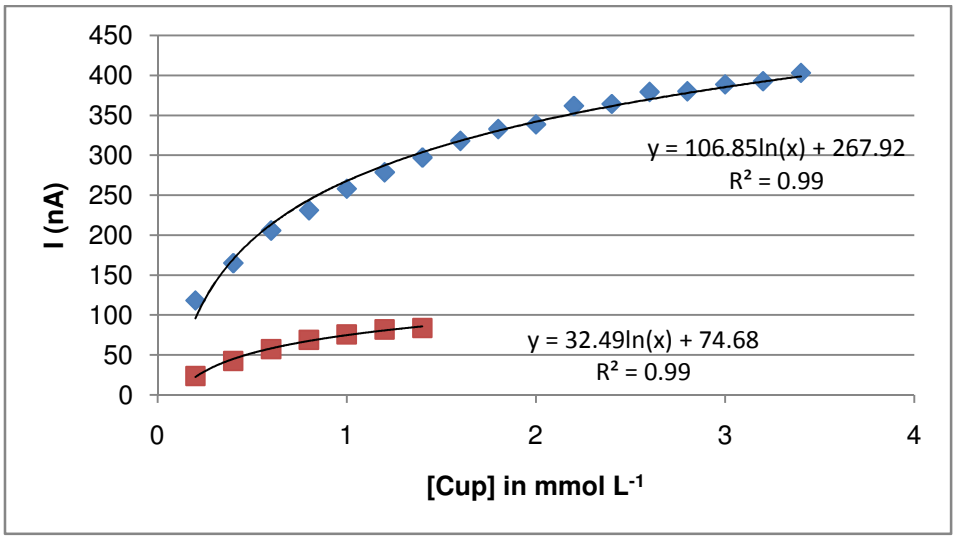

Figure 51. Plot of the peak current vs. the added cupferron concentrations. The blue squares show the increase of the peak current in MQ and the red squares show the increase of the peak current with the added cupferron in seawater

Table 5. Summary of cupferron-addtions (0.1 mol L^{-1}) and the composition of the calculated Nb:cupferron complexes.

pH	cupferron	Reagents*		Name
6.0	1	MQ	150µL $KBrO_3$	11051200_081006-CupfAdd01.dth
6.1	1	MQ		080606-Nb-MES-C2.dth
6.5	2	MQ		080606-Nb-MES-C1.dth
6.8	2	MQ		11061317_081007-CupfAdd03.dth
6.5	2	SW	150µL $KBrO_3$	11051327_081006-CupfAdd02.dth
7.1	2	SW		11061412_081007-CupfAdd04.dth

*In all of the determinations were used 10 mL MQ or seawater, 100 µL 1 mol L^{-1} buffer and 100 µL 11.09 µmol L^{-1} Nb. The $KBrO_3$ solution was 0.4 mmol L^{-1} (Baes and Mesmer 1976).

Table 5 shows a summary of the cupferron-additions in MQ and seawater and the determination of the Nb:cupferron complexes with the calculation of Baes and Mesmer (1976). In MQ until pH 6.1 a 1:1 Nb:cupferron complex was determined. It did not matter whether an oxidizing agent was used in the determination or not.

From pH 6.5 to 7.1 a 1:2 Nb:cupferron complex was determined. It made no difference if the determination was done in MQ or in seawater and whether KBrO3 was added or not.

5.1.5 Voltammetric/Polarographic Nb determination with N-benzoyl-N-phenylhydroxylamine (BPHA)

Name	07221417_080722-Nb-test04.dth
pH value	6.1
Peak position	-1.039 V
Reagents	10 mL MQ 100 µL 1 mol L^{-1} MES buffer 20 µL 11.09 µmol L^{-1} Nb 20 µL 0.1 mol L^{-1} BPHA
Additions	1st to 3rd addition: 20 µL 11.09 µmol L^{-1} Nb 4th: 100 µL 11.09 µmol L^{-1} Nb

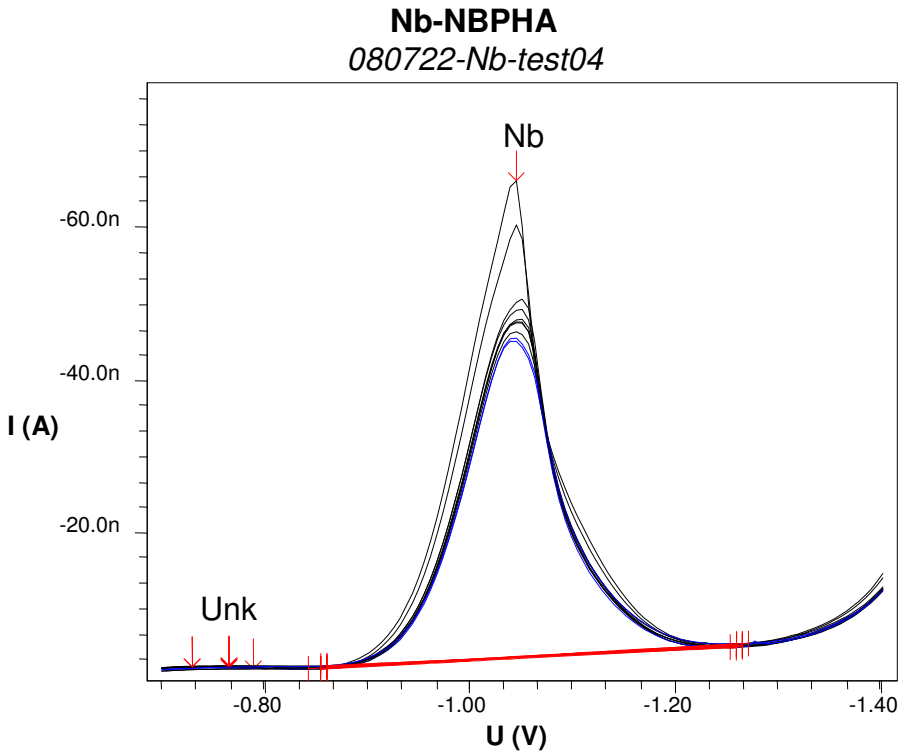

Figure 52. Current-voltage curves for 21.5, 42.9, 64.2, 85.4, 190.3 nmol L^{-1} Nb(V) in 10 mL 10 mmol L^{-1} MES buffer (pH 6.1) containing 200 µmol L^{-1} BPHA.

Comparing the complexing agents cupferron and BPHA, it can be seen that the peak position is shifted to a more negative potential with BPHA than with cupferron. Figure 52 shows the peak position for the polarogrographic determination of Nb at pH 6.1 in 10 mmol L^{-1} MES with 200 µmol L^{-1} BPHA at -1.039 V.

The replicates were far apart from each other and therefore the R^2 value was not acceptable with 0.93 (see Figure 53). The sensitivity of this polarographic determination of Nb with BPHA was S = 0.11 nA nmol^{-1} L.

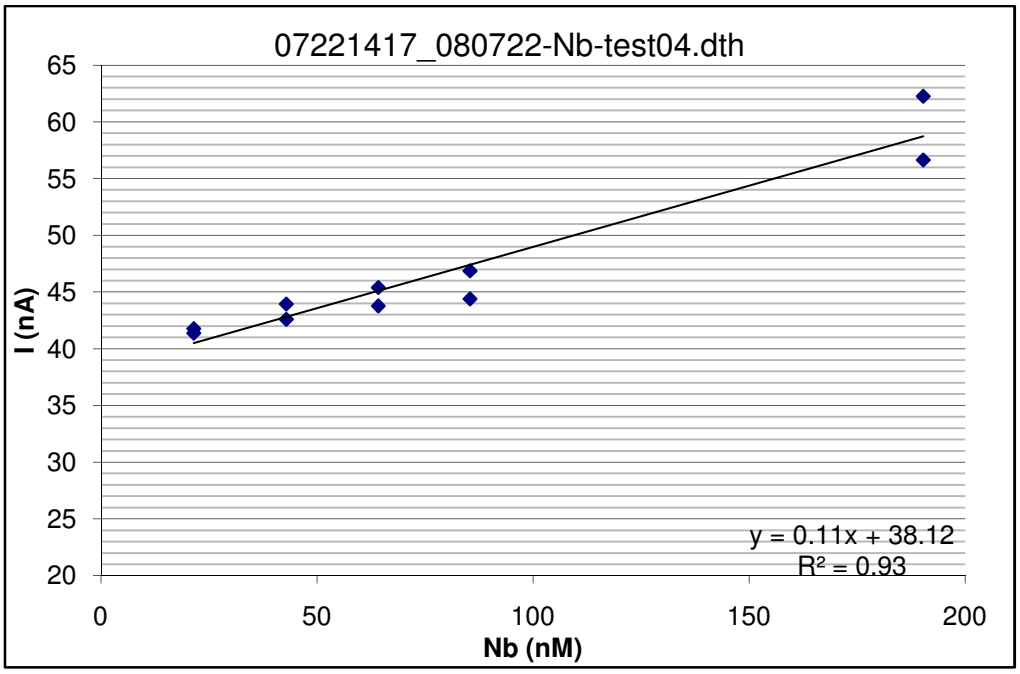

Figure 53. Plot of the measured peak currents as a function of the added Nb concentrations.

To be able to detect a peak around pH 8 in 10 mmol L^{-1} EPPS buffer containing 200 µmol L^{-1} BPHA, the Nb concentration had to be increased to 200 nmol L^{-1}.
Between pH 4 and 6 in 0.1 mol L^{-1} acetate buffer which contained 200 µmol L^{-1} BPHA only high Nb concentrations like 200 nmol L^{-1} could be detected, too. Another problem was that the peak shifted from -0.950 V with each addition of 200 nmol L^{-1} Nb -0.05 V to a more positive potential. Furthermore the peak current of the first addition was higher than for the second addition of 215 nmol L^{-1} Nb. Hence the correlation between the peak current and the added Nb concentration is not linear with a R^2 value of 0.73. The sensitivity of this Nb determination is fine with S = 0.51 nA nmol^{-1} L, but this only due to the high peak currents after the first addition and the fact that only two additions were conducted and not more (see Figure 54).

Name	07221621_080722-Nb-test08.dth
pH value	5.1
Peak position	-0.950 V to -0.859 V
Reagents	10 mL MQ 100 µL 1 mol L^{-1} acetate buffer 20 µL 110.9 µmol L^{-1} Nb 20 µL 0.1 mol L^{-1} BPHA
Additions	twice 20 µL 110.9 µmol L^{-1} Nb

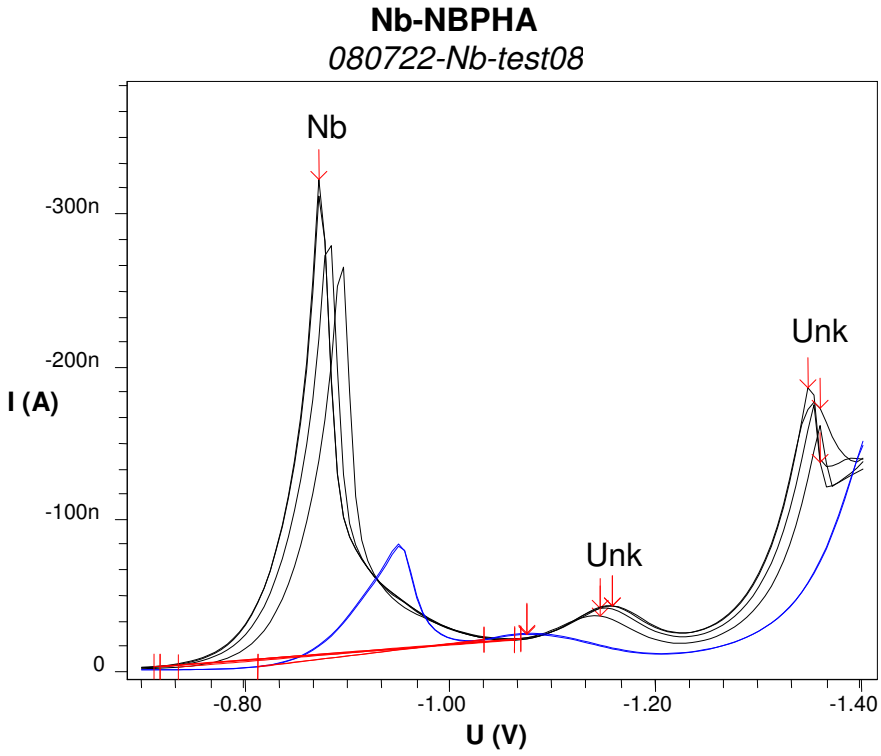

Figure 54. Current-voltage curves for 214.8, 428.8 and 641.9 nmol L^{-1} Nb(V) in 10 mL 0.1 mol L^{-1} acetate buffer (pH 5.1) containing 200 µmol L^{-1} BPHA.

In order to increase the sensitivity, first 150 µL 0.36 mmol L^{-1} $KBrO_3$ (200 µmol L^{-1} BPHA) were added and as a second test more BPHA (2 mmol L^{-1}) was used. Each polarographic determination was done under the same conditions in 10 mL 10 mmol L^{-1} MES buffer (pH 6). With an increase of the complexing agent concentration the same phenomena occurred as described above. With the first addition the peak current rose a lot, but with further additions only small changes were detected. Using this high concentrations of BPHA, sometimes a white precipitate could be seen after the measurement on the walls of the Teflon cell.

Name	07231400_080723-Nb-test06.dth
pH value	6.1
Peak position	-0.116 V
Reagents	10 mL MQ 100 µL 1 mol L^{-1} MES buffer 20 µL 11.09 µmol L^{-1} Nb 200 µL 0.1 mol L^{-1} BPHA
Additions	twice 20 µL 11.09 µmol L^{-1} Nb

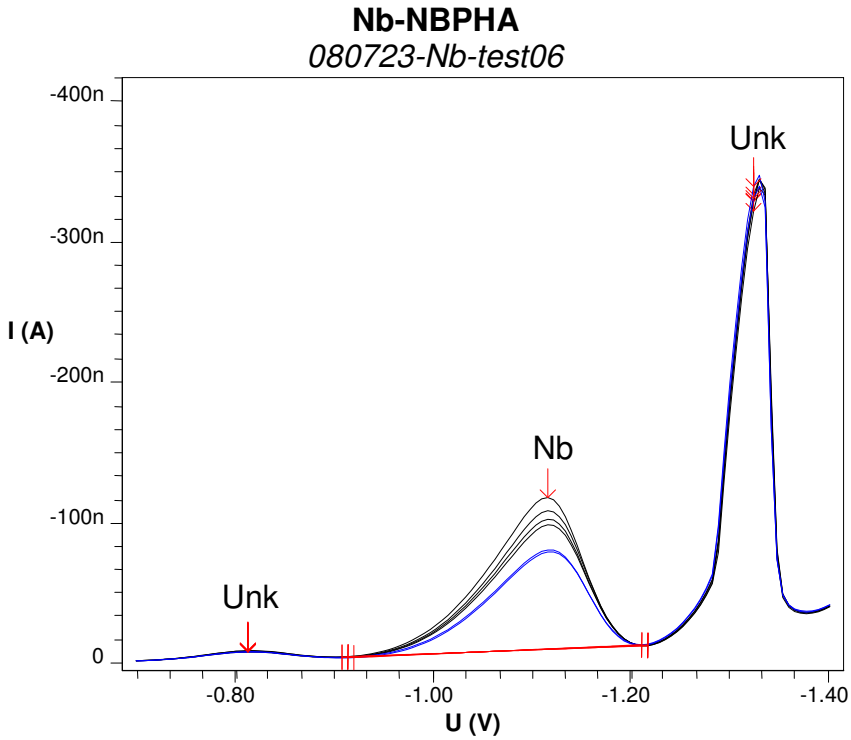

Figure 55. Current-voltage curves for 21.5, 42.9 and 64.2 nmol L^{-1} Nb(V) in 10 mL 0.1 mol L^{-1} MES buffer (pH 6.1) containing 2 mmol L^{-1} BPHA.

Figure 55 shows the current-voltage curves for smaller Nb additions (20 nmol L^{-1}) in 10 mL 10 mmol L^{-1} MES buffer (pH 6.12) containing 2 mmol L^{-1} BPHA. The peak current nicely increased without moving to a more positive potential, but the peak is quite broad and the values of the replicates of the second addition are not very close together. This can clearly be seen in Figure 55 and Figure 56. Still the R^2 value is fine with 0.94. The sensitivity is very good with S = 0.78 nA $nmol^{-1}$ L.

In a reproduction of this measurement the sensitivity was nearly as good as before with S = 0.70 nA $nmol^{-1}$ L, but the linear correlation of the Nb concentration and the peak current was poor with R^2 = 0.82. This was due to the fact that the peak currents

of the first addition and its replicate were high in comparison to the other peak currents.

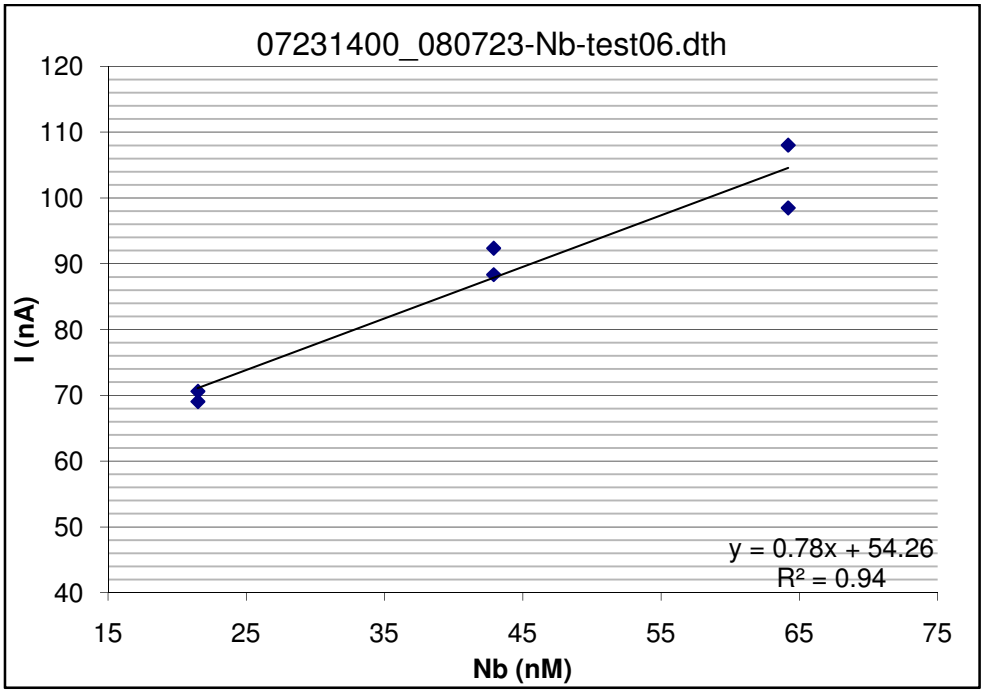

Figure 56. The measured peak currents are plotted as a function of the added Nb concentrations.

5.1.5.1 Nb determination by DPCSV with BPHA and an oxidizing agent in a MES buffered solution at pH 6

Name	07231449_080723-Nb-test08.dth
pH value	6.1
Peak position	-0.116 V
Reagents	10 mL MQ 100 µL 1 mol L^{-1} MES buffer 20 µL 11.09 µmol L^{-1} Nb 200 µL 0.1 mol L^{-1} BPHA 150 µL 0.36 mmol L^{-1} $KBrO_3$
Additions	twice 20 µL 11.09 µmol L^{-1} Nb

With the addition of the oxidizing agent the measurements were less sensitive under the same conditions. The sensitivity decreased from $S = 0.78$ nA nmol^{-1} L without $KBrO_3$ to $S = 0.29$ nA nmol^{-1} L with 5.4 µmol L^{-1} $KBrO_3$ (see Figure 57). Due to the fact that the peak currents of the replicates of the first addition (42.9 nmol L^{-1} Nb) were higher than those of the second addition (64.2 nmol L^{-1} Nb), the correlation is

not linear with $R^2 = 0.28$. Besides even without any addition the replicate measurements of 21.5 nmol L^{-1} Nb showed small agreement.

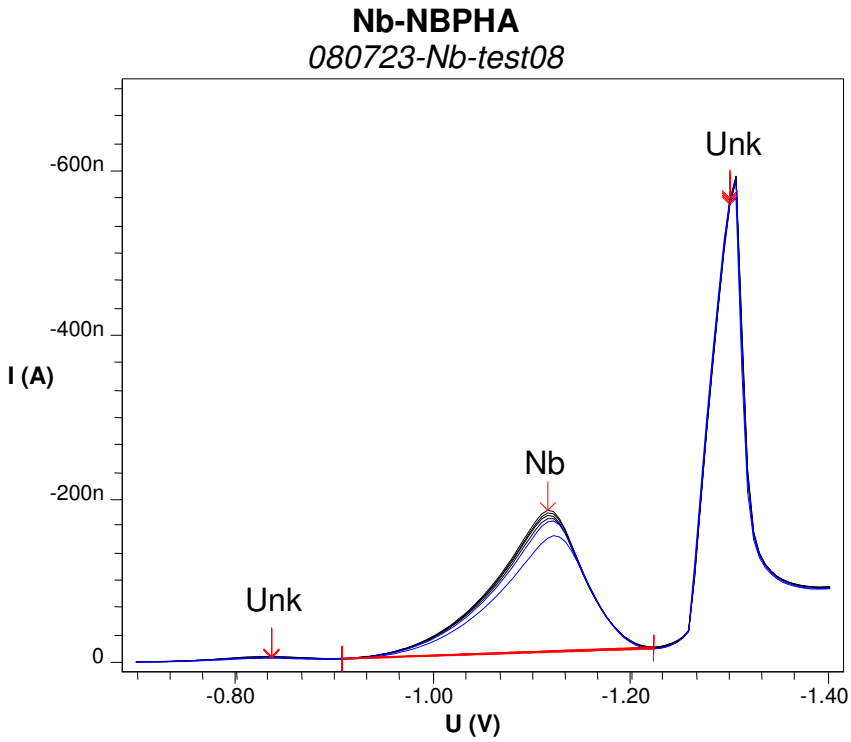

Figure 57. Current-voltage curves for 21.5, 42.9 and 64.2 nmol L^{-1} Nb(V) in 10 mL 10 mmol L^{-1} MES buffer (pH 6.1) containing 2 mmol L^{-1} BPHA and 5.39 µmol L^{-1} $KBrO_3$.

5.1.6 Polarographic determination of Nb with BPHA in seawater

Name	07231538_080723-Nb-test10.dth
pH value	6.47
Peak position	-1.236 V
Reagents	10 mL SW M68-3 100 µL 1 mol L^{-1} MES buffer 20 µL 11.09 µmol L^{-1} Nb 200 µL 0.1 mol L^{-1} BPHA
Additions	twice 20 µL 11.09 µmol L^{-1} Nb

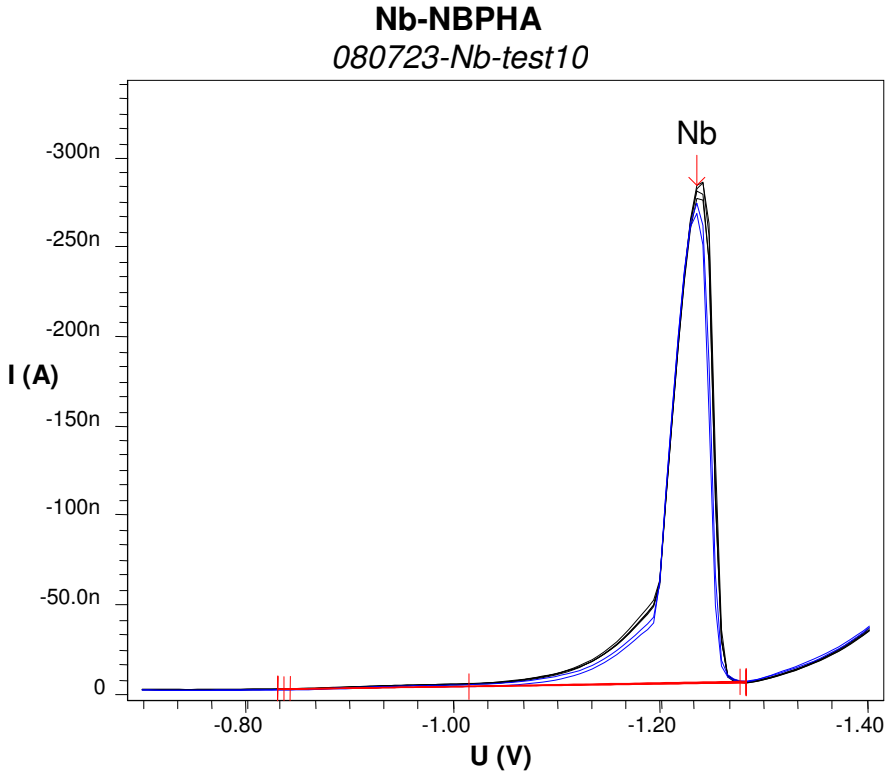

Figure 58. Current-voltage curves for 10 mL SW M 68-3 (pH 6.5) containing 0, 21.5, 42.9 nmol L^{-1} added Nb(V), 10 mmol L^{-1} MES buffer and 2 mmol L^{-1} BPHA.

Figure 58 shows the current-voltage curves for 10 mL seawater containing 10 mmol L^{-1} MES and 2 mmol L^{-1} BPHA with two additions of 20 µL 107.6 µmol L^{-1} Nb solution. The peak currents are enormous with 260-280 nA at -1.236 V.

Figure 59 displays the plot of the added Nb concentrations (0, 21.5, 42.9 nmol L^{-1}) as a function of these peak currents. Since the values of the replicates are not very close, R^2 is 0.86. The sensitivity of this measurement was good with a values of S = 0.30 nA $nmol^{-1}$ L.

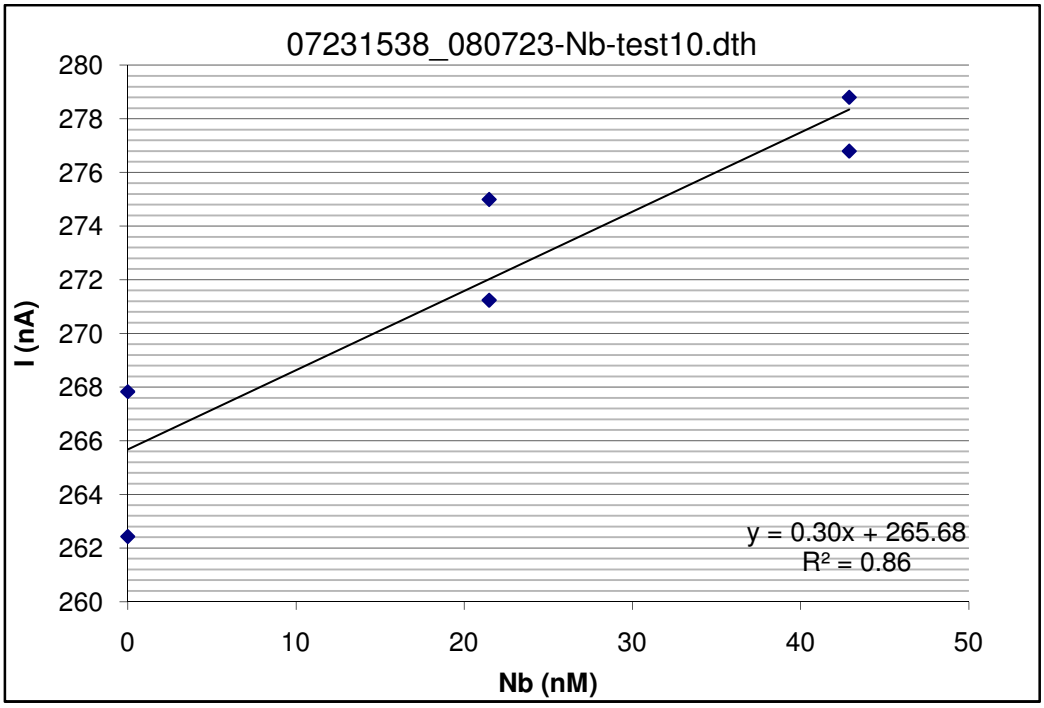

Figure 59. Plot of the measured peak current as a function of the added niobium concentrations for 10 mL SW M68-3 (pH 6.5) containing 10 mmol L^{-1} MES and 2 mmol L^{-1} BPHA.

5.1.6.1 Nb determination by DPCSV with BPHA and an oxidizing agent in seawater buffered by MES to pH 6

Name	07231512_080723-Nb-test09.dth
pH value	6.5
Peak position	-1.241 V
Reagents	10 mL SW M68-3 100 µL 1 mol L^{-1} MES buffer 200 µL 0.1 mol L^{-1} BPHA 150 µL 0.36 mmol L^{-1} $KBrO_3$ solution
Additions	twice 20 µL 11.09 µmol L^{-1} Nb

In Figure 60 the same measurement as in Figure 58 just with the addition of 5.4 µmol L^{-1} $KBrO_3$ can be observed. The high current-voltage curves give a good correlation to the added amount of Nb and therefore the R^2 value is 0.93.

With the addition of 150 µL 0.36 mmol L^{-1} $KBrO_3$-solution, the sensitivity could be increased from S = 0.30 nA $nmol^{-1}$ L to S = 0.36 nA $nmol^{-1}$ L.

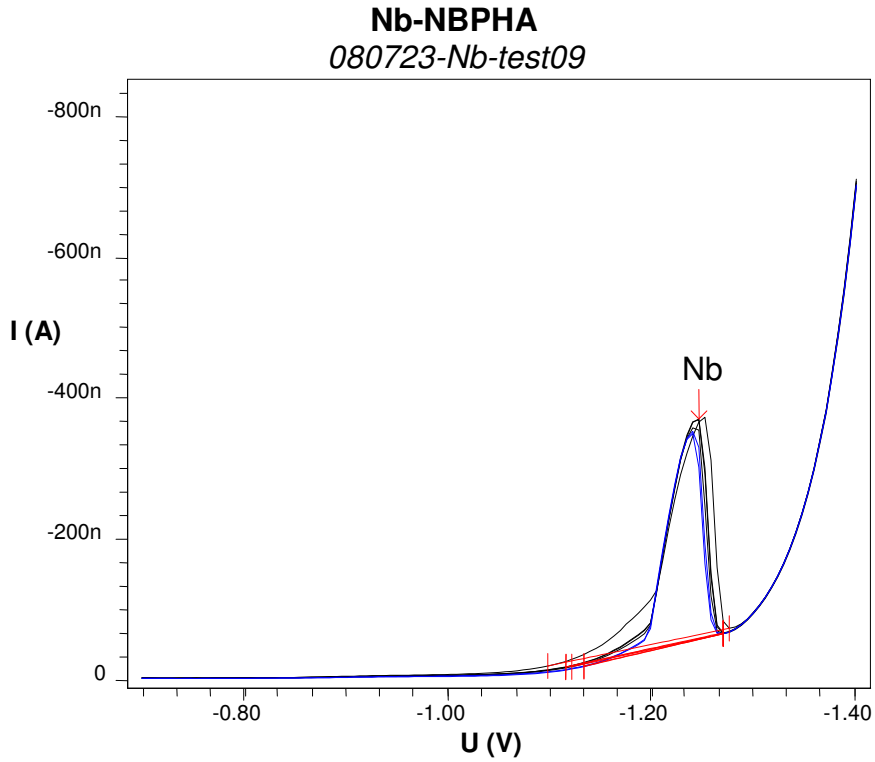

Figure 60. Current-voltage curves for 10 mL SW M 68-3 (pH 6.5) containing 0, 21.5, 42.9 nmol L^{-1} Nb(V), 10 mmol L^{-1} MES buffer, 5.4 µmol L^{-1} $KBrO_3$ and 2 mmol L^{-1} BPHA.

5.1.7 Summary of the Nb determination with N-benzoyl-N-phenylhydroxylamine (BPHA)

Because of the fact that the peak position of the polarographic Nb determination is shifted to a more negative potential, it seems that BPHA is a stronger chelator for Nb than cupferron. But the Nb-BPHA complex is less easily reduced than the Nb-cupferron complex, and therefore the catalytic cycle as with cupferron is not allowed to take place. Furthermore the catalytic cycle is not enhanced by the presence of the additional oxidizing agent $KBrO_3$ suggesting that the limiting factor is the reduction of the Nb-BPHA complex.

5.1.8 Spectrophotometric Nb determination with 4-(2-pyridylazo)-resorcinol

5.1.8.1 Spectrophotometric Nb determination with 4-(2-pyridylazo)-resorcinol and citrate in a 1 cm cuvette (Yamada et al. 1990)

Name	080817-Nb-PAR
pH value	4.5
Wavelength	550.28 nm
Reagents	As shown in Table 6
Cell	1 cm quartz cuvette

Table 6. Design for a 1 cm cell (Yamada et al. 1990). The buffer includes 200 µL 50 mmol L^{-1} citrate and 200 µL 0.85 mmol L^{-1} ammonia acetate Buffer (pH 4.5). λ_{max} = 550 nm.

Sample No.	MQ (mL)	Buffer (mL)	110 µmol L^{-1} Nb (µL)	5 mmol L^{-1} PAR (µL)	Total Vol (mL)	[Nb] µmol L^{-1}	expected absorbance	[PAR] µmol L^{-1}
1	4.5	0.4	0	100	5	0	0.000	100
2	4.4	0.4	100	100	5	2.16	0.074	100
3	4.3	0.4	200	100	5	4.31	0.148	100
4	4.2	0.4	300	100	5	6.46	0.222	100
5	4.1	0.4	400	100	5	8.61	0.296	100
6	4.0	0.4	500	100	5	10.77	0.370	100

Table 6 shows the design for the spectrophotometric determination of Nb with PAR in a 1 cm cell at pH 4.5 with similar concentrations like those used by Yamada et al. (1990).

Figure 61 shows the absorption spectra of Nb-PAR in solutions containing 2 mmol L^{-1} citrate, 34 µmol L^{-1} ammonia acetate buffer and 0.1 mmol L^{-1} PAR. With an increasing Nb concentration (0-10 µmol L^{-1}) the absorption at the wavelength 550 nm (marked by the green vertical line in Figure 61) increased obviously. In Figure 62 the absorbance is plotted versus the Nb concentration, there is a good linear correlation due to a R^2 value of 0.99. The molar absorptivity can be calculated by multiplying the value of the slope by the length of the cell.

The molar absorptivity here was ε_{mol} = 70,459 mol^{-1} dm^3 cm^{-1} with c(cit) = 2 mmol L^{-1}. This value is far higher than the published data by Yamada et al. (1990) with a molar absorptivity of ε_{mol} = 34,400 mol^{-1} dm^3 cm^{-1} and with a higher citrate concentration of 15-20 mmol L^{-1}.

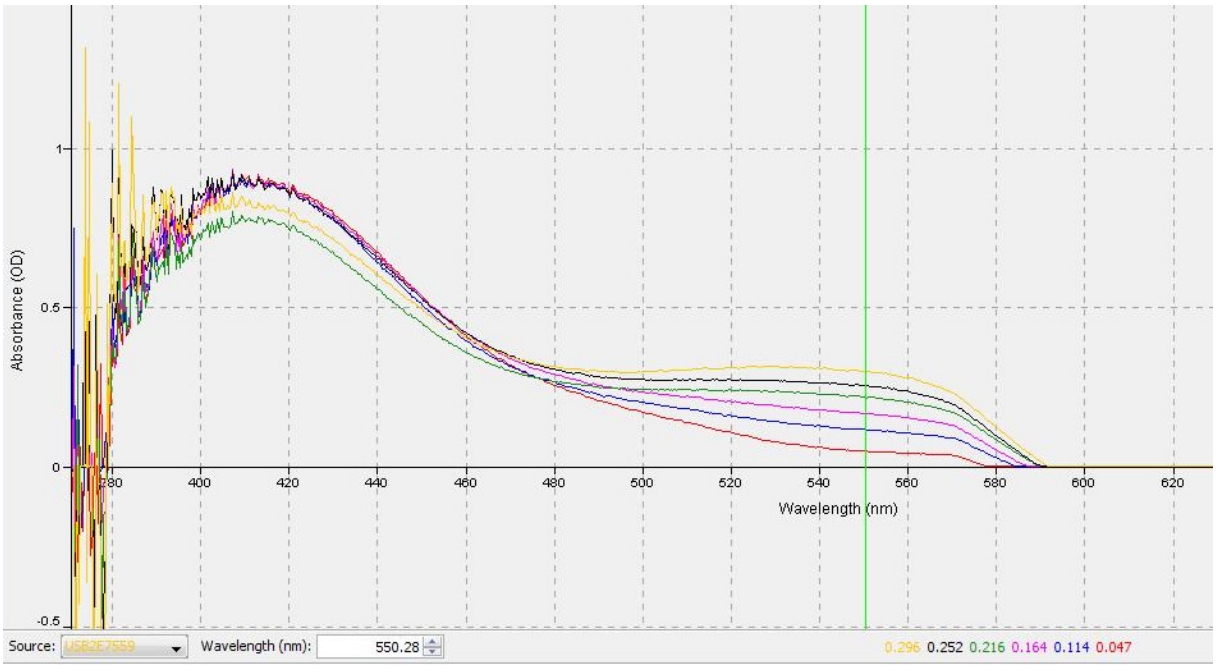

Figure 61. Absorption spectra of Nb-PAR-cit with 6 increasing Nb concentrations (0, 2.15, 4.30, 6.46, 8.61 and 10.76 µM) with the parameters: integration time: 200 msec, scans to average: 5, boxcar width: 10.

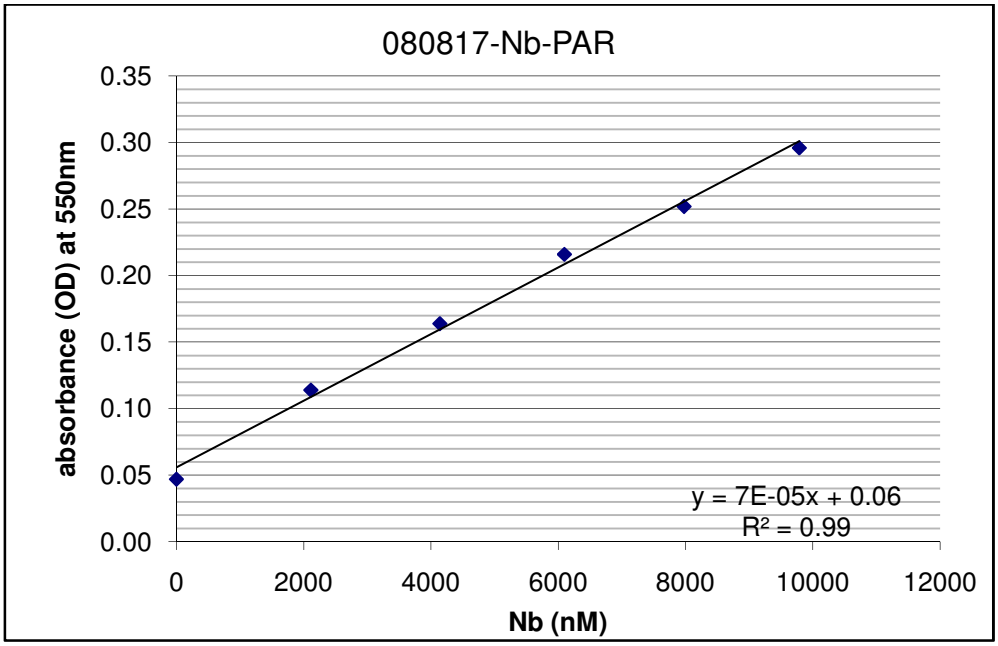

Figure 62. Plot of the absorbance (OD) changes at 550 nm as a function of the Nb concentrations (0, 2.15, 4.30, 6.46, 8.61 and 10.76 µmol L^{-1}).

5.1.8.2 Spectrophotometric Nb determination with 4-(2-pyridylazo)-resorcinol and citrate in a 10 cm quartz cuvette

Table 7. Design for a 10 cm cell. The buffer includes 60 µL 50 mmol L^{-1} citrate and 60 µL 1 mol L^{-1} buffer. λ_{max} = 550 nm.

Sample No.	MQ (mL)	Buffer (mL)	110 µmol L^{-1} Nb (µL	5 mmol L^{-1} PAR (µL)	Total Vol (mL)	[Nb] µmol L^{-1}	expected absorbance	[PAR] µmol L^{-1}
1	14.85	0.12	0	30	15	0	0.000	10
2	14.83	0.12	20	30	15	0.14	0.049	10
3	14.81	0.12	40	30	15	0.29	0.099	10
4	14.79	0.12	60	30	15	0.43	0.148	10
5	14.77	0.12	80	30	15	0.57	0.197	10
6	14.75	0.12	100	30	15	0.72	0.247	10

Table 7 shows the composition of the different reagents for a 10 cm cell. The pH is varied by using different 1 mol L^{-1} Good's buffers. The sample sets contained 10 nmol L^{-1} PAR and 20 nmol L^{-1} citrate. After preparing the sample set, they were allowed to stand for 1.5 h so that the coloured Nb-PAR complex had some time to form.

Name	080826-Nb-PAR-MES
pH value	6.0
Wavelength	550.18 nm
Reagents	As shown in Table 7 with 60 µL 1 mol L^{-1} MES buffer
Cell	10 cm quartz cuvette

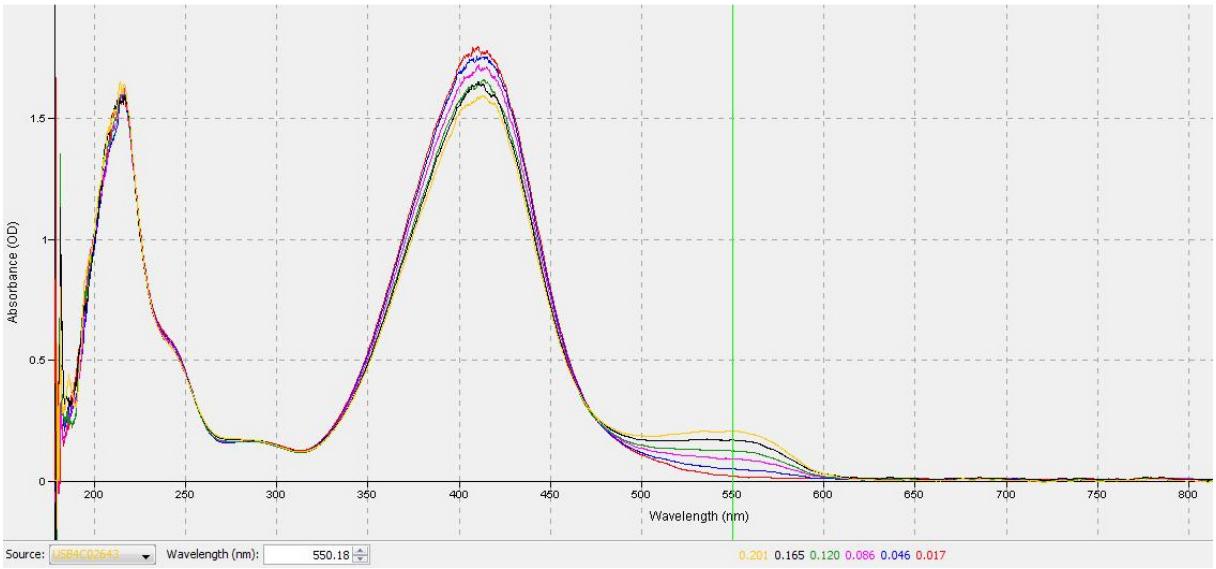

Figure 63. Absorption spectra of Nb-PAR-cit at pH 6 with six increasing niobium concentrations (0, 0.14, 0.28, 0.43, 0.57 and 0.71 µmol L^{-1}).

The correlation between the absorbance at 550 nm and the Nb concentration was linear with R^2 values from 0.96 to 1. Figure 63 shows an example for the absorption spectra for one measurement at pH 6 containing 8 mmol L^{-1} MES and 6 increasing amounts of Nb (0, 0.14, 0.28, 0.43, 0.57 and 0.71 µmol L^{-1}). It can be seen that the peak at 410 nm was decreasing while at 550 nm a peak was increasing.

Figure 64 shows the important detail of Figure 63. It is obvious that the peak around 550 nm developed with the increasing amount of Nb. The absorbance at 550 nm is plotted as a function of the Nb concentration in Figure 65. The apparent molar absorptivity is ε_{mol} = 26,579 mol^{-1} dm^3 cm^{-1}.

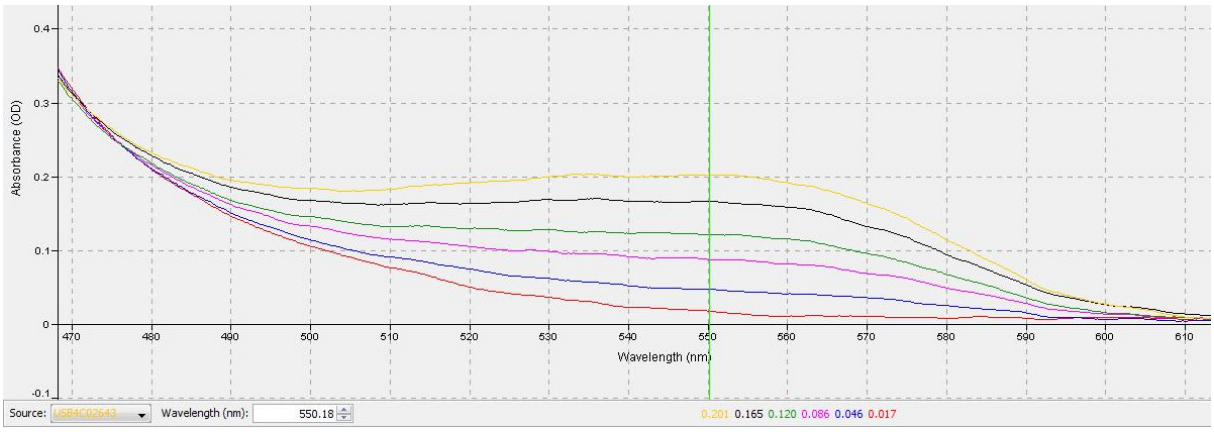

Figure 64. Detail of the absorption spectra of Nb-PAR-cit at pH 6 with 6 increasing Nb concentrations (0, 0.14, 0.28, 0.43, 0.57 and 0.71 µmol L^{-1}).

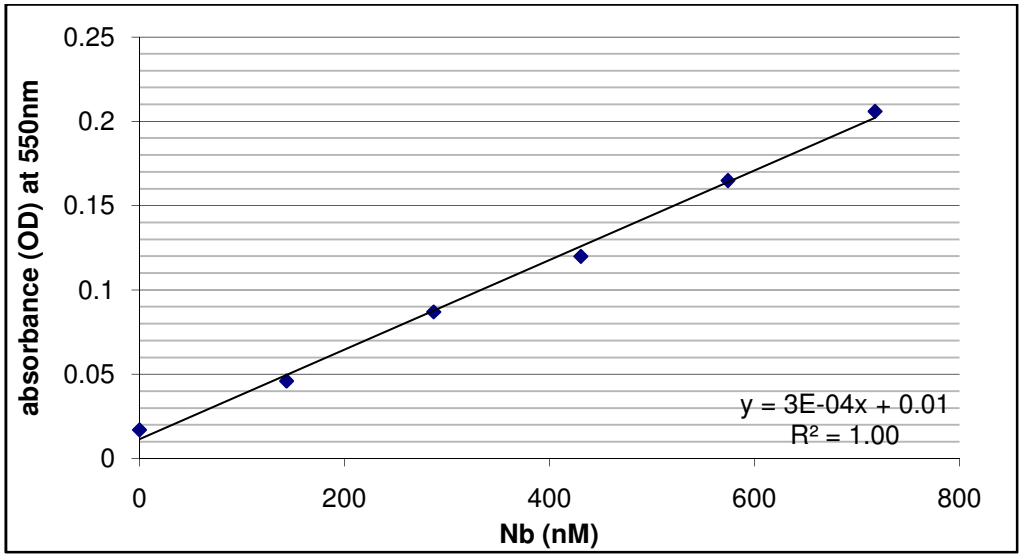

Figure 65. Plot of the absorbance (OD) changes at 550 nm as a function of the Nb concentrations (0, 0.14, 0.28, 0.43, 0.57 and 0.71 µmol L^{-1}).

5.1.8.3 Spectrophotometric Nb determination with 4-(2-pyridylazo)-resorcinol and citrate at varying pH

Table 8 shows the reagent design which was used in all of the spectrophotochemical measurements. The absorbance was measured at 550 nm and a 10 cm cell was used. A maximal value for the molar absorptivity of $\varepsilon_{mol}(max)$ = 70,000 mol^{-1} dm^3 cm^{-1} was assumed. By dividing the molar absorptivity through the maximal molar absorptivity the result is % Nb-PAR to know how much of this complex is formed under these pH conditions. Formula 5.1 shows the relative increase in the side reaction for hydroxide dominated Nb species.

$$\log(aNb(OH)) = \log \frac{1}{Nb(PAR)-1} \qquad (5.1)$$

Table 8. Results of the measurements at 550 nm with $\varepsilon_{mol}(max)$ = 70,000 mol^{-1} dm^3 cm^{-1}.

pH	ε_{mol} (mol^{-1} dm^3 cm^{-1})	%NbPAR	%NbOH	log(%NbOH)	Name
4.5	70,000	100.00%			080817-Nb-PAR
5.99	26,578	37.97%	62.03%	-0.21	080826 MES
6.26	21,741	31.06%	68.94%	-0.16	080827 PIPES1
6.63	11,442	16.35%	83.65%	-0.08	080829 PIPES2
6.87	6,651	9.50%	90.50%	-0.04	080827 PIPES0
6.92	3,507	5.01%	94.99%	-0.02	080826 PIPES

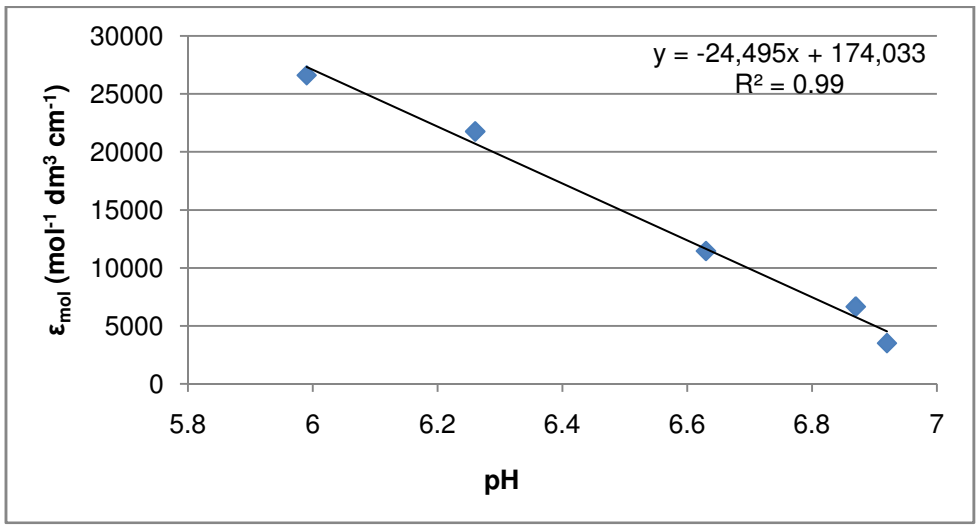

Figure 66. Molar absorptivity vs. pH. Data from Table 8.

Figure 66 shows that the molar absorptivity strongly decreases with the increase of the pH $\varepsilon_{mol}(pH)$ = 24,495 mol^{-1} dm^3 cm^{-1} pH^{-1}.

In Figure 67 the log(aNb(OH)) is plotted as a function of the pH. The slope of this plot is 0.2 at pH 6-7.

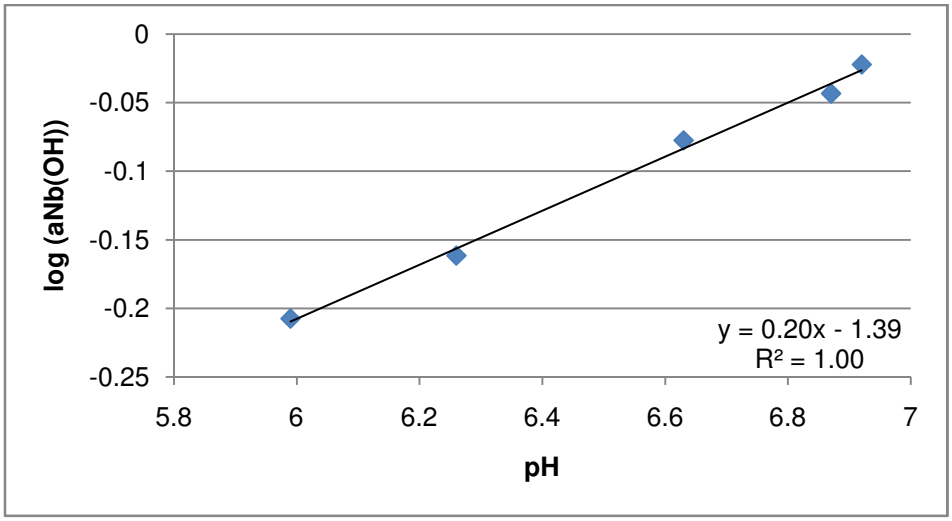

Figure 67. Plot of the log(% Nb(OH)) as a function of the pH value.

The point at which a 1:1 hydroxide dependency is reached, also implies a log pKa = 5.87 for the transition from $Nb(OH)_5$ to $Nb(OH)_6^-$ (see Table 8).
Figure 68 shows the plot of the percentage of each Nb species versus the pH. In this plot log pKa = 7.82 is implied for the transition from $Nb(OH)_5$ to $Nb(OH)_6^-$ (Baes and Mesmer 1976; Byrne 2002). In a calculation with the data published by Wagman et al. (1982) this takes place at log pKa = 7.34 (see Figure 69).

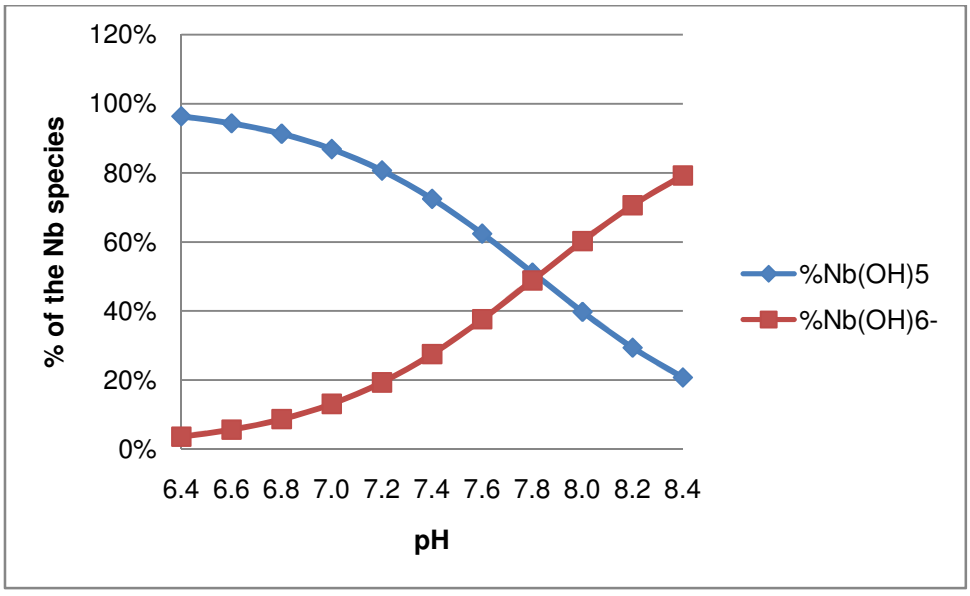

Figure 68. Plot of the percentage of the Nb species vs the pH (Baes and Mesmer 1996; Byrne 2002)

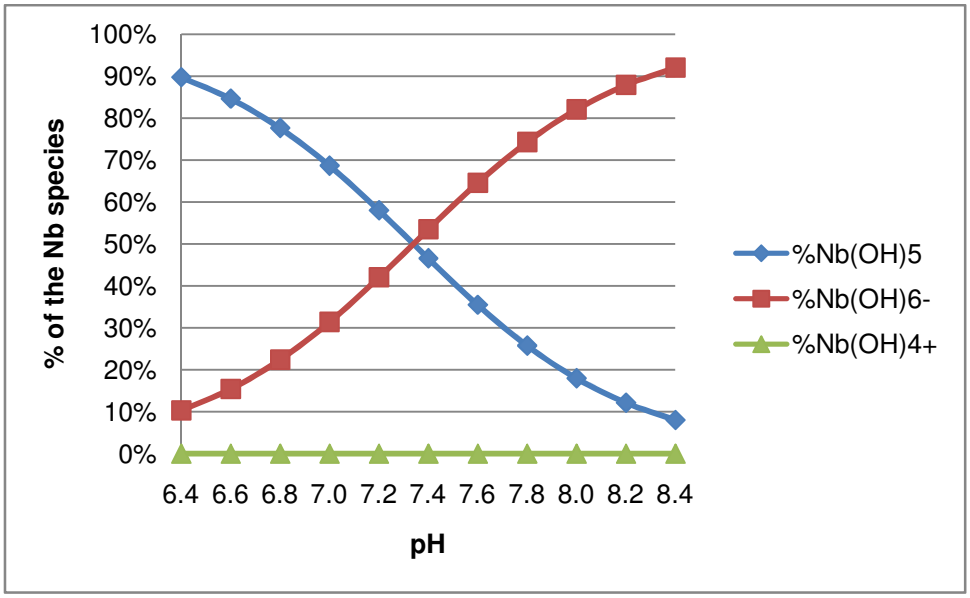

Figure 69. Plot of the percentage of the Nb species vs the pH (Wagman et al. 1982).

5.1.8.4 Spectrophotometric Nb determination with higher concentrations of 4-(2-pyridylazo)-resorcinol

For the increase of the apparent molar absorptivity a ten times higher PAR concentration (0.1 µmol L^{-1}) was used than before. The concentrations of the other reagents stayed the same and the design can be seen in Table 9.

Table 9. Design for a 10 cm cell with an increased amount of PAR.

Sample No.	MQ (mL)	Buffer (mL)	110 µmol L^{-1} Nb (µL	5 mmol L^{-1} PAR (µL)	Total Vol (mL)	[Nb] µmol L^{-1}	expected absorbance	[PAR] µmol L^{-1}
1	14.58	0.12	0	300	15	0	0.000	100
2	14.56	0.12	20	300	15	0.14	0.049	100
3	14.54	0.12	40	300	15	0.29	0.099	100
4	14.52	0.12	60	300	15	0.43	0.148	100
5	14.50	0.12	80	300	15	0.57	0.197	100
6	14.48	0.12	100	300	15	0.72	0.247	100

The apparent molar absorptivity was increased by increasing the PAR concentration, but the samples needed a longer equilibration time than 1.5 h. With an equilibration time of 1.5 h at pH 6.9 (080826-PIPES) with 10 mmol L^{-1} PAR the apparent molar absorptivity was ε_{mol} = 3,507 mol^{-1} dm^3 cm^{-1} and with 100 mmol L^{-1} PAR at pH 7.0 ε_{mol} = 32,602 mol^{-1} dm^3 cm^{-1} (080829-PIPES1). With an increase of the equilibration time to 7 h the molar absorptivity could be increased to ε_{mol} = 34,971 mol^{-1} dm^3 cm^{-1} (080903-PIPES1). With a 10 times higher PAR concentration, the apparent molar

absorptivity also increased by 10. This means, that the increase of the apparent molar absorptivity is essentially 1:1 with the PAR concentration indicating that at this pH still a 1:1 Nb-PAR complex is formed.

Figure 70 shows the plot of the absorbance at 550 nm as a function of the elapsed time. The dissociation rate for Nb-citrate was measured under the assumption that the Nb-PAR formation is faster (see equation 5.2):

$$\text{Nb-cit} \rightarrow \text{Nb} + \text{cit} \qquad (5.2)$$

Sample 6 with a Nb concentration of 0.72 µmol L^{-1} was used for this experiment. The blue data points are the measured absorbance. The red data points show the estimated data points. The difference between those two absorbances is quite small here. The estimated half life for the developing Nb-PAR species is therefore $\tau_{1/2}$ = 53.74 min in this 1st order reaction.

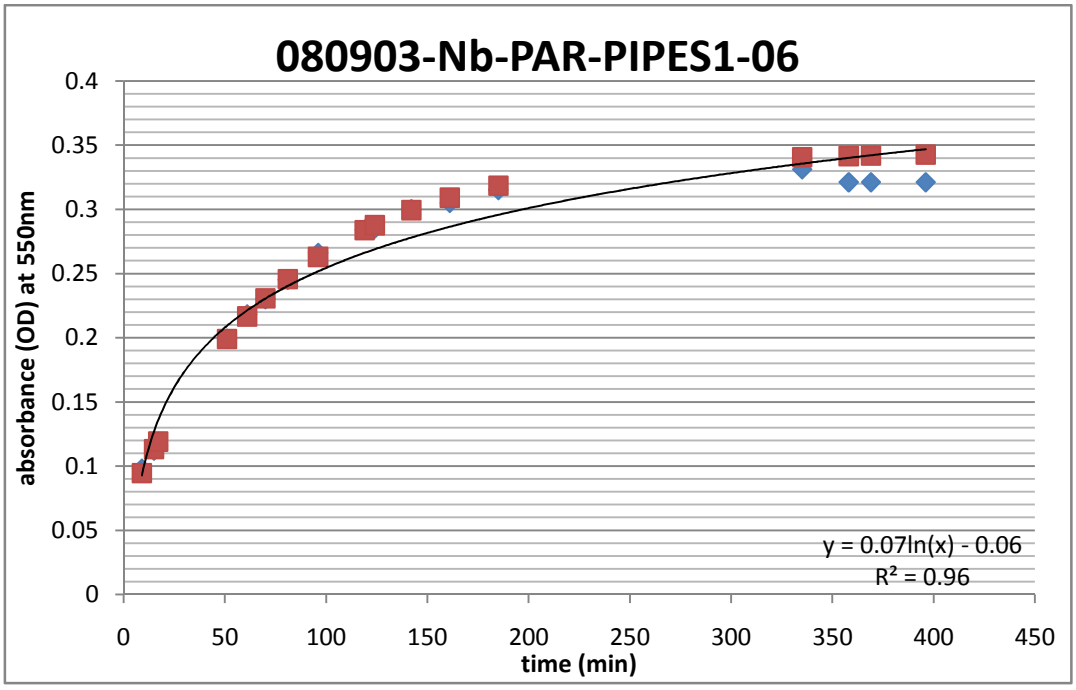

Figure 70. Plot of the absorbance (OD) at 550 nm vs. the elapsed time. Sample 6 with 0.72 µmol L^{-1} Nb at pH 7. Blue data points are the measured absorbance. The red data points show the estimated data points.

5.1.8.5 Spectrophotometric Nb determination with 4-(2-pyridylazo)-resorcinol but without citrate

Instead of 60 µL buffer and 60 µL citrate, 120 µL 1 mol L^{-1} EPPS buffer was used. Table 9 shows the amounts of the other reagents that were used. Alimarin and Savvin (1966) had published that the colour change is due to the formation of the ternary complex Nb-PAR-cit.

Again the sample no. 6 the one with the highest Nb concentration (0.72 µmol L^{-1}) was used to estimate the half life of 081007-Nb-PAR-MQ-EPPS1noCit as $\tau_{1/2}$ = 1.14 min. Figure 71 shows that the absorbance changed only very little with the time. But the measured absorbance (blue) and the estimated absorbance (pink) differed by the factor 4. The measured absorbance should have been higher than it was. The main reason for this lower value is the stronger hydroxide contribution at this pH.

The molar absorptivity at pH 8 was ε_{mol} = 7,116 mol^{-1} dm^3 cm^{-1} for this experiment

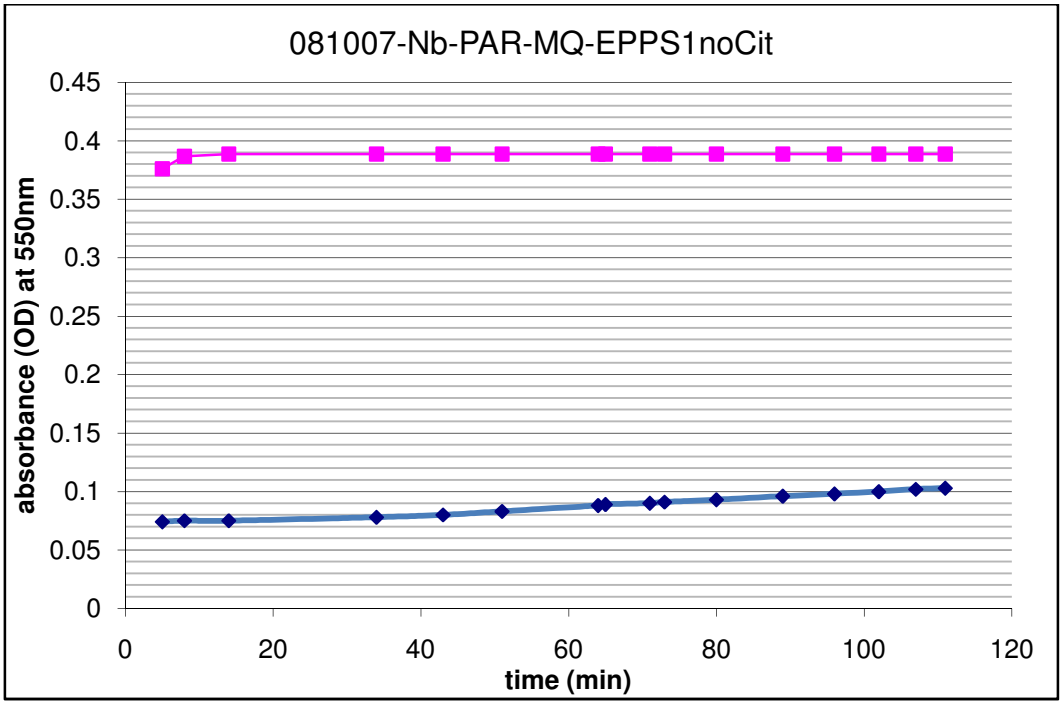

Figure 71. Absorbance (OD) at 550 nm vs. the elapsed time. Sample 6 with 0.72 µmol L^{-1} Nb at pH 8. Blue data points show the measured absorbance. The pink data points show the estimated data points.

5.1.9 Spectrophotometric Nb determination with 4-(2-pyridylazo)-resorcinol and citrate in seawater at varying pH

Table 10. Design for a 10 cm cell for the spectrophotochemical determination of Nb in seawater.

Sample No.	SW M68-3 (mL)	1 mol L^{-1} Buffer (mL)	110 µmol L^{-1} Nb (µL)	5 mmol L^{-1} PAR (µL)	Total Vol (mL)	[Nb] µmol L^{-1}	expected absorbance	[PAR] µmol L^{-1}
1	14.58	0.12	0	300	15	0	0.000	100
2	14.56	0.12	20	300	15	0.14	0.049	100
3	14.54	0.12	40	300	15	0.29	0.099	100
4	14.52	0.12	60	300	15	0.43	0.148	100
5	14.50	0.12	80	300	15	0.57	0.197	100
6	14.48	0.12	100	300	15	0.72	0.247	100

Table 10 shows the reagents and their concentrations which were used in the following spectrochemical Nb determinations in seawater. The baseline of the measured seawater samples mostly shifted quite a bit and therefore the baseline shifts had to be substracted to get comparable values.

Name	080903-Nb-PAR-PIPES-SW1
pH value	6.8
Wavelength	550.18 nm
Reagents	As shown in Table 10 with 60 µL 1 mol L^{-1} PIPES buffer
Cell	10 cm quartz cuvette

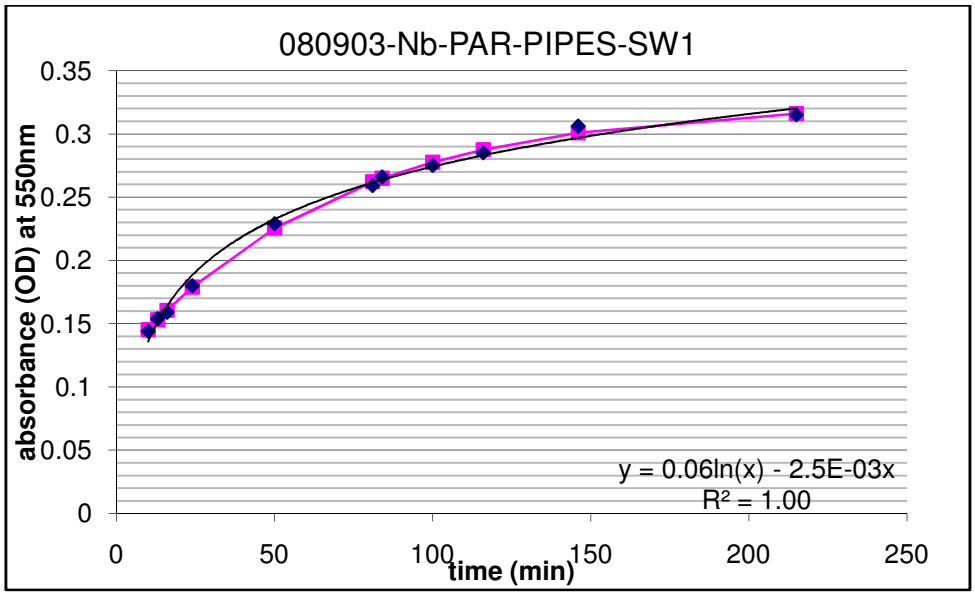

Figure 72. Absorbance (OD) at 550 nm vs. the elapsed time in seawater at pH 6.8. Blue data points show the measured absorbance. The pink data points show the estimated data points.

Figure 72 shows the increasing development of the absorbance at 550 nm as a function of the elapsed time. The correlation is exponential. The seawater sample (no. 6) contained 712.8 nmol L^{-1} Nb.

In Figure 73 can be seen the absorbance at 550 nm versus the Nb concentration. The apparent molar absorptivity is ε_{mol} = 23,848 mol^{-1} dm^3 cm^{-1}. The correlation is linear with R^2 = 0.99.

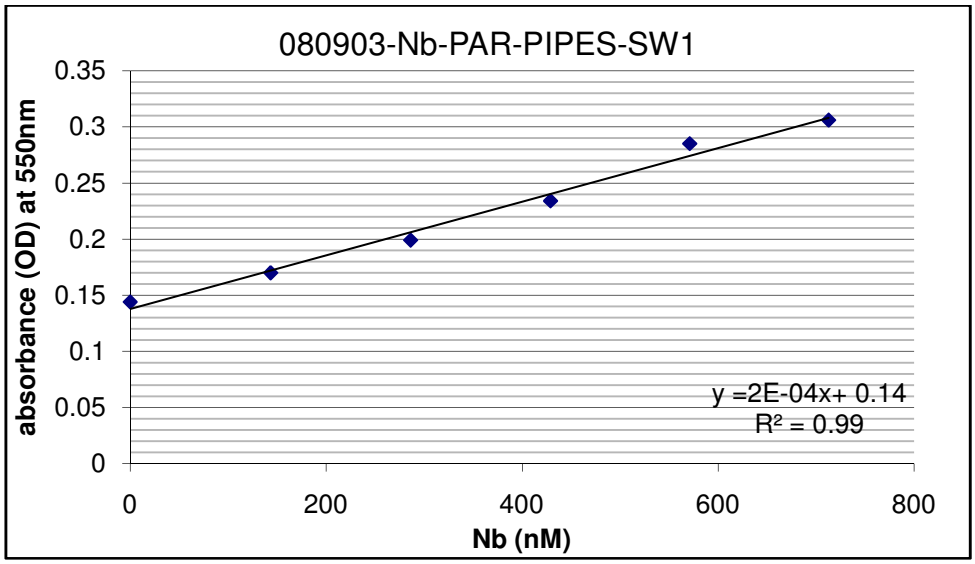

Figure 73. Absorbance (OD) at 550 nm vs. Nb concentration in seawater at pH 6.8.

Table 11. Estimated parameters of the measured seawater samples.

pH	slope absorbance $nmol^{-1}$ L	Name	Emissivity mol^{-1} dm^3 cm^{-1}	Nb nmol L^{-1}	k min	half-life min
6.8	0.00024	080903 PIPES-SW1	23847.7	594.71	0.015	46.55
7.1	0.00025	080905 PIPES-SW2	25127.7	832.87	0.011	60.38
7.9	0.00018	080905 EPPS-SW	18178.3	621.21	0.024	29.27

Table 11 shows the half-lives of the seawater samples that were in the range of the comparable one in MQ which can be seen in Figure 70 with a half-life of $\tau_{1/2}$ = 53.74 min. The estimated Nb concentration of the second (pH 7.1) determination somehow is higher than the really added Nb concentration (712.8 nmol L^{-1}). The calculations of the half-lives were based on the model of the first order process. It seems as if in the presence of citrate it is the dissociation reaction that causes the long half-lives.

5.1.9.1 Spectrophotometric Nb determination in seawater with 4-(2-pyridylazo)-resorcinol but without citrate

Instead of 120 µL half buffer and half citrate, the total amount of 1 mol L^{-1} buffer was used. Table 10 shows the design of the other reagents.

The correlations and therefore the R^2 values of all of these measurements were good, except for 080912-Nb-PAR-EPPS-SW where the absorbance shifted strongly and therefore R^2 is only 0.7.

The apparent emissivities of the measured seawater samples were in the same range. Table 11 shows that below this pH the emissivites of the seawater samples with citrate increased with decreasing pH. And furthermore, the half-lives of the seawater samples without citrate are far shorter than those with citrate. At pH 7.9 the half-live with citrate was $\tau_{1/2}$ = 29.27 min and without citrate it was of $\tau_{1/2}$ = 1.13 min. This could show that there is no ternary complex formed. It could simply be a competition between complexation of Nb by citrate and PAR and hydrolysis at high concentrations.

Table 12. Estimated parameters of the measured seawater samples without any citrate.

pH	slope absorbance $nmol^{-1}$ L	ε_{mol} mol^{-1} dm^3 cm^{-1}	Nb nmol L^{-1}	k min	half-life min	name
6.5	0.000387	38704.86	571.88	0.30	2.33	080912-Nb-PAR-PIPES-SW01
7.0	0.000347	34693.70	647.86	0.18	3.89	080912-Nb-PAR-PIPES-SW02
7.9	0.000188	18752.03	401.02	0.61	1.13	080912-Nb-PAR-EPPS-SW

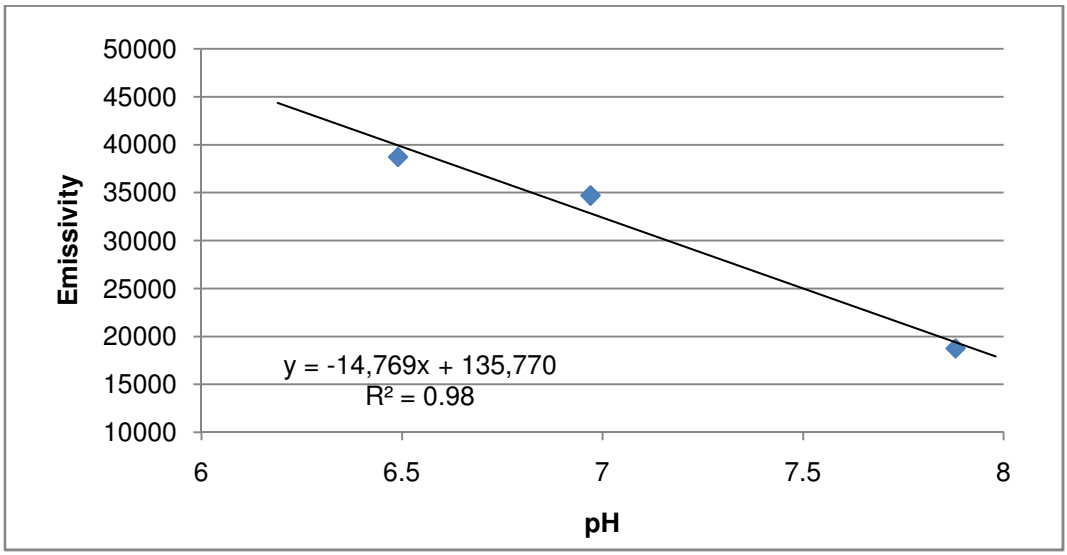

Figure 74. Apparent molar absorptivity vs. pH. λ = 550 nm. Seawater samples without citrate.

5.2 Methods of Zirconium determination

5.2.1 Voltammetric/Polarographic Zr determination with cupferron at a varying pH

Name	06261231_080626-Zr-MES-01.dth
pH value	6.1
Peak position	-1.190 V
Reagents	10 mL MQ 100 µL 1 mol L^{-1} MES buffer 20 µL 10.96 µmol L^{-1} Zr 200 µL 0.005 mol L^{-1} cupferron
Additions	1st and 2nd: 20 µL 10.96 µmol L^{-1} Zr 3rd and 4th: 100 µL 10.96 µmol L^{-1} Zr

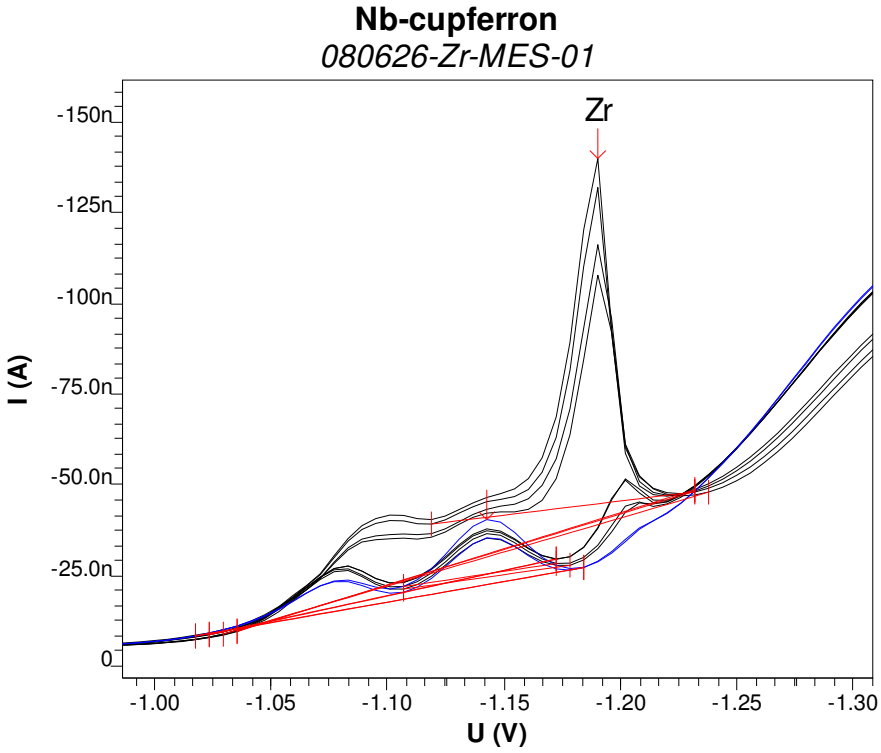

Figure 75. Current-voltage curves for 21.9, 43.7, 65.4, 172.6, 277.8 nmol L^{-1} Zr(IV) in 10 mL 0.1 mol L^{-1} MES buffer (pH 6.1) containing 200 µmol L^{-1} cupferron.

In the attempt to locate the Zr-cupferron peak position MQ buffered with 100 µL 1 mol L^{-1} MES to pH 6.1 containing 200 µmol L^{-1} cupferron and 21.9 nmol L^{-1} Zr was used. In the first two Zr additions no real increase of the peak could be determined by

the voltammeter and therefore the added amount of Zr was increased. A huge and sharp peak developed, but it increased only very little with the last addition of Zr. The described scan can be seen in Figure 75. The sensitivity was very low with S = 0.01 nA nmol^{-1} L and the peaks were rather scattered than linearly arranged. In the calculation the R^2 value of 0.07 showed no linear correlation between the Zr concentration and the peak current.

At pH 4 there was a huge peak at -0.76 V and the Zr peak was situated on the shoulder of this peak at -1.00 V and therefore was hardly detectable at all. Between pH 4 and 6 in 10 mmol L^{-1} acetate buffer and around pH 6.5 in 0.1 mol L^{-1} PIPES buffer it was not possible to find the peak position of Zr. Between pH 4 and 6 there were a lot of peaks and only with huge Zr additions like 108.5 nmol L^{-1} small peak changes could be observed. In the position of the Zr peak there were already other huge peaks, therefore no linear correlation could be observed. Around pH 6.5 it was not possible to detect the Zr peak position neither with an increasing amount of cupferron to 1 mmol L^{-1} nor with the addition of the oxidizing agent $KBrO_3$. Then measurements above pH 8 were tried.

Name	06271030_080627-Zr-EPPS1.dth
pH value	8.4
Peak position	-1.256 V
Reagents	10 mL MQ 100 µL 1 mol L^{-1} EPPS buffer 20 µL 10.96 µmol L^{-1} Zr 200 µL 0.005 mol L^{-1} cupferron
Additions	1st and 2nd: 20 µL 10.96 µmol L^{-1} Zr 3rd: 40 µL 10.96 µmol L^{-1} Zr 4th: 80 µL 10.96 µmol L^{-1} Zr

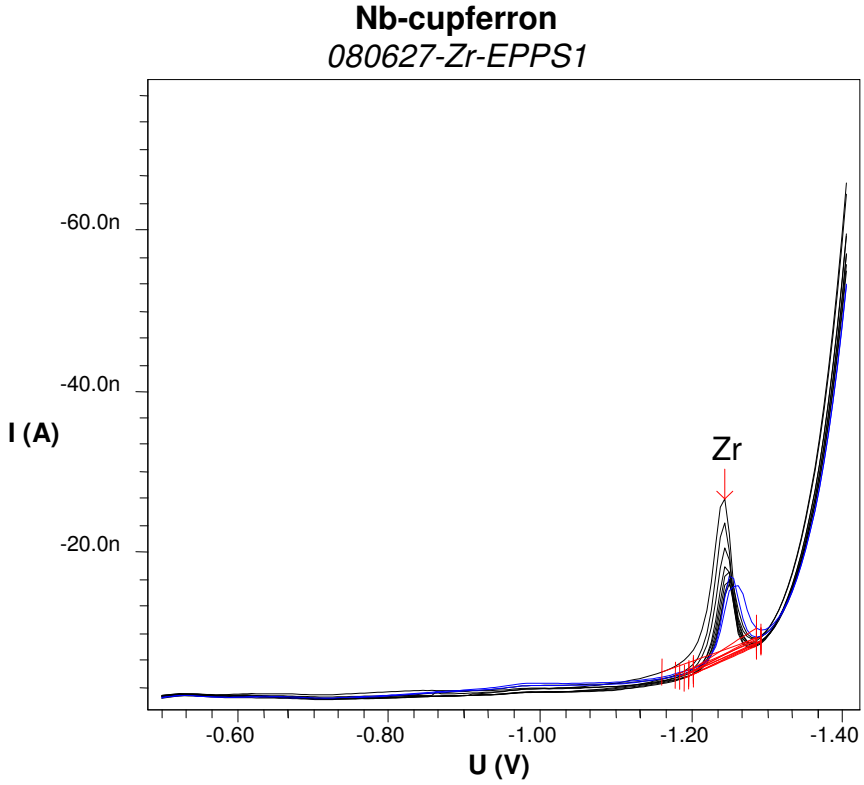

Figure 76. Current-voltage curves for 21.9, 43.7, 65.4, 108.5, 193.8 nmol L^{-1} Zr(IV) in 10 mL 0.1 mol L^{-1} EPPS buffer (pH 8.4) altogether containing 100 µmol L^{-1} cupferron.

In Figure 76 it can be seen that in 10 mmol L^{-1} EPPS buffer at pH 8.4 it was possible to locate the peak position of Zr. It is positioned at a very negative potential (-1.25 V) and on the shoulder of the hydrogen wave. The sensitivity was $S = 0.06$ nA $nmol^{-1}$ L with an R^2 value of 0.93. The cupferron concentration was 100 µmol L^{-1}.

In the attempt to increase the sensitivity of the polarographic determination, twice as much cupferron was used in the next determination. Figure 77 shows the polarogram and Figure 78 shows the plot of the peak currents versus the Zr concentration. The sensitivity increased to $S = 0.08$ nA $nmol^{-1}$ L and the R^2 value to 0.97, but the

voltammeter could not determine the first two peak currents, because the values were too small.

Name	06271113_080627-Zr-EPPS2.dth
pH value	8.4
Peak position	-1.250 V
Reagents	10 mL MQ 100 µL 1 mol L^{-1} EPPS buffer 20 µL 10.96 µmol L^{-1} Zr 20 µL 0.1 mol L^{-1} cupferron
Additions	4 times 20 µL 10.96 µmol L^{-1} Zr

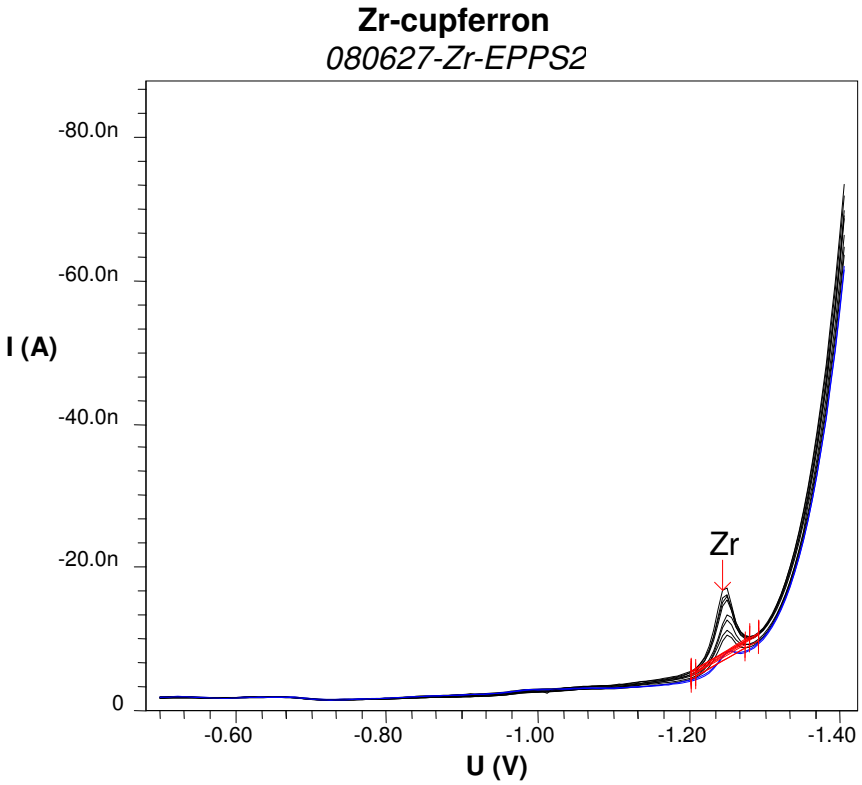

Figure 77. The applied current is plotted as a function of the voltage for 21.9, 43.7, 65.4, 87.0, 108.5 nmol L^{-1} Zr(IV) in 10 mL 0.1 mol L^{-1} EPPS buffer (pH 8.4) altogether containing 200 µmol L^{-1} cupferron.

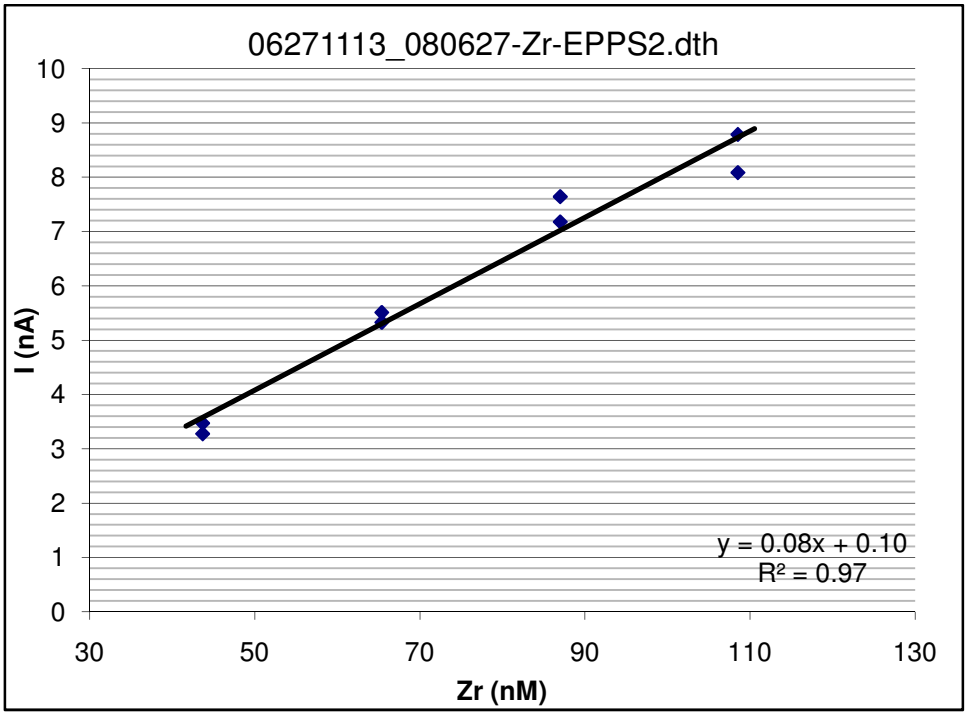

Figure 78. The measured peak currents are plotted as a function of the added Zr concentrations.

For a further increase of the sensitivity, the cupferron concentration was doubled again in a further determination. With a cupferron concentration of 400 µmol L^{-1} in 10 mmol L^{-1} EPPS buffer at pH 8.4 neither the R^2 value (0.93) could be further increased, nor the sensitivity (S = 0.06 nA $nmol^{-1}$ L), due to the fact that the hydrogen wave also increased. The replication of the current-voltage curves of each Zr addition was fine.

To increase the sensitivity of the polarographic determination of Zr $KBrO_3$ was added as an oxidizing agent.

5.2.1.1 Polarographic Zr determination with cupferron and an oxidizing agent

Name	07011051_080701-Zr-EPPS01.dth
pH value	8.3
Peak position	-1.244 V
Reagents	10 mL MQ 100 µL 1 mol L^{-1} EPPS buffer 20 µL 10.96 µmol L^{-1} Zr 20 µL 0.1 mol L^{-1} cupferron 150 µL 0.36 mmol L^{-1} $KBrO_3$ solution
Additions	1st: 20 µL 10.96 µmol L^{-1} Zr 2nd: 40 µL 10.96 µmol L^{-1} Zr 3rd: 80 µL 10.96 µmol L^{-1} Zr 4th: 160 µL 10.96 µmol L^{-1} Zr

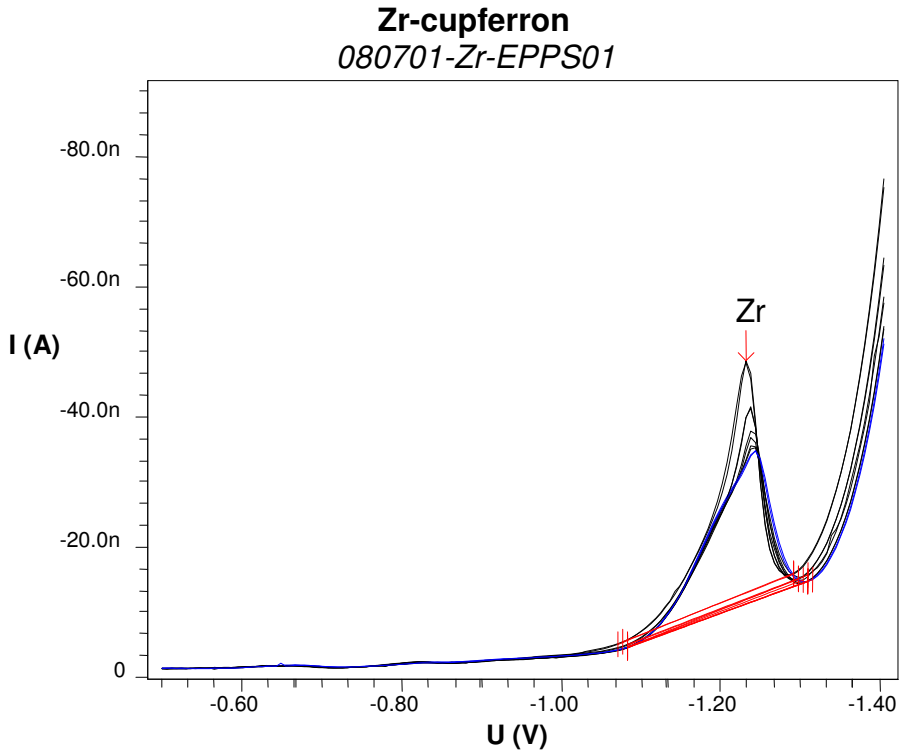

Figure 79. Current-voltage curves for 21.9, 43.7, 87.0, 172.5, 339.9 nmol L^{-1} Zr(IV) in 10 mL 0.1 mol L^{-1} EPPS buffer (pH 8.3) containing 200 µmol L^{-1} cupferron and 5.4 µmol L^{-1} $KBrO_3$.

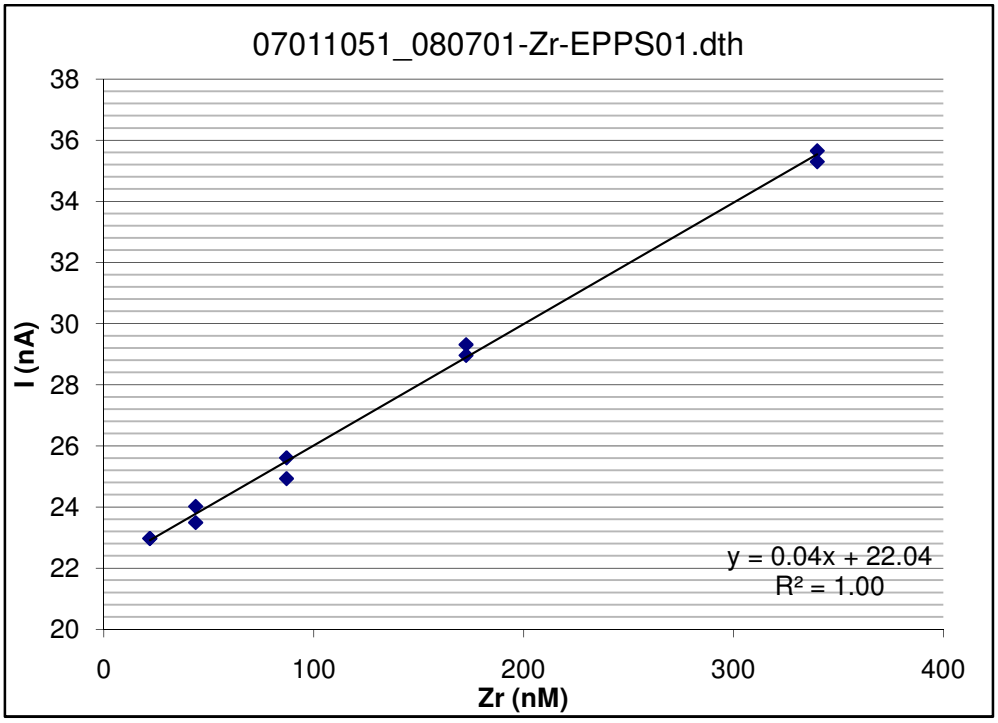

Figure 80. Plot of the measured peak currents as a function of the added Zr concentrations.

Figure 79 and Figure 80 show that the replications are good and therefore the linear correlation between the Zr concentrations and the peak currents is $R^2 = 1$. But the sensitivity did not increase with the addition of the oxidizing reagent. Without $KBrO_3$ and the same cupferron concentration the sensitivity was $S = 0.08$ nA nmol^{-1} L. With a $KBrO_3$ concentration of 5.4 µmol L^{-1} the sensitivity was cut in half to $S = 0.04$ nA nmol^{-1} L.

Zr apparently differs from Ti. Ti(III) is very reactive and a catalytic cycle is formed with cupferron and $KBrO_3$ while Zr(III) is not formed, and instead it is probably just the ligand which is reduced. Thus the oxidizing agent has no affect on the Zr peak.

5.2.2 Polarographic Zr determination with cupferron in seawater

Name	07011623_080701-Zr-EPPS07.dth
pH value	8.2
Peak position	-1.205 V
Reagents	10 mL SW M68-3 100 µL 1 mol L^{-1} EPPS buffer 20 µL 0.1 mol L^{-1} cupferron
Additions	twice 20 µL 10.96 µmol L^{-1} Zr 3rd: 100 µL 10.96 µmol L^{-1} Zr 4th: 500 µL 10.96 µmol L^{-1} Zr

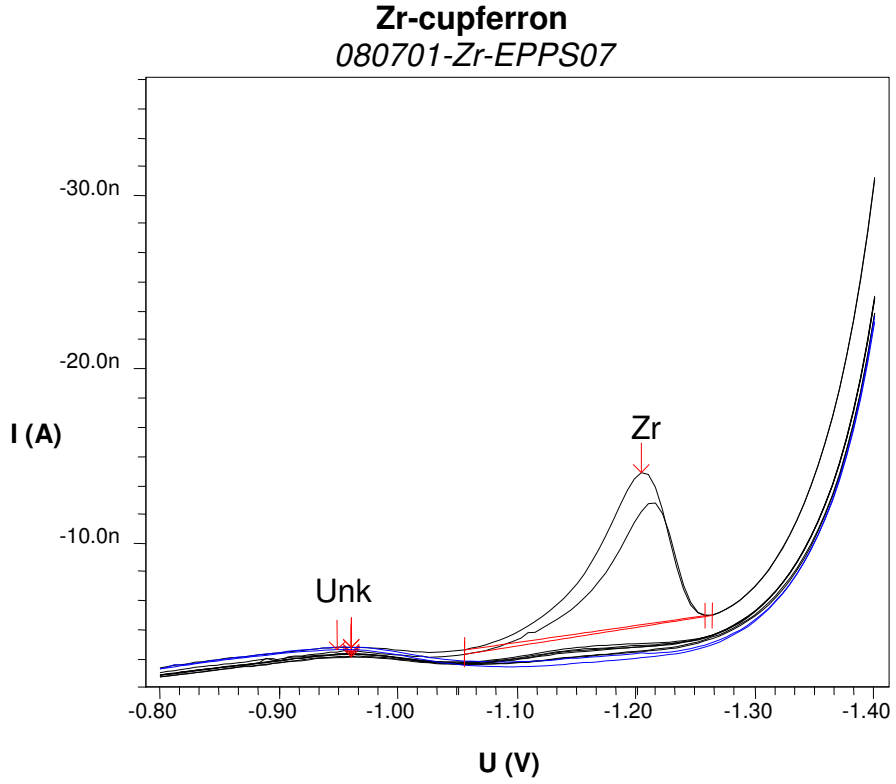

Figure 81. Current-voltage curves for the Zr additions of 0, 21.9, 43.7, 151.3, 561.6 nmol L^{-1} in 10 mL seawater containing 0.1 mol L^{-1} EPPS buffer (pH 8.22) and 20 µmol L^{-1} cupferron.

In Figure 81 can be seen that only with very high Zr concentrations of 561.6 nmol L^{-1} a peak could be observed in seawater. Under the same conditions the polarographic detection of Zr worked in MQ. The peak current of the replication was far lower than the first peak.

To increase the sensitivity of the measurements 150 µL 0.36 mmol L^{-1} $KBrO_3$ solution were added, but only at Zr concentrations of 561.6 nmol L^{-1} a real peak appeared.

Another possibility to increase the sensitivity is to increase the concentration of the complexing agent. Hence the concentration of cupferron in seawater was risen to 2 mmol L^{-1} and its polarogram can be seen in Figure 82.

Name	07151101_080715-Zr-EPPS01.dth
pH value	8.3
Peak position	-1.272 V
Reagents	10 mL SW M68-3 100 µL 1 mol L^{-1} EPPS buffer 200 µL 0.1 mol L^{-1} cupferron
Additions	1st and 2nd: 20 µL 10.96 µmol L^{-1} Zr 3rd and 4th: 100 µL 10.96 µmol L^{-1} Zr

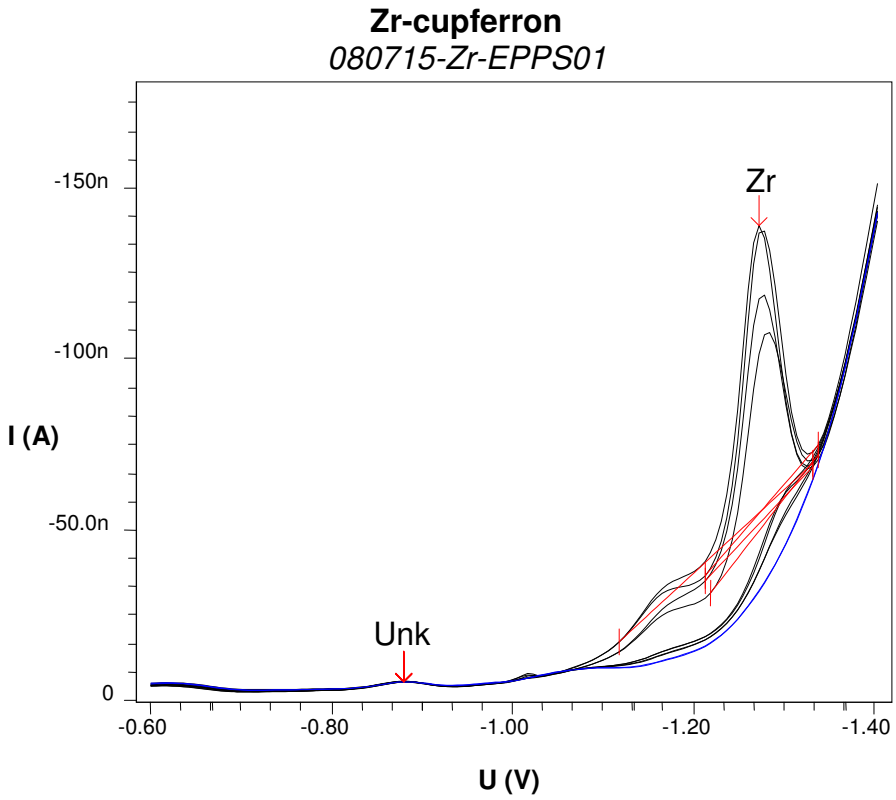

Figure 82. Current-voltage curves for the Zr additions of 0, 21.9, 43.7, 151.3, 256.9 nmol L^{-1} in 10 mL seawater containing 0.1 mol L^{-1} EPPS buffer (pH 8.29) and 200 µmol L^{-1} cupferron.

In Figure 82 the Zr concentration could only be determined starting with a concentration of 150 nmol L^{-1}. For the last two additions of Zr the peaks are clearly visible on the shoulder of another peak. Again the replication was far lower than the first determination. The same decrease could be observed in seawater at a pH that was lower than 8. Therefore 277.8 nmol L^{-1} Zr were added to the seawater containing

10 mmol L^{-1} MES buffer (pH 6.52) and 200 µmol L^{-1} cupferron and the peak current was measured every few minutes. This is shown in Figure 83. The peak current decreases with nearly 1 nA $nmol^{-1}$ L min^{-1}. This means that the Zr-cupferron complex is obviously not stable at this pH range (6-8).

Name	07151415_080715-Zr-MES-02.dth
pH value	6.5
Peak position	-1.272 V
Reagents	10 mL SW M68-3 100 µL 1 mol L^{-1} MES buffer 20 µL 0.1 mol L^{-1} cupferron 260 µL 10.96 µmol L^{-1} Zr

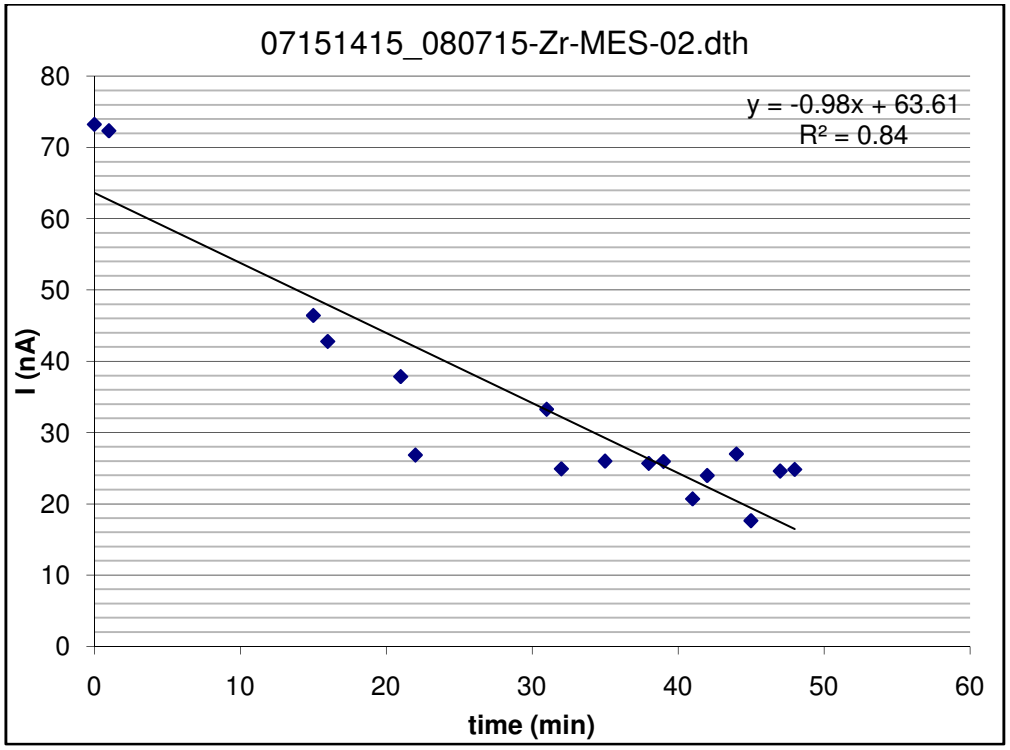

Figure 83. Plot of the peak current as a function of the time with seawater containing 277.8 nmol L^{-1} Zr, 0.1 M MES buffer (pH 6.52) and 200 µmol L^{-1} cupferron.

5.2.3 Polarographic Zr determination with BPHA as complexing agent

In various buffers and therefore at a pH range from 4 to 9 no Zr-BPHA peak could be detected. This did not change with varying amounts of Zr, BPHA or the addition of $KBrO_3$.

5.2.4 Zirconium speciation

Figure 84 shows the Zr-Speciation under fresh and seawater conditions at a pH range from 0 to 9. The data of this plot are based on the pK-values published by Turner et al. (1981). It is assumed that Zr(OH) species are in a cumulative form in terms of H^+.

Figure 84 shows that with increasing pH the dominating Zr species are more and more hydrolyzed. It can be seen that under seawater conditions around pH 8 the dominating species is $Zr(OH)_5^-$. There is also a little bit of $Zr(OH)_4$. This is in good agreement with Byrne (2002).

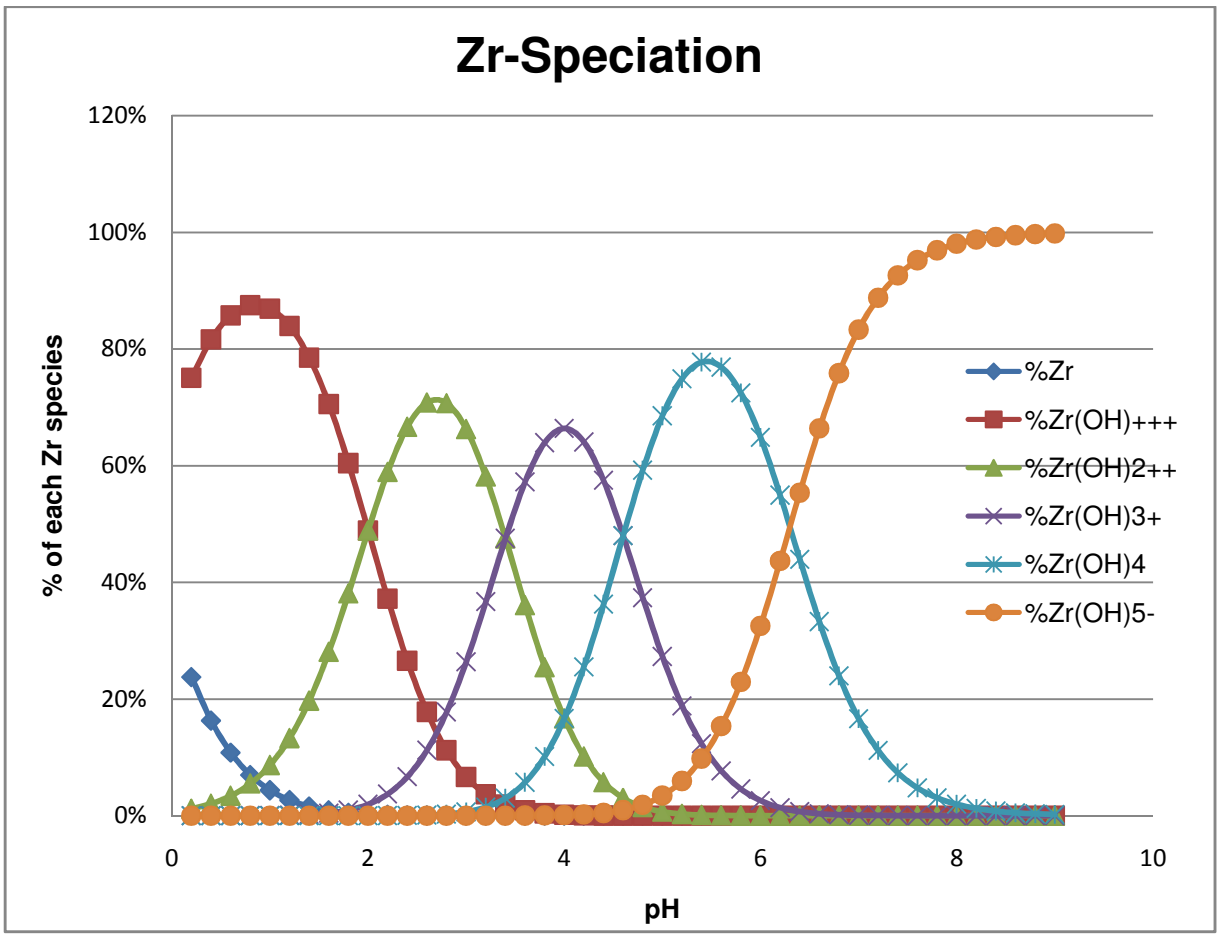

Figure 84. Zr-Speciation under water and seawater conditions. T = 298.15 K.

6 Conclusions and future perspectives

The focus of this diploma thesis was on the speciation of Nb and Zr species in seawater, and on the development of electrochemical and spectrochemical methods for the determination of Nb and Zr in seawater.

Nb can be determined by DPCSV with cupferron at pH 4 as published by Wang et al. (1992a). It was shown that this is also efficiently the case at a slightly higher pH range of 4.4-6.6, though with increasing pH a higher cupferron concentration is needed to achieve the same sensitivity. For the Nb determination in seawater a higher cupferron concentration is necessary than in MQ, because of Mg and Ca in seawater which also form complexes with cupferron. Therefore less complexing agent is left for the complexation with Nb.

It was shown that the Nb determination with cupferron, which can act as both complexing agent and oxidizing agent, works fine in seawater in the pH range of 3.9-6.5. To increase the sensitivity and enhance catalytically the overall reaction, $KBrO_3$ was added as an effective complexing agent under these pH conditions. With 1 mmol L^{-1} cupferron as a chelator and 5.4 mmol L^{-1} $KBrO_3$ as an additional oxidizing agent a very good sensitivity of S = 0.55 nA $nmol^{-1}$ L can be achieved at pH 6.4. At pH 7 the Nb determination was disturbed by another peak which was also situated at the same peak position as the Nb peak. It was found that the peak position moves to a more negative potential with an increasing pH in MQ and seawater which is in good agreement with Ferrett et al. (1955).

The results of this thesis suggest that a 1:1 Nb:cupferron complex is formed at pH 6. At a higher pH (6.5-7.1) a 1:2 Nb:cupferron complex seems to be formed in MQ.

The replacement of cupferron by BPHA as a chelator was not successful, due to the fact that the catalytic cycle cannot be formed. Though BPHA is the stronger chelator than cupferron, the Nb-BPHA complex readily is reduced.

PAR and Nb form a 1:1 Nb-PAR complex at pH 5-6 in tartrate, oxalate and citrate buffered solutions (Belcher et al. 1962a; Yamada et al. 1988; Yamada et al. 1990). Earlier studies found that the maxima of these ternary complex occurs at λ_{max} = 550 nm. The results of this thesis suggest that at pH 7 there is still a Nb-PAR complex formed, although it was examined that it requires longer formation time than at pH 5-6. In the spectrochemical Nb determination with PAR, but without the additional tartrate, oxalate and citrate, it could be shown that for the Nb determination in seawater and MQ no citrate is needed for the formation of a ternary complex.

Furthermore it was found that the Nb-PAR complex forms faster without citrate which indicates the absence of any competing complexation reactions.

The dominating oxidation state of Nb in seawater is likely to be +5. Nb is strongly hydrolyzed and significant species were postulated to be mainly $Nb(OH)_6^-$ and marginally $Nb(OH)_5$ (Greenwood and Earnshaw 1990; Sohrin et al. 1998a; Byrne 2002). According to Astrom et al. (2008) dissolved Nb is present in an anionic form in acidic streams (pH = 4.5-6.2). The results of the experiments in this thesis rather match with an anionic Nb species in seawater for pH higher than 5.8, too. Further works needs to be done to see which species is really predominating in seawater. Astrom et al. (2008) discovered that the Nb concentration in streams depends on dissolved humic substances and colloidal Fe. It would be of interest so see whether this is also the case in seawater. Nb hydrolyzes easily and it is very difficult to keep it in solution, even in slightly acidic solutions. Therefore they have to be prepared directly before the spectrochemical Nb determination. The addition of a complexing agent like oxalate was found to reduce the hydrolysis of Nb.

Zr and Ti both belong to the 4^{th} group in the Periodic System of Elements and it was therefore hoped that their elemental properties would be similar. Then Zr could also be determined electrochemically with cupferron in seawater. But the behaviour of Zr differs from the behaviour of Ti. Zr is less reactive than Ti and Zr(III) is not formed. Therefore Zr does not form a catalytic cycle and has no redox chemistry [Zr(IV)/Zr(III)] under the conditions used here. In the future further electrochemical Zr determinations could be tried out with other complexing agents which are related to cupferron.

In the plot that is based on the pK-values published by Turner et al. (1981) it was shown that Zr is more strongly hydrolyzed with the increase of the pH. Under seawater conditions the predominating species is $Zr(OH)_5^-$, but also $Zr(OH)_4$ is formed which is in good agreement with Byrne (2002).

6.1 Zusammenfassung

Der Fokus dieser Diplomarbeit lag auf der elektrochemischen und spektrochemischen Untersuchung von Niob- und Zirkonium-Speziation im Seewasser. Die im Seewasser gemessen Konzentration liegen im Bereich von nmol L^{-1} bis pmol L^{-1}. Alle bisher veröffentlichten Untersuchungen von Nb- und Zr-Speziation wurden bei Konzentrationen im Bereich von µmol L^{-1} durchgeführt. Wobei es sein könnte, dass die *in situ* Speziation stark von der im Seewasser abweicht. Bei Konzentrationen im Bereich von µmol L^{-1} sind die Löslichkeitsergebnisse gekoppelt mit der Bildung von dimeren oder polymeren Hydroxyden, welche die Untersuchungen im Seewasser verkomplizieren. Deshalb sind momentan die Kenntnisse über die wirkliche Speziation und ihre mögliche Rolle in der organischen Komplexierung im Seewasser sehr beschränkt. Zudem gehören Nb und Zr zu der Gruppe der „high field strength elements“ (HFSE) (Barth et al. 2001; Rudnick und Gao 2005). Sie sind deshalb von großem Interesse in der Geochemie und werden momentan als ozeanographische Indikatoren zur Bestimmung von Wassermassen untersucht (McKelvey und Orians 1998). Folglich ist es dringend erforderlich neue Methoden zu entwickeln mit deren Hilfe Nb- und Zr-Speziation in niedrigen Konzentrationen bestimmt werden können, so dass unser Verständnis von der grundlegenden Biogeochemie dieser Metalle verbessert werden kann.

Wang et al. (1992a) veröffentlichten eine empfindliche elektrochemische Methode zur Bestimmung von Nb mit 5 µmol L^{-1} Kupferron (dem Ammonium Salz von *N*-nitroso-*N*-phenylhydroxylamine) in 0.1 mol L^{-1} Acetatpuffer bei pH 4. Diese Methode beruht auf der kathodischen Differenz-Puls-Inversvoltammetrie (DPCSV). In dieser Arbeit wurde die Methode weiterentwickelt, so dass sie mit einer deutlich höheren Kupferron Konzentration effizient auch im pH-Bereich von 4.4-6.6 angewendet werden konnte. Mit steigendem pH war es notwendig die Kupferron Konzentration zu erhöhen, um die Empfindlichkeit der Methode steigern zu können, wobei sich die Lage des Peaks dabei zu negativerem Potential verschob. Dies stimmt mit den Beobachtungen von Ferrett et al. (1955) überein. Es wurde zudem gezeigt, dass diese Methode auch im Seewasser zur Bestimmung von Nb angewendet werden kann. Hierfür musste die verwendete Kupferron Konzentration weiter gesteigert werden, da Magnesium und Calcium ebenfalls mit Kupferron Komplexe bilden.

Es wurde gezeigt, dass Nb im Seewasser mit Kupferron in einem pH-Bereich von 3.9-6.5 bestimmt werden kann. Die Empfindlichkeit der Messung kann auf

S = 0.55 nA nmol^{-1} L durch die Zugabe von 1 mmol L^{-1} Kupferron als chelatbildende Verbindung und 5.4 mmol L^{-1} $KBrO_3$ als Oxidationsmittel bei einem pH von 6.4 gesteigert werden. Die Gesamtreaktion wird durch das Oxidationsmittel katalytisch verstärkt, wobei Kupferron sowohl als Komplexierungsreagenz als auch als Oxidationsmittel fungieren kann. In diesem pH-Bereich ist $KBrO_3$ jedoch das bessere Oxidationsmittel. Der gesamte katalytische Zyklus besteht aus der Reduktion des Nb(V)-Kupferron Komplexes zu Nb(IV) und der Reoxidation zurück zu Nb(V) in Gegenwart des Oxidationsmittels. Bei dem Versuch, die Nb-Bestimmung mit Kupferron bei pH 7 durchzuführen, zeigte sich, dass ein anderer Peak an der gleichen Lage des Nb-Peaks störte.

Die Ergebnisse dieser Arbeit deuten an, dass bei pH 6 ein 1:1 Nb:Kupferron Komplex gebildet wird, wohingegen bei einem höheren pH von 6.5-7.1 ein 1:2 Komplex gebildet wird.

Es wurde ausprobiert, ob Kupferron als Komplexierungsreagenz bei der polarographischen Nb-Bestimmung durch das verwandte *N*-benzoyl-*N*-phenylhydroxylamine (BPHA) ersetzen werden könnte. Dies war leider nicht erfolgreich, da der katalytische Zyklus wie mit Kupferron nicht gebildet werden kann. BPHA ist zwar ein stärkeres Komplexierungsreagenz für Nb als Kupferron, aber der Nb-BPHA Komplex wird zu leicht reduziert.

In den bisher veröffentlichen Artikeln wurde beschrieben, dass Nb mit 4-(2-pyridylazo)-resorcinol (PAR) ternäre, rot gefärbte Komplexe in der Anwesenheit von entweder Citrate, Oxalate oder Tartrate bei pH 5-6 bildet. Diese ternären Komplexe können spektrochemisch nachgewiesen werden, da sie das Licht bei einer Wellenlänge von λ_{max} = 550 nm absorbieren. Die Zusammensetzung des Nb-PAR Komplexes ist hierbei 1:1 (Belcher et al. 1962a; Yamada et al. 1988; Yamada et al. 1990). Die Ergebnisse dieser Arbeit zeigen, dass bis zu einem pH-Wert von 7 immer noch 1:1 Nb-PAR Komplexe gebildet werden. Die Zeit die für die Bildung benötigt wird, ist wesentlich länger als bei niedrigerem pH-Wert. Der Nb-PAR Komplex wurde ohne Citrate deutlich schneller gebildet, was auf die Abwesenheit einer konkurrierenden chelatbildenden Verbindung schließen lässt.

Sehr wenig ist bekannt über die Meereschemie von Nb und Zr. Im Seewasser ist das Verhalten von Nb wahrscheinlich von der Oxidationsstufe +5 geprägt. Nb ist im Seewasser stark hydrolysiert und es wurde postuliert, dass die bedeutenden Verbindungen hauptsächlich $Nb(OH)_6^-$ und in geringerer Konzentration $Nb(OH)_5$ sind

(Greenwood and Earnshaw 1990; Sohrin et al. 1998a; Byrne 2002). Laut Astrom et al. (2008) liegt gelöstes Nb in sauren Flüssen (pH = 4.5-6.2) jedoch in anionischer Form vor. Die Ergebnisse der Experimente in dieser Diplomarbeit sprechen auch für anionisches Nb im Seewasser ab einem pH von 5.8. Es ist jedoch weitere Arbeit vonnöten, um herausfinden, welche Formen im Seewasser dominieren. Astrom et al. (2008) fand zudem heraus, dass die Nb Konzentration in Flüssen abhängig ist von den gelösten Humusverbindungen und vom kolloidalen Eisen. Es wäre interessant herauszufinden, ob dies ebenfalls der Fall im Seewasser ist.

Da Nb so leicht hydrolysiert, ist es sehr schwierig es in Lösung zu behalten, sogar in leicht sauren Lösungen. Deshalb musste die Nb Lösung direkt vor jeder spektrochemischen Messreihe angesetzt werden. Es wurde festgestellt, dass die Zugabe eines Komplexierungsreagenzes wie Oxalate dazu beiträgt, dass Nb besser in Lösung bleibt.

Zr und Ti gehören beide zur 4. Gruppe des Periodensystems der Elemente und es wurde deshalb gehofft, dass ihre elementaren Eigenschaften ähnlich sein würden. In diesem Fall könnte Zr im Seewasser ebenfalls mit Kupferron polarographisch bestimmt werden. Es ist aber leider so, dass das Verhalten von Zr stark von dem von Ti abweicht. Zr ist weniger reaktiv als Ti und es wird kein Zr(III) gebildet. Dadurch kann Zr keinen katalytischen Zyklus bilden und es hat keine Redoxchemie [Zr(IV)/Zr(III)] bei diesen Bedingungen. In weiteren Experimenten könnte man die elektrochemische Nb-Bestimmung mit anderen Komplexierungsreagenzien versuchen, die mit Kupferron verwandt sind.

Die dominierende Oxidationsstufe von Zr bei Seewasserbedingungen ist wahrscheinlich +4. Mit Hilfe der graphischen Darstellung von pK-Werten, welche von Turner et al. (1981) veröffentlicht wurden, konnte gezeigt werden, dass mit steigendem pH-Wert Zr stärker hydrolysiert. Bei Seewasserbedingungen ist $Zr(OH)_5^-$ dominierend, aber es liegt teilweise $Zr(OH)_4$ vor, was in guter Übereinstimmung mit Untersuchungen von Byrne (2002) steht.

7 Acknowledgements

First of all I would like to thank Prof. Dr. Douglas W. Wallace for the possibility to realize this diploma thesis at the IFM-GEOMAR in the “Forschungsbereich Marine Biogeochemie”.

Very special thanks to Dr. Peter Croot for the interesting topic of this diploma thesis, the good supervision and all of the great advice you gave me. Thanks for all the hours spending with me helping out, discussing and explaining.

I also would like to thank his working group. I really enjoyed working with all of you in the clean lab, because the working atmosphere is fantastic. I am looking forward to continue working with you all.

Thanks to Peter Streu who explained everything to me in the clean lab and with whom we had some good laughs while working.

I would like to thank Maija Heller who read and corrected my diploma thesis and who always found some time for me.

Thanks to Christian Schlosser for helping me out with the voltammeter a lot of times, when it did not work the way it should.

I would like to thank Anna Dammshäuser for the correction of the all the little “formal faults”.

I wish to thank the whole “high productivity area” for all the sweets, tea, chats and laughs. I am glad that that I got the chance to sit in that beautiful room with all of you and I hope that we will have a great time the next years.

I would like to thank the whole “Forschungsbereich Marine Biogeochemie” for the kind introduction and help whenever it is needed, too.

I also would like to make some private acknowledgements:

Many thanks to all the great friends I made over the period of my chemistry studies first in Freiburg, then in Alicante and in the end in Kiel. I hope that we'll stay in contact.

I am grateful to Nils. Million thanks for laughing, talking, cooking with me and pushing me in the end. Kiel is my home, because of you.

And at the end an unbelievably huge "thank you" to my mother. Thank you for correcting and helping me with this work. Without you it would have been a lot harder. Thanks for all the support and love you gave me the past 25years. I am looking forward to the next vacation and visits.

8 Erklärung

Die vorliegende Diplomarbeit wurde in dem Zeitraum von Mai 2008 bis November 2008 im IFM-GEOMAR, Leibniz-Institut für Meereswissenschaften an der Christian-Albrechts-Universität Kiel unt erder Leitung von Dr. Peter L. Croot durchgeführt.

Hiermit versichere ich, Kathrin Wuttig, dass ich diese Arbeit selbständig und nur unter Zuhilfenahme der angegebenen Literatur angefertigt habe.

Kiel, den 05.11.2008

9 References

Adler, N. and Hiskey, C. F. (1957a). "Composition of the Peroxy Complexes of Niobium(V) in Sulfuric Acid." Journal of the American Chemical Society **79**(8): 1831-1834.

Adler, N. and Hiskey, C. F. (1957b). "Spectra of the Peroxy Complexes of Niobium in Sulfuric Acid." Journal of the American Chemical Society **79**(8): 1827-1830.

Agarwala, B. V. and Dey, A. K. (1967). "4-(2-Pyridylazo) Resorcinol as a Sensitive Reagentfor Vanadium, Niobium, and Tantalum." Microchemical Journal **12**: 162-167.

Agarwala, B. V. and Dey, A. K. (1969). "Spectrophotometric Determination of Vanadium and Niobium: Xylenol Orange as a Chromogenic Reagent." Mikrochim. Acta, No. 3, 664-7 (1969).

Aja, S. U., Wood, S. A., et al. (1995). "The Aqueous Geochemistry of Zr and the Solubility of Some Zr-Bearing Minerals." Applied Geochemistry **10**(6): 603-620.

Alimarin, I. P. and Savvin, S. B. (1966). "Photometric Determination of Niobium with Azo-Dyestuffs." Talanta **13**(5): 689-700.

Alimarin, I. P. and Tse, Y. (1962). "Determination of Zirconium Using N-Benzoylphenylhydroxylamine." Talanta (England); Vol: 9: Pages: 9-13.

Astrom, M. E., Peltola, P., et al. (2008). "Niobium in Boreal Stream Waters and Brackish-Water Sediments." Geochemistry-Exploration Environment Analysis **8**: 139-148.

Atkins, P. W. (2001). Physikalische Chemie Wiley-VCH.

Baes, C. F. and Mesmer, J. R. E. (1976). The Hydrolysis of Cations. New York, John Wiley.

Bard, A. J. and Faulkner, L. R. (2001). Elctrochemical Methods: Fundamentals and Applications, John Wiley & Sons, Inc. .

Barth, M. G., Rudnick, R. L., et al. (2001). "Geochemistry of Xenolithic Eclogites from West Africa, Part I: A Link between Low Mgo Eclogites and Archean Crust Formation." Geochimica et Cosmochimica Acta **65**(9): 1499-1527.

Belcher, R., Ramakrishna, T. V., et al. (1962a). "4-(2-Pyridylazo)Resorcinol as a Selective and Sensitive Spectrophotometric Reagent for Niobium." Talanta (England); Vol: 9: Pages: 943-5.

Belcher, R., Ramakrishna, T. V., et al. (1962b). "4-(2-Pyridylazo)Resorcinol as a Selective and Sensitive Spectrophotometric Reagent for Niobium(V)." Preliminary Communications: 943-945.

Belcher, R., Ramakrishna, T. V., et al. (1963). "Absorptiometric Determination of Niobiumv with 4-(2-Pyridylazo)-Resorcinol as Reagent." Talanta **10**(9): 1013-1022.

Bielig, H. and Bayer, E. (1954). "Über Die Molekulargrösse Des Hämovanadins." Cellular and Molecular Life Sciences (CMLS) **10**(7): 300-302.

Bobrowski, A. and Zarebski, J. (2000). "Catalytic Systems in Adsorptive Stripping Voltammetry." Electroanalysis **12**(15): 1177-1189.

Bone, Q. (1998). The Biology of Pelagic Tunicates, Oxford Univ. Press.

Boodts, J. F. C., Sluyters-Rehbach, M., et al. (1986). "The Electrochemical Behaviour of Nb(Iv) in Aqueous Citrate Solutions Studied at the Dropping Mercury Electrode." Journal of Electroanalytical Chemistry **206**(1-2): 153-165.

Boswell, S. M. and Elderfield, H. (1988). "The Determination of Zirconium and Hafnium in Natural Waters by Isotope Dilution Mass Spectrometry." Marine Chemistry **25**(3): 197.

Broecker, W. S. and Peng, T. H. (1982). Tracers in the Sea, Eldigio Press.

Byrne, R. (2002). "Inorganic Speciation of Dissolved Elements in Seawater: The Influence of Ph on Concentration Ratios." Geochemical Transactions **3**(1): 11.

Carlisle, D. B. (1958). "Niobium in Ascidians." Nature **181**(4613): 933-933.

Carlisle, D. B. and Hummerstone, L. G. (1958). "Niobium in Sea-Water." Nature **181**(4614): 1002-1003.

Cozzi, D. and Vivarelli, S. (1953). "Reduction of Hydrochloric Solutions of Niobic Acid at the Dropping Mercury Electrode " Ricerca sci. **23**: 2244-2249.

Donoson, G. N., Chadwick, I. W., et al. (1975). "The Polarographic Determination of Traces of Titanium-(Iv) in the Presence of N-Benzoyl-N-Phenylhydroxylamine." Analytica Chimica Acta **77**: 1-8.

Eisenhardt, I. (1991). Polarography and Voltammetry. Weinheim, VCH.

Elson, R. E. (1953). "The Chemistry of Niobium and Tantalum.I. Reduction in Solution." Journal of the American Chemical Society **75**(17): 4193-4195.

Elving, P. J. and Olson, E. C. (1955). "Gravimetric and Titrimetric Determination of Titanium, Zirconium, and Hafnium with Cupferron - Application to Fluoride Solution." Analytical Chemistry **27**(11): 1817-1820.

Elving, P. J. and Olson, E. C. (1956a). "Analysis of Samples Containing Uranium, Niobium, and Zirconium." Analytical Chemistry (U.S.) Formerly Ind. Eng. Chem., Anal. Ed.; Vol: 28: Pages: 338-42.

Elving, P. J. and Olson, E. C. (1956b). "Titrimetric Determination of Zirconium in Magnesium Alloys." Analytical Chemistry **28**(2): 251-252.

Faure, G. (1998). Principles and Applications of Geochemistry, Prentice Hall. 2nd Edition, 53ff.

Ferrett, D. J. and Milner, G. W. C. (1955). "Reversible Polarographic Reduction of Niobium." Nature **175**(4454): 477-477.

Ferrett, D. J. and Milner, G. W. C. (1956). "The Polarography of Niobium." Journal of the Chemical Society (England) Divided into J. Chem. Soc. A, J. Chem. Soc. B, etc.: Pages: 1186-92.

Firdaus, M. L., Norisuye, K., et al. (2008). "Dissolved and Labile Particulate Zr, Hf, Nb, Ta, Mo and W in the Western North Pacific Ocean." Journal of Oceanography **64**(2): 247-257.

Firdaus, M. L., Norisuye, K., et al. (2006). "Determination and Distribution of Zr, Hf, Nb, Ta and W in the North Pacific Ocean." Geochimica et Cosmochimica Acta **70**(18, Supplement 1): A175-A175.

Firdaus, M. L., Norisuye, K., et al. (2007). "Preconcentration of Zr, Hf, Nb, Ta and W in Seawater Using Solid-Phase Extraction on Tsk-8-Hydroxyquinoline Resin and Determination by Inductively Coupled Plasma-Mass Spectrometry." Analytica Chimica Acta **583**(2): 296.

Godfrey, L. V., White, W. M., et al. (1996). "Dissolved Zirconium and Hafnium Distributions across a Shelf Break in the Northeastern Atlantic Ocean." Geochimica et Cosmochimica Acta **60**(21): 3995-4006.

Gomes, M. D. G. and Franco, D. W. (1995). "Electrochemical Behaviour of Nb(V)-Edta and Nb(V)-Citrate Systems in Aqueous Solutions." Electroanalysis **7**(8): 778-781.

Good, N. E., Winget, G. D., et al. (1966). "Hydrogen Ion Buffers for Biological Research." Biochemistry **5**(2): 467-477.

Gorbushina, A. A., Kort, R., et al. (2007). Life in Darwin's Dust: Intercontinental Transport and Survival of Microbes in the Nineteenth Century. **9:** 2911-2922.

Greenway, G. M. and Wolfbauer, G. (1995). "On-Line Determination of Vanadium by Adsorptive Stripping Voltammetry." Analytica Chimica Acta **312**(1): 15-25.

Greenwood, N. N. (2003). "Vanadium to Dubnium: From Confusion through Clarity to Complexity." Catalysis Today **78**(1-4): 5-11.

Greenwood, N. N. and Earnshaw, A. (1990). Chemie Der Elemente, Wiley-VCH. (Korr. Nachdr. d. 1. Aufl. 1988) 1225-1287.

Hála, J. (1967). "The Solvent Extraction of Hafnium (Iv) and Zirconium (Iv) by N-Benzoyl-N-Phenylhydroxylamine and 2-Thenoyltrifluoroacetone from Strongly Acidic Solutions." Journal of Inorganic and Nuclear Chemistry **29**(1): 187-198.

Hall, G. E. M. and Pelchat, J. C. (1993). "Determination of Palladium and Platinum in Fresh Waters by Inductively Coupled Plasma Mass Spectrometry and Activated Charcoal Preconcentration." J. Anal. At. Spectrom. **8**: 1059 - 1065.

Henrion, G. and Adler, F. (1975). "Zum Polarographischen Verhalten Von Niob." Zeitschrift der Chemie **15**(8): 321-322.

Henze, M. (1911). "Untersuchungen Über Das Blut Der Ascidien I: Die Vanadiumverbindung Der Blutkörperchen." Hoppe Seyler's Z. Physiol. Chem. **72**: 494-501.

Hollemann, A. F. and Wiberg, N. (1995). Lehrbuch Der Anorganischen Chemie, Walter de Gruyter GmbH & Co. KG. Edition 101, 1399ff.

Hunt, E. C., North, A. A., et al. (1955). "Application of Paper-Chromatographic Methods of Analysis to Geochemical Prospecting." Analyst **80**(948): 172-&.

Irving, H., Freiser, H., et al. (1978). International Union of Pure and Applied Chemistry, Compendium of Analytical Nomenclature. Oxford, Chemistry Pergamon Press.

Jochum, K. P., Seufert, H. M., et al. (1986). "The Solar-System Abundances of Nb, Ta, and Y, and the Relative Abundances of Refractory Lithophile Elements in Differentiated Planetary Bodies." Geochimica et Cosmochimica Acta **50**(6): 1173-1183.

Kalk, M. (1963). "Absorption of Vanadium by Tunicates." Nature **198**(4884): 1010-1011.

Kennedy, J. H. (1960). "Polarography of Niobium and Tantalum Peroxide Complexes." J. Am. Chem. Soc. **54**: 1590-1592.

Kennedy, J. H. (1961). "Polarography of Niobium(V) in (Ethylenedinitrilo)-Tetraacetic Acid and Citric Acid Media." Analytical Chemistry (U.S.) Formerly Ind. Eng. Chem., Anal. Ed.; Vol: 33: Pages: 943-6.

Kirby, R. and Freiser, H. (1963). "Polarography of Niobium-Edta Complexes." Analytical Chemistry (U.S.) Formerly Ind. Eng. Chem., Anal. Ed.; Vol: 35: Pages: 122-5.

Kokubu, N. and Hidaka, T. (1965). "Tantalum and Niobium in Ascidians." Nature **205**(4975): 1028-1029.

Kolthoff, I. M. and Sandell, E. B. (1952). Textbook of Quantitative Inorganic Analysis. New York, Macmillan Co. 3, p. 84.

Land, J. E. and Sanchez-Caldas, J. R. (1967). "The Niobium(V)-N-Phenyl-N-Nitrosohydroxylamine Complex." Journal of the Less Common Metals **12**(1): 41-45.

Laubengayer, A. W. and Eaton, R. B. (1940). "The Reducibility of Quadrivalent Zirconium." J. Am. Chem. Soc. **62**(10): 2704-2706.

Libes, S. M. (1992). Marine Biogeochemistry, John Wiley & Sons, Inc. 81ff.

Lichtig, J. and Andrade, R. F. (2001). "Determination of Niobium in Pyrochlore Ore by Differential Pulse Polarography." Fresenius J. Anal. Chem. **371**(4): 559-561.

Macara, I. G. (1980). "Vanadium - an Element in Search of a Role." Trends in Biochemical Sciences **5**(4): 92-94.

Macara, I. G., Leod, G. C., et al. (1979). "Tunichromes and Metal Ion Accumulation in Tunicate Blood Cells." Comp. Biochem. Physiol. **63B**: 229-302.

Majumdar, A. K. and Mukherjee, A. K. (1958). "Separation of Niobium and Tantalum with N-Benzoyl-N-Phenylhydroxylamine." Analytica Chimica Acta **19**: 23-26.

Majumdar, A. K. and Mukherjee, A. K. (1959). "Direct Estimation of Niobium by N-Benzoyl-N-Phenylhydroxilamine." Analytica Chimica Acta **21**: 245-247.

Majumdar, A. K. and Pal, B. K. (1961). "Separation of Niobium and Tantalum by N-Benzoyl-N-Phenylhydroxylamine." Analytica Chimica Acta **24**: 497-498.

Majumdar, A. K. and Ray Chowdhury, J. B. (1958). "Separation of Niobium and Tantalum with Cupferron." Analytica Chimica Acta **19**: 18-22.

Mauchline, J. and Templeton, W. L. (1964). "Artificial and Natural Radioisotopes in the Marine Environment." Oceanogr. Mar. Biol. Ann. Rev.; Vol: 2: Pages: 229-79.

McKelvey, B. A. and Orians, K. J. (1993). Dissolved Zirconium in the North Pacific Ocean. Geochimica et Cosmochimica Acta ; Vol/Issue: 57:15. United States**:** Pages: 3801-3805.

McKelvey, B. A. and Orians, K. J. (1998). "The Determination of Dissolved Zirconium and Hafnium from Seawater Using Isotope Dilution Inductively Coupled Plasma Mass Spectrometry." Marine Chemistry **60**(3-4): 245.

McLeod, G. C., Ladd, K. V., et al. (1975). "Extraction of Vanadium (V) from Seawater by Tunicates: A Revision of Concepts " Limnology and Oceanography **20**(3): 491-493.

Metrohm. (2008). from http://products.metrohm.com/polarograph/va-systems/prod-MVA-01.aspx.

Michibata, H., Terada, T., et al. (1986). The Accumulation and Distribution of Vanadium, Iron, and Manganese in Some Solitary Ascidians. **171:** 672-681.

Michibata, H., Uyama, T., et al. (2002). "Vanadocytes, Cells Hold the Key to Resolving the Highly Selective Accumulation and Reduction of Vanadium in Ascidians." Microscopy Research and Technique **56**(6): 421-434.

Monniot, C. (1969). Les Molgulidae Des Mers Européennes, Broché Mémoires du Muséum d' Histoire Naturelle. 172-272.

Moshier, R. W. and Schwarberg, J. E. (1957). "Tantalum Determination in Presence of Niobium by Precipitation with N-Benzoyl-N-Phenylhydroxylamine." Analytical Chemistry (U.S.) Formerly Ind. Eng. Chem. **29**: 947-51.

Nechay, B. R. (1984). Mechanisms of Action of Vanadium. **24:** 501-524.

Nozaki, Y. (1997). "A Fresh Look at Element Distribution in the North Pacific." Eos, Transactions American Geophysical Union **78**(21): 221-221.

Olson, E. C. and Elving, P. J. (1954). Amperometric Titration of Zirconium. Application to Fluoride Solution. Analytical Chemistry (U.S.) Formerly Ind. Eng. Chem., Anal. Ed.; Vol: 26. Not Available**:** Pages: 1747-50.

Orshulyak, O. O. and Levitskaya, G. D. (2008). "Voltammetric Determination of Zirconium Using Azo Compounds." Journal of Analytical Chemistry **63**(3): 271-274.

Palilla, F. C., Adler, N., et al. (1953). "Analytical Chemistry of Niobium and Tantalum." Anal. Chem. **25**(6): 926-931.

Plank, T. and Langmuir, C. H. (1992). "Effects of the Melting Regime on the Composition of the Oceanic Crust." Journal of Geophysical Research **97**(B13): 19,749-19,770.

Plank, T. and Langmuir, C. H. (1998). "The Chemical Composition of Subducting Sediment and Its Consequences for the Crust and Mantle." Chemical Geology **145**(3-4): 325-394.

Pobi, M. and Das, J. (1993). "Separation of Niobium and Tantalum Using a Chelating Ion Exchange Resin with N-Benzoyl Phenyl Hydroxyl Amine as Functional Group." Analytical Letters **26**(4): Pages: 793-800.

Powell, M., Ball, J. C., et al. (2000). Square Wave Anodic Stripping Voltammetry at Mercury-Plated Electrodes. Simulation of Surface Morphology Effects on Electrochemically Reversible, Irreversible, and Quasi-Reversible Processes: Comparison of Thin Films and Microdroplets. **104:** 8268-8278.

Rach, P., Seiler, H., et al. (1985). Polarographie Und Voltammetrie in Der Spurenanalytik. Heidelberg, Dr. Alfred Hüthig Verlag GmbH.

Rayner-Canham, G. W. (1984). "Some Niobium(V) Complexes and Their Relevance to the Uptake of Niobium by Ascidians." Polyhedron **3**(8): 1029-1031.

Reed, J. F. (1963). "Extraction of the Cupferron Complex of Niobium." Talanta **10**(4): 347-350.

Reimann, C. and Caritat, P. d. (1998). Chemical Elements in the Environment. Berlin, Springer.

Rowley, A. F. (1982). "Ultrastructural and Cytochemical Studies on the Blood Cells of the Sea Squirt,Ciona Intestinalis." Cell and Tissue Research **223**(2): 403-414.

Rowley, A. F. (1983). "Preliminary Investigations on the Possible Antimicrobial Properties of Tunicate Blood Cell Vanadium." The Journal of experimental zoology **227**(2): 319-322.

Rudnick, R. L. and Gao, S. (2003). "Composition of the Continental Crust." Treatise on Geochemistry **3**: 1-64.

Sandell, E. B. (1959). Colorimetric Determination of Traces of Metals. New York, Interscience Publishers, Inc.

Sastry, V. N., Krishnamoorthy, T. M., et al. (1969). "Microdetermination of Zirconium in Marine Environment." Curr. Sci. (India), 38: 279-81(June 20, 1969).

Shendrikar, A. D. (1969). "Substituted Hydroxylamines as Analytical Reagents." Talanta **16**: 51-53.

Siroki, M. and Djordjev, C. (1971). "Spectrophotometric Determination of Niobium with 4-(2-Pyridylazo)Resorcinol and Colored Complexes Separated from Oxalic and Tartaric Acid Systems." Analytical Chemistry **43**(11): 1375-&.

Sohrin, Y., Fujishima, Y., et al. (1998a). "Dissolved Niobium and Tantalum in the North Pacific." Geophysical Research Letters **25**(7): 999-1002.

Sohrin, Y., Iwamoto, S., et al. (1998b). "Determination of Trace Elements in Seawater by Fluorinated Metal Alkoxide Glass-Immobilized 8-Hydroxyquinoline Concentration and High-Resolution Inductively Coupled Plasma Mass Spectrometry Detection." Analytica Chimica Acta **363**(1): 11-19.

Swinehart, J. H., Biggs, W. R., et al. (1974). "The Vanadium and Selected Metal Contents of Some Ascidians." The Biological Bulletin **146**(2): 302-312.

Taylor, S. R. and McLennan, S. M. (1995). "The Geochemical Evolution of the Continental Crust." Reviews of Geophysics **33**(2): 241-265.

Turner, D. R., Whitfield, M., et al. (1981). "The Equilibrium Speciation of Dissolved Components in Freshwater and Sea Water at 25°C and 1 Atm Pressure." Geochimica et Cosmochimica Acta **45**(6): 855-881.

Wagman, D. D., Evans, W. H., et al. (1982). The Nbs Tables of Chemical Thermodynamic Properties. Selected Values for Inorganic and C1 and C2 Organic Substances in Si Units. Washington, D.C. , American Inst. Phys.

Wang, J. (1985). Stripping Analyses: Principles, Instrumentation and Applications, VCH Publishers, Inc.

Wang, J. (2006). Analytical Electrochemistry, John Wiley & Sons, Inc.

Wang, J., Lu, J., et al. (1992a). "Adsorptive Stripping Voltammetric Measurements of Trace Niobium Levels Following Chelation with Cupferron." Electroanalysis **4**(10): 981-985.

Wang, J., Tian, B., et al. (1992b). "Adsorptive--Catalytic Stripping Measurements of Ultratrace Vanadium in the Presence of Cupferron and Bromate." Talanta **39**(10): 1273-1276.

Wang, J., Tuzhi, P., et al. (1987). "Adsorptive Preconcentration for Voltammetric Measurements of Trace Levels of Zirconium." Talanta **34**(6): 561-566.

Yamada, S., Anma, H., et al. (1988). "Kinetic Determination of Tantalum in the Presence of Niobium." Analytical Sciences **4**(1): 49-52.

Yamada, S., Taki, N., et al. (1990). "Kinetic and Thermodynamic Effects of Auxiliary Complexing Agents on the Color-Reactions of Niobium and Tantalum with 4-(2-Pyridylazo)Resorcinol." Analytical Sciences **6**(4): 567-572.

Zhang, X., Ma, C., et al. (1995). "Voltammetric Behaviour of the Zirconium-Phenylfluorone-Hexadecyl Pyridinium Chloride System and the Sensitizing Effect of Surfactants." Fresenius' Journal of Analytical Chemistry **351**(7): 618-621.

Zhao, G. and Chasteen, N. D. (2006). "Oxidation of Good's Buffers by Hydrogen Peroxide." Analytical Biochemistry **349**(2): 262-267.

Zittel, H. E. and Florence, T. M. (1967). "Voltammetric and Spectrophotometric Study of the Zirconium-Alizarine Red S Complex." Analytical Chemistry **39**(3): 320-326.

Zubi, T. (2006). from http://www.starfish.ch/c-invertebrates/chordata.html.

10 Appendices

10.1 Nb determination with cupferron

Name	080508-Nb-Test2-3b.dth	080514-Nb-acetate(pH 5)-1b.dth	080521-Nb-acetate(pH 5)-3b.dth	05271125_080527-Nb-MES-1b.dth	06121336_080612-Nb-PIPES1.dth	06121441_080612-Nb-PIPES3.dth	06130929_080613-Nb-PIPES1.dth
	11.79	4.35	53.70	5.5	11.87	3.81	6.34
	11.74	4.28	53.10	5.41	12.43	3.48	6.36
	13.51	7.70	72.00	14.05	22.85	6.68	9.06
I_p	14.32	7.47	72.80	12.42	22.53	6.09	8.68
(nA)	16.71	9.33	85.40	19.96	34.89	9.47	11.52
	16.76	9.92	86.50	18.56	34.64	8.67	11.38
	18.99	12.17	97.40	27.37	44.6	12.16	14.42
	19.07	12.06	98.40	25.85	43.82	11.66	13.93
	20.77	14.21	108.90	32.28	53.95	14.18	16.53
	20.99	14.18	110.70	31.46	53.11	14.33	17.05
Sensitivity (nA $nmol^{-1}$ L)	0.11	0.11	0.65	0.31	0.49	1.39	1.36

10.2 Nb determination with cupferron in seawater

Name	080513-Nb-Test3-3b.dth	05281606_080528-Nb-ac4-S1b.dth	05281638_080528-Nb-ac5-S1b.dth	05281502_080528Nb-MES-S1b.dth	08131015_080813-Nb-test01.dth	08131138_080813-Nb-test05.dth	08131058_080813-Nb-test03.dth	08131035_080813-Nb-test02.dth	06191130_080619-Nb-PIPES2.dth
	2.89	4.12	3.17	0.48	13.49	22.88	25.27	16.43	16.03
	2.87	4.29	3.16	0.47	14.44	21.21	24.35	15.89	15.87
	4.11	23.39	14.74	2.15	16.19	26.27	34.98	24.37	24.48
I_p	4.69	24.88	14.74	2.03	16.45	25.36	33.43	23.65	24.88
(nA)	6.13	40.09	26.75	3.10	19.77	29.81	51.21	37.79	26.69
	6.04	41.54	26.43	2.87	19.7	29.25	46.1	35.9	26.18
	7.78	53.21	36.98	4.01					31.24
	7.91	54.40	36.64	3.78					30.58
	8.67	64.95	46.54	4.65					33.68
	9.45	66.51	45.78	4.61					32.86
Sensitivity (nA $nmol^{-1}$ L)	0.07	0.72	0.51	0.05	0.12	0.17	0.56	0.48	0.19

10.3 Nb determination with N-benzoyl-N-phenylhydroxylamine

Name	07221417_080722-_Nb-test04.dth	07221642_080722-_Nb-test09.dth	07231400_080723-_Nb-test06.dth	07231449_080723-_Nb-test08.dth	07231538_080723-_Nb-test10.dth	07231512_080723-_Nb-test09.dth
I_p (nA)	41.36	69.50	70.61	142.05	262.43	294.13
	41.75	67.90	69.06	159.65	267.83	297.70
	43.93	311.40	92.36	168.53	274.99	302.14
	42.59	253.40	88.36	171.89	271.24	306.95
	45.39	300.50	108.05	161.46	276.79	311.63
	43.77	268.00	98.52	165.07	278.80	310.86
	46.86					
	44.39					
	62.27					
	56.64					
Sensitivity (nA $nmol^{-1}$ L)	0.11	0.51	0.78	0.29	0.30	0.36

10.4 Nb determination with 4-(2-pyridylazo)-resorcinol

Parameters used in the following calculations:

Nb (M = 92.91 g/mol) standard stock solution: 11.086 mmol L^{-1}

1st Nb working standard: 110.86 µmol L^{-1}

Name	080817-Nb-PAR	080826-Nb-PAR-MES	080827 PIPES1	080829 PIPES2	080827 PIPES0	080826 PIPES	080829-Nb-PAR-PIPES1	080903-Nb-PAR-PIPES-SW1	081007-Nb-PAR-MQ-EPPS1noCit
absorbance at 550 nm	0.05	0.02	0.01	0.01	0.01	0.00	0.06	0.14	0.07
	0.11	0.05	0.03	0.03	0.01	0.01	0.10	0.17	0.08
	0.16	0.09	0.06	0.04	0.02	0.01	0.13	0.20	0.09
	0.22	0.12	0.09	0.05	0.03	0.02	0.18	0.23	0.10
	0.25	0.17	0.12	0.07	0.04	0.02	0.23	0.29	0.11
	0.30	0.21	0.17	0.09	0.06	0.03	0.29	0.31	0.12
Emissivity (mol^{-1} dm^3 cm^{-1})	70459	26579	21742	11442	6652	3507	32602	23848	7017

10.5 Nb determination with 4-(2-pyridylazo)-resorcinol in seawater

Name	080903-Nb-PAR-PIPES-SW1	080905-Nb-PAR-PIPES-SW2	080905 EPPS-SW	080912-Nb-PAR-PIPES-SW01	080912-Nb-PAR-PIPES-SW02	080912-Nb-PAR-EPPS-SW
absorbance at 550 nm	0.14	0.14	0.24	0.09	0.10	0.17
	0.17	0.16	0.24	0.15	0.15	0.18
	0.20	0.19	0.27	0.20	0.20	0.22
	0.23	0.25	0.26	0.26	0.26	0.26
	0.29	0.27	0.29	0.31	0.30	0.28
	0.31	0.32	0.40	0.36	0.35	0.29
Emissivity (mol^{-1} dm^3 cm^{-1})	23848	25128	18178	38705	34694	18752

10.6 Zr determination with cupferron

Parameters used in the following calculations:

Zr (M = 91.224 g/mol) standard stock solution: 10.963 mmol L^{-1}

1st Zr working standard: 10.96 µmol L^{-1}

2nd Zr working standard: 109.63 nmol L^{-1}

Name	06261231_0806 26-Zr-MES-01.dth	06271030_0806 27-Zr-EPPS1.dth	06271113_0806 27-Zr-EPPS2.dth	07011127_0807 01-Zr-EPPS02.dth	07011623_0807 01-Zr-EPPS07.dth	07151101_0807 15-Zr-EPPS01.dth	07151415_0807 15-Zr-MES-02.dth
I_p (nA)	17.90	-6.96					25.71
	12.90	-9.37					27.67
	10.70	-9.10	-3.47	-3.41			32.74
	11.10	-9.02	-3.27	-3.51			31.20
	12.00	-10.28	-5.32	-5.82			36.67
	12.40	-9.48	-5.51	-5.76			34.35
	75.90	-13.60	-7.64	-7.97		65.74	39.89
	67.40	-11.60	-7.18	-7.37		55.29	35.00
	100.80	-18.70	-8.79	-8.89	8.78	83.97	83.43
	87.00	-16.32	-8.09	-8.99	7.02	82.01	63.94
Sensitivity (nA $nmol^{-1}$ L)	0.19	-0.06	-0.07	-0.07			0.17